SAND2018-1356C

DRAFT DO NOT CITE OR RETAIN COPIES

# Parameter Development for New EQ3/6 Database

*DOE-EPA Technical Exchange Meeting, February 13-15, 2018; Albuquerque, NM*

Yongliang Xiong, Ph.D., Paul Domski; Christi Leigh, Ph.D.
Repository Investigations Department; Sandia National Laboratories

Sandia National Laboratories is a multimission laboratory managed and operated by National Technology and Engineering Solutions of Sandia, LLC., a wholly owned subsidiary of Honeywell International, Inc., for the U.S. Department of Energy's National Nuclear Security Administration under contract DE-NA-0003525.
This research is funded by the WIPP programs administered by the Office of Environmental Management (EM) of the U.S Department of Energy. SAND2018-xxxxP

Sandia National Laboratories

# OUTLINE OF PRESENTATION

- What Parameters Are we Discussing?
- Activity Coefficient Corrections
- Data Selection
- History of the thermodynamic database
- Database Updates
  - **Value for Hydromagnesite**
  - **Equilibrium Constant for $AmHB_4O_7^{2+}$**
  - **Revised Stability Constant for $CaEDTA^{2-}$**
  - **Equilibrium Constant for $Nd(OH)_3(am)$**
  - **Stability Constant for $MgSO_4(aq)$**
  - **Stability Constant for $AmEDTA^-$**
  - **Stability Constant for $NaB(OH)_4(aq)$**
  - **Lead Chemistry**
- Summary

Sandia National Laboratories

# What Parameters Are we Discussing?

- Sometimes the solubility constant (dissolution of solids)
- Sometimes the equilibrium constant (interaction of aqueous species)
- Sometimes the activity coefficients

The WIPP thermodynamic database at 25°C uses the **Pitzer model** for calculation of activity coefficients of aqueous species.

# INTRODUCTION: Activity Coefficient Correction

- Accurate prediction of concentrations of aqueous species is important to modeling various geochemical processes, including the performance assessment (PA) of geological repositories for nuclear waste.
- Concentrations of aqueous species are calculated according to thermodynamic activities and their activity coefficients, usually on molality scale:

$$a_i = m_i \gamma_i$$

# INTRODUCTION: Activity Coefficient Models

- Davies Equation:

$$\log \gamma_i = -A_\gamma z_i^{\,2} \left( \frac{\sqrt{I_m}}{1+\sqrt{I_m}} + 0.3 I_m \right)$$

- Advantages:
  - It is universal (one needs to know $z_i$). It only depends on ionic strength.
- Limitations:
  - Valid to ionic strength of 0.1 m
  - Only used for temperatures close to 25°C.
- Computer Codes using Davies equation:
  - PHREEQC (USGS), EQ3/6 (LLNL), Visual MINTEQ (EPA)

# INTRODUCTION: Activity Coefficient Models

- Extended Debye-Hückel (or WATEQ Debye-Hückel) Equation:

$$\log \gamma_i = -A_\gamma z_i^{\,2} \times \frac{\sqrt{\mathrm{I}_m}}{1 + B_{DH} a_i^0 \sqrt{I_m}} - b_i I_m$$

- Advantages:
  - If values for all parameters are available, it is good up to ionic strength of 0.8 m.
  - It is valid at elevated temperatures.
- Limitations:
  - Quite limited species have values for $b_i$ parameters
- Computer Codes using Extended Debye-Hückel equation:
  - PHREEQC (USGS), Visual MINTEQ (EPA)

# INTRODUCTION: Activity Coefficient Models

- B dot Equation:

$$\log \gamma_i = -A_\gamma z_i^{\,2} \times \frac{\sqrt{I_m}}{1 + B_{DH} a_i^0 \sqrt{I_m}} + \dot{B} I_m$$

- Advantages:
  - It has the universality similar to Davies equation.
  - It can be applied up to 300°C.
- Limitations:
  - Valid to ionic strength of 1.0 m.
  - The model was developed from NaCl solutions.
- Computer Codes using B dot equation:
  - EQ3/6 (LLNL), EQBRMB (Princeton-University of Idaho), GWB (University of Illinois).

# INTRODUCTION: Activity Coefficient Models

- Brønsted-Guggenheim-Scatchard Specific Ion Interaction Theory (SIT) Model

$$\log \gamma_i = -A_\gamma z_i^{\,2} \times \frac{\sqrt{I_m}}{1+1.5\sqrt{I_m}} + \sum_k \varepsilon(i,k) m_k$$

- Advantages:
  - Valid to ionic strength of 4.0 m
  - If values for parameters are available, it can be applied at high temperatures.
  - Mathematically simple; it is linear.
  - Less extensive experimental data sets are needed for obtaining SIT parameters.
- Limitations:
  - Experimental data are needed for evaluation of SIT parameters.
  - Majority of parameters are at 25°C, but there are some up to 200°C.
- Computer Codes using SIT model
  - PHREEQC version 2.17 (USGS), Visual MINTEQ version 3.0 (EPA)

# INTRODUCTION: Activity Coefficient Models

- Pitzer Model, using mean activity coefficient for NaCl as an example:

$$\ln \gamma_{\pm} = -A_{\phi}\left[\frac{\sqrt{I_m}}{1+1.2\sqrt{I_m}} + \frac{2}{1.2}\ln(1+1.2\sqrt{I_m})\right] + m\left\{2\beta^{(0)} + \frac{2\beta^{(1)}}{\alpha^2 \times I_m}\left[1-(1+\alpha\sqrt{I_m} - \frac{\alpha^2 I_m}{2})e^{-\alpha\sqrt{I_m}}\right]\right\} + \frac{3m^2}{2}C^{\phi}$$

- Advantages:
  - Reproduction of experimental data with high precision, if the model is well parameterized.
  - Valid to high ionic strength, up to saturation of most salts.
- Limitations:
  - Extensive data are needed for evaluation of Pitzer parameters.
- Status of Pitzer parameters
  - Majority of them are at 25°C.
  - YMP high temperature database, data0.ypf, up to 200°C for limited species.
  - Na-Ca-Cl-$SO_4$ system to 250°C (Moller, 1988).
- Computer Codes using Pitzer model:
  - EQ3/6 (LLNL), FMT (SNL), FREZCHEM (US Army Corps of Engineers; Desert Research Institute), GWB (University of Illinois), PHREEQC version 2.12 or higher (USGS).

# Data Selection

- Thorough literature search for data relevant to the near-field geochemistry of the WIPP by using the following search engines:
  - Web of Sciences®.
  - Google Scholar®.
  - Elsevier Scopus®.
  - ACS Chemical Abstracts®
- We apply the similar criteria for selecting data for establishment of actinide uncertainty distributions to include/exclude literature data for parameterization.
- We prioritize to updates those parameters that impact actinide solubilities and the near-field geochemistry.
- We also prioritize to updates those parameters that impact the engineered barrier, MgO.
- We also prioritize to include those parameters for the elements that have high inventories in the WIPP, such as lead and iron.

# Database History

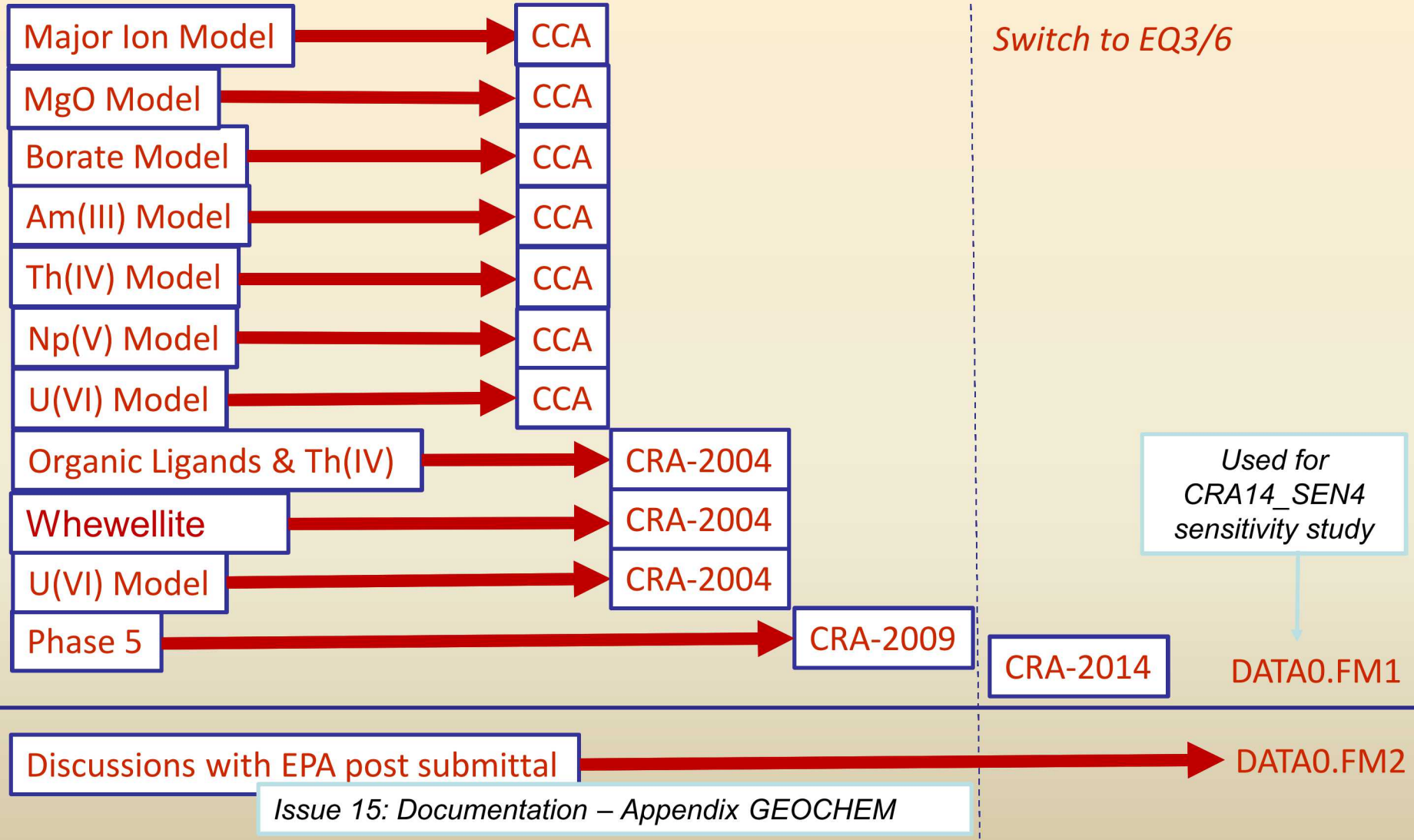

# Database History

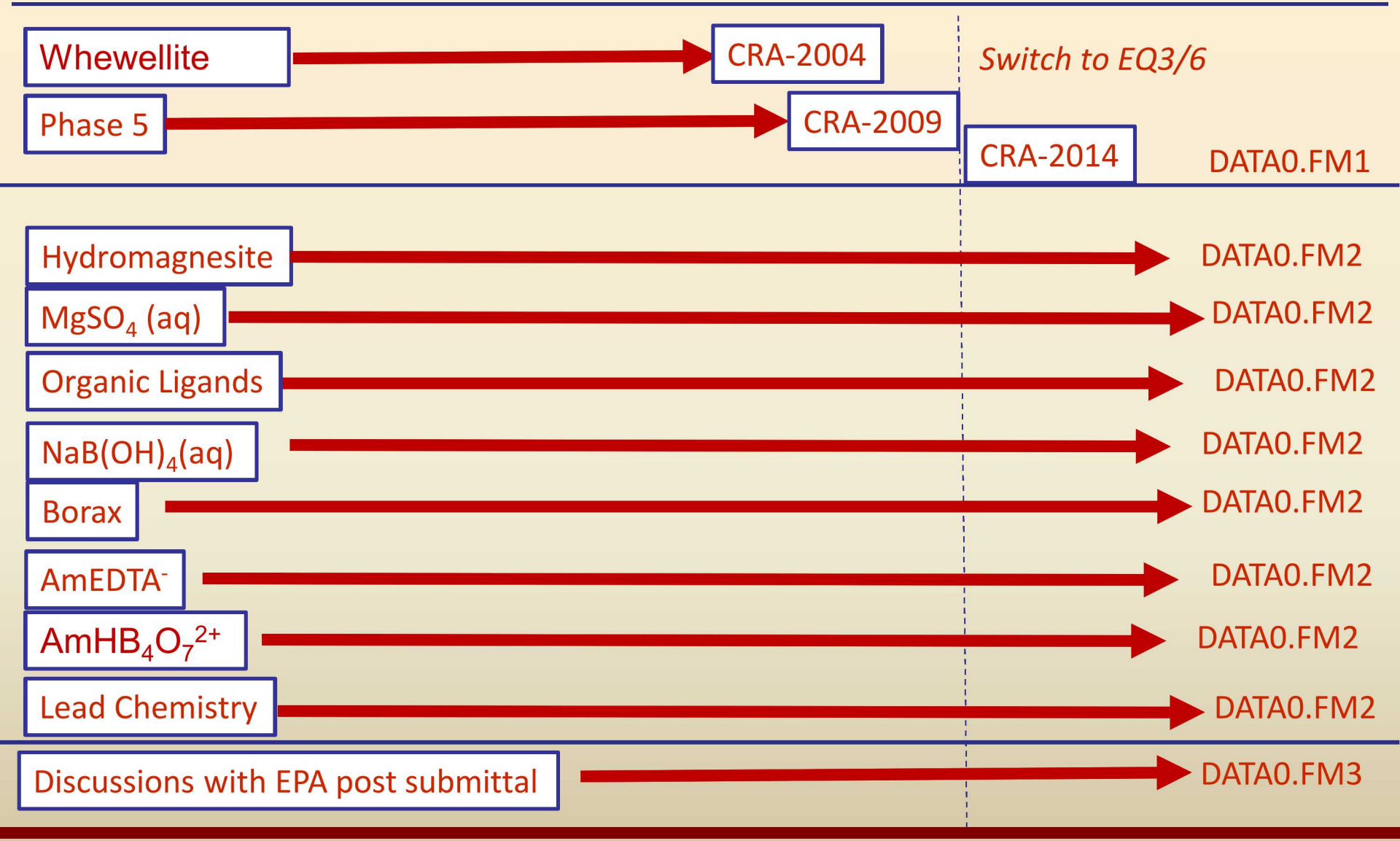

# Database History

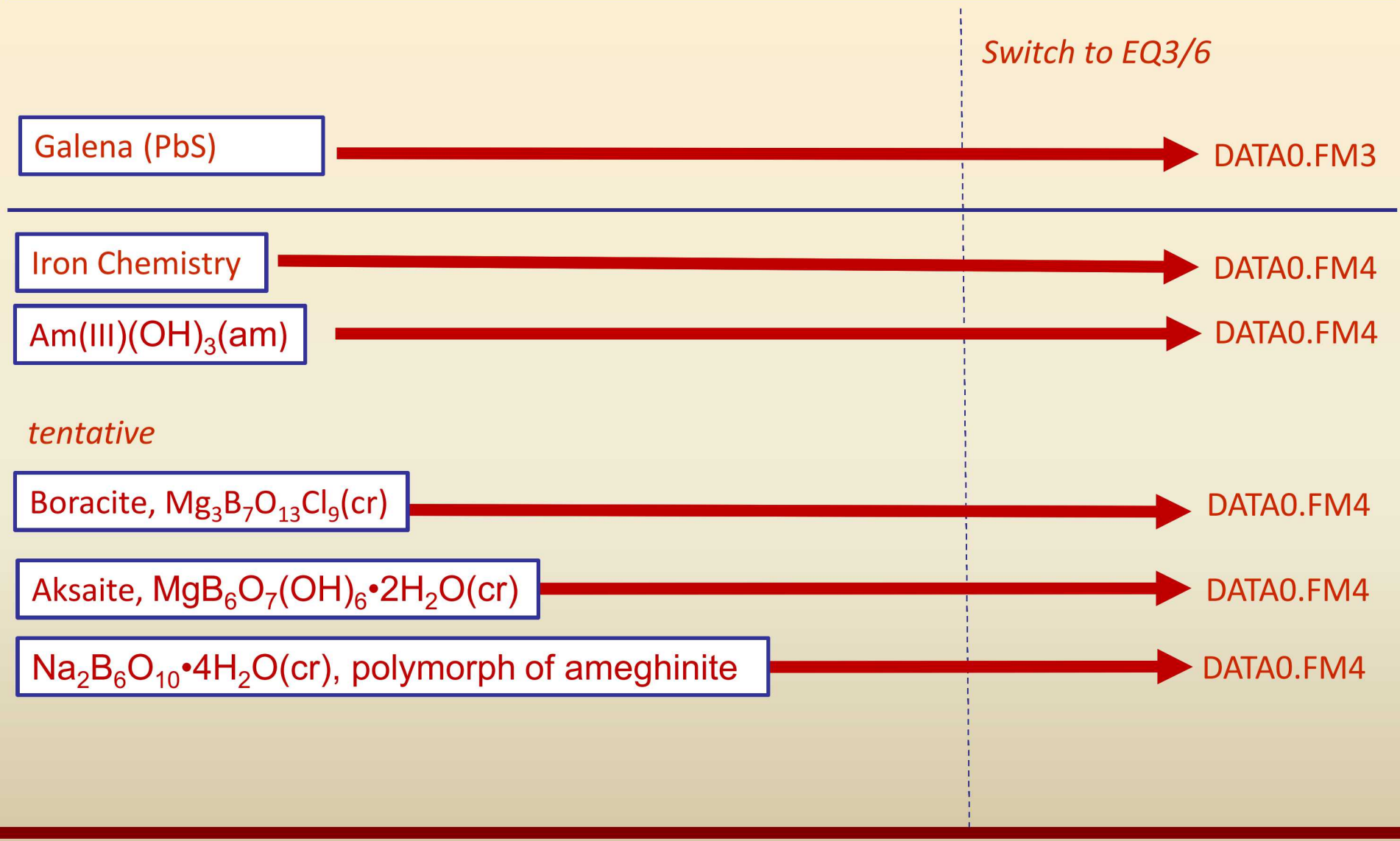

# WIPP Thermodynamic Database: Major ions

(I-1) $H_2O = OH^- + H^+$

(I-2) $Ca^{2+} + 2H_2O = Ca(OH)_2(\text{portlandite}) + 2H^+$

(I-3) $Na^+ + Cl^- = NaCl(\text{halite})$

(I-4) $K^+ + Cl^- = KCl(\text{sylvite})$

(I-5) $Ca^{2+} + 2Cl^- + 4H_2O = CaCl_2{\bullet}4H_2O(cr)$

(I-6) $4Ca^{2+} + 2Cl^- + 19H_2O = Ca_4Cl_2(OH)_6{\bullet}13H_2O(\text{CaOxychloride\_A}) + 6H^+$

(I-7) $2Ca^{2+} + 2Cl^- + 3H_2O = Ca_2Cl_2(OH)_2{\bullet}H_2O(\text{CaOxychloride\_B}) + 2H^+$

(I-8) $K^+ + Mg^{2+} + 3Cl^- + 6H_2O = KMgCl_3{\bullet}6H_2O(\text{carnallite})$

(I-9) $H^+ + HCO_3^- = CO_2(aq) + H_2O$

(I-10) $HCO_3^- = CO_3^{2-} + H^+$

(I-11) $Na^+ + HCO_3^- = NaHCO_3(\text{nahcolite})$

(I-12) $3Na^+ + 2HCO_3^- + 2H_2O = Na_3H(CO_3)_2{\bullet}2H_2O(\text{trona}) + H^+$

(I-13) $2Na^+ + HCO_3^- + 10H_2O = Na_2CO_3{\bullet}10H_2O(\text{natron}) + H^+$

(I-14) $2Na^+ + HCO_3^- + 7H_2O = Na_2CO_3{\bullet}7H_2O(cr) + H^+$

(I-15) $2Na^+ + HCO_3^- + H_2O = Na_2CO_3{\bullet}H_2O(\text{thermonatrite}) + H^+$

(I-16) $K^+ + HCO_3^- = KHCO_3(\text{kalicinite})$

(I-17) $2K^+ + HCO_3^- + 1.5H_2O = K_2CO_3{\bullet}3/2H_2O(cr) + H^+$

(I-18) $8K^+ + 6HCO_3^- + 3H_2O = K_8H_4(CO_3)_6{\bullet}3H_2O(cr) + 2H^+$

(I-19) $K^+ + Na^+ + HCO_3^- + 6H_2O = KNaCO_3{\bullet}6H_2O(cr) + H^+$

(I-20) $2K^+ + Na^+ + 2HCO_3^- + 2H_2O = K_2NaH(CO_3)_2{\bullet}2H_2O(\text{K-trona}) + H^+$

(I-21) $Ca^{2+} + HCO_3^- = CaCO_3(\text{aragonite}) + H^+$

(I-22) $Ca^{2+} + HCO_3^- = CaCO_3(\text{calcite}) + H^+$

(I-23) $Ca^{2+} + 2Na^+ + 2HCO_3^- + 5H_2O = CaNa_2(CO_3)_2{\bullet}5H_2O(\text{gaylussite}) + 2H^+$

(I-24) $2Na^+ + Ca^{2+} + 2HCO_3^- + 2H_2O = Na_2Ca(CO_3)_2{\bullet}2H_2O(\text{pirssonite}) + 2H^+$

(I-25) $SO_4^{2-} + H^+ = HSO_4^- + H^+$

(I-26) $Ca^{2+} + SO_4^{2-} = CaSO_4(\text{anhydrite})$

(I-27) $Ca^{2+} + SO_4^{2-} + 2H_2O = CaSO_4{\bullet}2H_2O(\text{gypsum})$

(I-28) $2K^+ + SO_4^{2-} = K_2SO_4(\text{arcanite})$

(I-29) $8K^+ + 6H^+ + 7SO_4^{2-} = K_8H_6(SO_4)_7(\text{misenite})$

(I-30) $3K^+ + H^+ + 2SO_4^{2-} = K_3H(SO_4)_2(cr)$

(I-31) $K^+ + Ca^{2+} + 2SO_4^{2-} + H_2O = K_2Ca(SO_4)_2{\bullet}H_2O(\text{syngenite})$

Source: Harvie-Moller-Weare
Na-K-H-Ca-Mg-Cl-SO4-CO2-H2O
Phosphate: Rai and Felmy

No changes made by DOE

(I-32) $2Na^+ + SO_4^{2-} + 10H_2O = Na_2SO_4{\bullet}10H_2O(\text{mirabilite})$

(I-33) $2Na^+ + SO_4^{2-} = Na_2SO_4(\text{thenardite})$

(I-34) $Na^+ + H^+ + 2SO_4^{2-} = Na_3H(SO_4)_2(cr)$

(I-35) $Na^+ + 3K^+ + 2SO_4^{2-} = NaK_3(SO_4)_2(\text{aphthitalite, galerite})$

(I-36) $2Na^+ + Ca^{2+} + 2SO_4^{2-} = Na_2Ca(SO_4)_2(\text{glauberite})$

(I-37) $4Na^+ + Ca^{2+} + 3SO_4^{2-} + 2H_2O = Na_4Ca(SO_4)_3{\bullet}2H_2O(\text{labile salt})$

(I-38) $HPO_4^{2-} + 2H^+ = H_3PO_4(aq)$

(I-39) $HPO_4^{2-} + H^+ = H_2PO_4^- + H^+$

(I-40) $HPO_4^{2-} = PO_4^{3-} + H$

# WIPP Thermodynamic Database: MgO

(II-1) $Mg^{2+} + H_2O = MgOH^+ + H^+$

(II-2) $Mg^{2+} + 2H_2O = Mg(OH)_2(brucite) + 2H^+$

(II-3) $Mg^{2+} + 2Cl^- + 6H_2O = MgCl_2 \bullet 6H_2O(bischofite)$

(II-4) $2Mg^{2+} + Cl^- + 7H_2O = Mg_2Cl(OH)_3 \bullet 4H_2O(phase\ 3) + 3H^+$

Source:
Harvie-Moller-Weare

(II-6) $2Mg^{2+} + Ca^{2+} + 6Cl^- + 12H_2O = Mg_2CaCl_6 \bullet 12H_2O(tachyhydrite)$

(II-7) $K^+ + Mg^{2+} + 3Cl^- + 6H_2O = KMgCl_3 \bullet 6H_2O(carnallite)$

(II-8) $Mg^{2+} + HCO_3^- = MgCO_3(magnesite) + H^+$

(II-9) $Mg^{2+} + HCO_3^- + 3H_2O = MgCO_3 \bullet 3H_2O(nesquehonite) + H^+$

(II-10) $4Mg^{2+} + 3HCO_3^- + 5H_2O = Mg_4(CO_3)_3(OH)_2 \bullet 3H_2O(hydromagnesite4323) + 5H^+$

(II-11) $5Mg^{2+} + 4HCO_3^- + 6H_2O = Mg_5(CO_3)_4(OH)_2 \bullet 4H_2O(hydromagnesite5424) + 6H^+$

(II-12) $2K^+ + Mg^{2+} + 2SO_4^{2-} + 4H_2O = K_2Mg(SO_4)_2 \bullet 4H_2O(leonite)$

(II-14) $2Na^+ + Mg^{2+} + 2SO_4^{2-} + 2H_2O = Na_2Mg(SO_4)_2 \bullet 4H_2O(boedite)$

(II-15) $Mg^{2+} + SO_4^{2-} + 7H_2O = MgSO_4 \bullet 7H_2O(epsomite)$

(II-16) $Mg^{2+} + SO_4^{2-} + 6H_2O = MgSO_4 \bullet 6H_2O(hexahydrite)$

(II-17) $Mg^{2+} + SO_4^{2-} + H_2O = MgSO_4 \bullet H_2O(kieserite)$

(II-18) $K^+ + Mg^{2+} + Cl^- + SO_4^{2-} + 3H_2O = KMgClSO_4 \bullet 3H_2O(kainite)$

# WIPP Thermodynamic Database: MgO

(II-1) $Mg^{2+} + H_2O = MgOH^+ + H^+$

(II-2) $Mg^{2+} + 2H_2O = Mg(OH)_2(brucite) + 2H^+$

(II-3) $Mg^{2+} + 2Cl^- + 6H_2O = MgCl_2 \bullet 6H_2O(bischofite)$

(II-4) $2Mg^{2+} + Cl^- + 7H_2O = Mg_2Cl(OH)_3 \bullet 4H_2O(phase\ 3) + 3H^+$

(II-5) $3Mg^{2+} + Cl^- + 9H_2O = Mg_3Cl(OH)_5 \bullet 4H_2O(phase\ 5) + 5H^+$

(II-6) $2Mg^{2+} + Ca^{2+} + 6Cl^- + 12H_2O = Mg_2CaCl_6 \bullet 12H_2O(tachyhydrite)$

(II-7) $K^+ + Mg^{2+} + 3Cl^- + 6H_2O = KMgCl_3 \bullet 6H_2O(carnallite)$

(II-8) $Mg^{2+} + HCO_3^- = MgCO_3(magnesite) + H^+$

(II-9) $Mg^{2+} + HCO_3^- + 3H_2O = MgCO_3 \bullet 3H_2O(nesquehonite) + H^+$

(II-10) $4Mg^{2+} + 3HCO_3^- + 5H_2O = Mg_4(CO_3)_3(OH)_2 \bullet 3H_2O(hydromagnesite4323) + 5H^+$

(II-11) $5Mg^{2+} + 4HCO_3^- + 6H_2O = Mg_5(CO_3)_4(OH)_2 \bullet 4H_2O(hydromagnesite5424) + 6H^+$

(II-12) $2K^+ + Mg^{2+} + 2SO_4^{2-} + 4H_2O = K_2Mg(SO_4)_2 \bullet 4H_2O(leonite)$

(II-14) $2Na^+ + Mg^{2+} + 2SO_4^{2-} + 2H_2O = Na_2Mg(SO_4)_2 \bullet 4H_2O(boedite)$

(II-15) $Mg^{2+} + SO_4^{2-} + 7H_2O = MgSO_4 \bullet 7H_2O(epsomite)$

(II-16) $Mg^{2+} + SO_4^{2-} + 6H_2O = MgSO_4 \bullet 6H_2O(hexahydrite)$

(II-17) $Mg^{2+} + SO_4^{2-} + H_2O = MgSO_4 \bullet H_2O(kieserite)$

(II-18) $K^+ + Mg^{2+} + Cl^- + SO_4^{2-} + 3H_2O = KMgClSO_4 \bullet 3H_2O(kainite)$

Changes:
Phase 5 solid added

# WIPP Thermodynamic Database: MgO

(II-1) $Mg^{2+} + H_2O = MgOH^+ + H^+$

(II-2) $Mg^{2+} + 2H_2O = Mg(OH)_2$(brucite) $+ 2H^+$

(II-3) $Mg^{2+} + 2Cl^- + 6H_2O = MgCl_2 \bullet 6H_2O$(bischofite)

(II-4) $2Mg^{2+} + Cl^- + 7H_2O = Mg_2Cl(OH)_3 \bullet 4H_2O$(phase 3) $+ 3H^+$

(II-5) $3Mg^{2+} + Cl^- + 9H_2O = Mg_3Cl(OH)_5 \bullet 4H_2O$(phase 5) $+ 5H^+$

(II-6) $2Mg^{2+} + Ca^{2+} + 6Cl^- + 12H_2O = Mg_2CaCl_6 \bullet 12H_2O$(tachyhydrite)

(II-7) $K^+ + Mg^{2+} + 3Cl^- + 6H_2O = KMgCl_3 \bullet 6H_2O$(carnallite)

(II-8) $Mg^{2+} + HCO_3^- = MgCO_3$(magnesite) $+ H^+$

(II-9) $Mg^{2+} + HCO_3^- + 3H_2O = MgCO_3 \bullet 3H_2O$(nesquehonite) $+ H^+$

(II-10) $4Mg^{2+} + 3HCO_3^- + 5H_2O = Mg_4(CO_3)_3(OH)_2 \bullet 3H_2O$(hydromagnesite4323) $+ 5H^+$

(II-11) $5Mg^{2+} + 4HCO_3^- + 6H_2O = Mg_5(CO_3)_4(OH)_2 \bullet 4H_2O$(hydromagnesite5424) $+ 6H^+$

(II-12) $2K^+ + Mg^{2+} + 2SO_4^{2-} + 4H_2O = K_2Mg(SO_4)_2 \bullet 4H_2O$(leonite)

(II-14) $2Na^+ + Mg^{2+} + 2SO_4^{2-} + 2H_2O = Na_2Mg(SO_4)_2 \bullet 4H_2O$(boedite)

(II-15) $Mg^{2+} + SO_4^{2-} + 7H_2O = MgSO_4 \bullet 7H_2O$(epsomite)

(II-16) $Mg^{2+} + SO_4^{2-} + 6H_2O = MgSO_4 \bullet 6H_2O$(hexahydrite)

(II-17) $Mg^{2+} + SO_4^{2-} + H_2O = MgSO_4 \bullet H_2O$(kieserite)

(II-18) $K^+ + Mg^{2+} + Cl^- + SO_4^{2-} + 3H_2O = KMgClSO_4 \bullet 3H_2O$(kainite)

(II-19) $Mg^{2+} + SO_4^{2-} = MgSO_4$(aqueous)

Changes:
$MgSO_4$(aq) added
Revised hydromagnesite

*Issue 21*

*EPA comments but not identified as an issue*

# WIPP Thermodynamic Database: Borate Species

(VIII-1) $B(OH)_4^- + H^+ = B(OH)_3(aq) + H_2O$

(VIII-2) $CaB(OH)_4^+ = Ca^{2+} + B(OH)_4^-$

(VIII-3) $MgB(OH)_4^+ = Mg^{2+} + B(OH)_4^-$

(VIII-4) $B_3O_3(OH)_4^- + 5H_2O = 3B(OH)_4^- + 2H^+$

(VIII-5) $B_4O_5(OH)_4^{2-} + 7H_2O = 4B(OH)_4^- + 2H^+$

Source: Felmy-Weare Model Na-K-H-Ca-Mg-Cl-SO4-CO2-B(OH)3-H2O

(VIII-7) $Na_2B_4O_7 \bullet 10H_2O(Na\text{-tetraborate}) = 2Na^+ + 4B(OH)_4^- + 2H^+ + H_2O$

(VIII-8) $B(OH)_3(cr) + H_2O = B(OH)_4^- + H^+$

(VIII-9) $KB_5O_8 \bullet 4H_2O(K\text{-pentaborate}) + 8H_2O = K^+ + 5B(OH)_4^- + 4H^+$

(VIII-10) $K_2B_4O_7 \bullet 4H_2O(K\text{-tetraborate}) + 5H_2O = 2K^+ + 4B(OH)_4^- + 2H^+$

(VIII-11) $NaBO_2 \bullet 4H_2O(Na\text{-metaborate}) = Na^+ + B(OH)_4^- + 2H_2O$

(VIII-12) $NaB_5O_8 \bullet 5H_2O(Na\text{-pentaborate}) + 7H_2O = Na^+ + 5B(OH)_4^- + 4H^+$

(VIII-13) $NaBO_2 \bullet NaCl \bullet 2H_2O(teepleite) = 2Na^+ + B(OH)_4^- + Cl^-$

# WIPP Thermodynamic Database: Borate Species

(VIII-1) $B(OH)_4^- + H^+ = B(OH)_3(aq) + H_2O$

(VIII-2) $CaB(OH)_4^+ = Ca^{2+} + B(OH)_4^-$

(VIII-3) $MgB(OH)_4^+ = Mg^{2+} + B(OH)_4^-$

(VIII-4) $B_3O_3(OH)_4^- + 5H_2O = 3B(OH)_4^- + 2H^+$

(VIII-5) $B_4O_5(OH)_4^{2-} + 7H_2O = 4B(OH)_4^- + 2H^+$

(VIII-6) $NaB(OH)_4(aq) = Na^+ + B(OH)_4^-$

(VIII-7) $Na_2B_4O_7 \bullet 10H_2O(Na\text{-tetraborate}) = 2Na^+ + 4B(OH)_4^- + 2H^+ + H_2O$

(VIII-8) $B(OH)_3(cr) + H_2O = B(OH)_4^- + H^+$

(VIII-9) $KB_5O_8 \bullet 4H_2O(K\text{-pentaborate}) + 8H_2O = K^+ + 5B(OH)_4^- + 4H^+$

(VIII-10) $K_2B_4O_7 \bullet 4H_2O(K\text{-tetraborate}) + 5H_2O = 2K^+ + 4B(OH)_4^- + 2H^+$

(VIII-11) $NaBO_2 \bullet 4H_2O(Na\text{-metaborate}) = Na^+ + B(OH)_4^- + 2H_2O$

(VIII-12) $NaB_5O_8 \bullet 5H_2O(Na\text{-pentaborate}) + 7H_2O = Na^+ + 5B(OH)_4^- + 4H^+$

(VIII-13) $NaBO_2 \bullet NaCl \bullet 2H_2O(teepleite) = 2Na^+ + B(OH)_4^- + Cl^-$

Changes:
$NaB(OH)_4(aq)$ added
Revised Borax (Sodium Tetraborate)

# WIPP Thermodynamic Database: Organic Ligands

(III-1) $Mg^{2+} + Acetate^{-} = MgAcetate^{+}$

(III-2) $Ca^{2+} + Acetate^{-} = CaAcetate^{+}$

(III-3) $Citrate^{3-} + 3H^{+} = H_3Citrate\ (aq)$

(III-4) $Citrate^{3-} + 2H^{+} = H_2Citrate^{-}$

(III-5) $Citrate^{3-} + H^{+} = HCitrate^{2-}$

(III-6) $Mg^{2+} + Citrate^{3-} = MgCitrate^{-}$

(III-7) $Ca^{2+} + Citrate^{3-} = CaCitrate^{-}$

(III-9) $EDTA^{4-} + 4H^{+} = H_4EDTA(aq)$

(III-10) $EDTA^{4-} + 3H^{+} = H_3EDTA^{-}$

(III-11) $EDTA^{4-} + 2H^{+} = H_2EDTA^{2-}$

(III-12) $EDTA^{4-} + H^{+} = HEDTA^{3-}$

(III-13) $Mg^{2+} + EDTA^{4-} = MgEDTA^{2-}$

(III-14) $Ca^{2+} + EDTA^{4-} = CaEDTA^{2-}$

(III-16) $Oxalate^{2-} + 2H^{+} = H_2Oxalate(aq)$

(III-17) $Oxalate^{2-} + H^{+} = HOxalate^{-}$

(III-18) $Mg^{2+} + Oxalate^{2-} = MgOxalate(aq)$

(III-19) $Ca^{2+} + Oxalate^{2-} = CaOxalate(aq)$

(III-20) $Oxalate^{2-} + 2H^{+} + 2H_2O = H_2Oxalate \bullet 2H_2O$

(III-21) $Na^{+} + H^{+} + Oxalate^{2-} + H_2O = NaHOxalate \bullet H_2O$

(III-22) $2Na^{+} + Oxalate^{2-} = Na_2Oxalate$

(III-23) $Ca^{2+} + Oxalate^{2-} + H_2O = CaOxalate \bullet H_2O$

(III-24) $Lactate^{-} + H^{+} = HLactate(aq)$

Sources for Organic Species:
FSU, SNL (Bob Moore)

Added to +III

Added to +IV

Added to +V

Giambalvo update for Th(IV)

# WIPP Thermodynamic Database: Organic Ligands

(III-1) $Mg^{2+} + Acetate^{-} = MgAcetate^{+}$

(III-2) $Ca^{2+} + Acetate^{-} = CaAcetate^{+}$

(III-3) $Citrate^{3-} + 3H^{+} = H_3Citrate\ (aq)$

(III-4) $Citrate^{3-} + 2H^{+} = H_2Citrate^{-}$

(III-5) $Citrate^{3-} + H^{+} = HCitrate^{2-}$

(III-6) $Mg^{2+} + Citrate^{3-} = MgCitrate^{-}$

(III-7) $Ca^{2+} + Citrate^{3-} = CaCitrate^{-}$

(III-9) $EDTA^{4-} + 4H^{+} = H_4EDTA(aq)$

(III-10) $EDTA^{4-} + 3H^{+} = H_3EDTA^{-}$

(III-11) $EDTA^{4-} + 2H^{+} = H_2EDTA^{2-}$

(III-12) $EDTA^{4-} + H^{+} = HEDTA^{3-}$

(III-13) $Mg^{2+} + EDTA^{4-} = MgEDTA^{2-}$

(III-14) $Ca^{2+} + EDTA^{4-} = CaEDTA^{2-}$

(III-16) $Oxalate^{2-} + 2H^{+} = H_2Oxalate(aq)$

(III-17) $Oxalate^{2-} + H^{+} = HOxalate^{-}$

(III-18) $Mg^{2+} + Oxalate^{2-} = MgOxalate(aq)$

(III-19) $Ca^{2+} + Oxalate^{2-} = CaOxalate(aq)$

(III-20) $Oxalate^{2-} + 2H^{+} + 2H_2O = H_2Oxalate \bullet 2H_2O$

(III-21) $Na^{+} + H^{+} + Oxalate^{2-} + H_2O = NaHOxalate \bullet H_2O$

(III-22) $2Na^{+} + Oxalate^{2-} = Na_2Oxalate$

(III-23) $Ca^{2+} + Oxalate^{2-} + H_2O = CaOxalate \bullet H_2O$

(III-24) $Lactate^{-} + H^{+} = HLactate(aq)$

Changes: Added Whewelite

# WIPP Thermodynamic Database: Organic Ligands

(III-1) $Mg^{2+} + Acetate^{-} = MgAcetate^{+}$

(III-2) $Ca^{2+} + Acetate^{-} = CaAcetate^{+}$

(III-3) $Citrate^{3-} + 3H^{+} = H_3Citrate\ (aq)$

(III-4) $Citrate^{3-} + 2H^{+} = H_2Citrate^{-}$

(III-5) $Citrate^{3-} + H^{+} = HCitrate^{2-}$

(III-6) $Mg^{2+} + Citrate^{3-} = MgCitrate^{-}$

(III-7) $Ca^{2+} + Citrate^{3-} = CaCitrate^{-}$

(III-8) $Ca_3(Citrate)_2 \bullet 4H_2O\ (earlandite) = 3Ca^{2+} + 2Citrate^{3-} + 4H_2O$

(III-9) $EDTA^{4-} + 4H^{+} = H_4EDTA(aq)$

(III-10) $EDTA^{4-} + 3H^{+} = H_3EDTA^{-}$

(III-11) $EDTA^{4-} + 2H^{+} = H_2EDTA^{2-}$

(III-12) $EDTA^{4-} + H^{+} = HEDTA^{3-}$

(III-13) $Mg^{2+} + EDTA^{4-} = MgEDTA^{2-}$

(III-14) $Ca^{2+} + EDTA^{4-} = CaEDTA^{2-}$

(III-15) $Ca_2EDTA \bullet 7H_2O(s) = 2Ca^{2+} + EDTA^{4-} + 7H_20$

(III-16) $Oxalate^{2-} + 2H^{+} = H_2Oxalate(aq)$

(III-17) $Oxalate^{2-} + H^{+} = HOxalate^{-}$

(III-18) $Mg^{2+} + Oxalate^{2-} = MgOxalate(aq)$

(III-19) $Ca^{2+} + Oxalate^{2-} = CaOxalate(aq)$

(III-20) $Oxalate^{2-} + 2H^{+} + 2H_2O = H_2Oxalate \bullet 2H_2O$

(III-21) $Na^{+} + H^{+} + Oxalate^{2-} + H_2O = NaHOxalate \bullet H_2O$

(III-22) $2Na^{+} + Oxalate^{2-} = Na_2Oxalate$

(III-23) $Ca^{2+} + Oxalate^{2-} + H_2O = CaOxalate \bullet H_2O$

(III-24) $Lactate^{-} + H^{+} = HLactate(aq)$

Changes: Added
Earlandite (Calcium Citrate)
$Ca_2EDTA \bullet 7H_2O(s)$
Revised $CaEDTA^{2-}$

*EPA comments but not identified as an issue*

# WIPP Thermodynamic Database: Am(III) Model

(IV-1) $AmCO_3^+ + H^+ = Am^{3+} + HCO_3^-$

(IV-2) $Am(CO_3)_2^- + 2H^+ = Am^{3+} + 2HCO_3^-$

(IV-3) $Am(CO_3)_3^{3-} + 3H^+ = Am^{3+} + 3HCO_3^-$

(IV-4) $Am(CO_3)_4^{5-} + 4H^+ = Am^{3+} + 4HCO_3^-$

(IV-5) $Am(OH)^{2+} + H^+ = Am^{3+} + H_2O$

(IV-6) $Am(OH)_2^+ + 2H^+ = Am^{3+} + 2H_2O$

(IV-7) $Am(OH)_3(aq) + 3H^+ = Am^{3+} + 3H_2O$

(IV-8) $AmCl^{2+} = Am^{3+} + Cl^-$

(IV-9) $AmCl_2^+ = Am^{3+} + 2Cl^-$

(IV-10) $AmSO_4^+ = Am^{3+} + SO_4^{2-}$

(IV-11) $Am(SO_4)_2^- = Am^{3+} + 2SO_4^{2-}$

Source:
Am(III) Model: Literature, PNNL, SNL (Craig Novak)

(IV-17) $AmOHCO_3(s) + 2H^+ = Am^{3+} + H_2O + HCO_3^-$

(IV-18) $Am(OH)_3(s) + 3H^+ = Am^{3+} + 3H_2O$

(IV-19) $NaAm(CO_3)_2 \bullet 6H_2O(s) + 2H^+ = Na^+ + Am^{3+} + 2HCO_3^- + 6H_2O$

(IV-20) $AmPO_4(cr) + H^+ = Am^{3+} + HPO_4^{2-}$

# WIPP Thermodynamic Database: Am(III) Model

(IV-1) $AmCO_3^+ + H^+ = Am^{3+} + HCO_3^-$

(IV-2) $Am(CO_3)_2^- + 2H^+ = Am^{3+} + 2HCO_3^-$

(IV-3) $Am(CO_3)_3^{3-} + 3H^+ = Am^{3+} + 3HCO_3^-$

(IV-4) $Am(CO_3)_4^{5-} + 4H^+ = Am^{3+} + 4HCO_3^-$

(IV-5) $Am(OH)^{2+} + H^+ = Am^{3+} + H_2O$

(IV-6) $Am(OH)_2^+ + 2H^+ = Am^{3+} + 2H_2O$

(IV-7) $Am(OH)_3(aq) + 3H^+ = Am^{3+} + 3H_2O$

(IV-8) $AmCl^{2+} = Am^{3+} + Cl^-$

(IV-9) $AmCl_2^+ = Am^{3+} + 2Cl^-$

(IV-10) $AmSO_4^+ = Am^{3+} + SO_4^{2-}$

(IV-11) $Am(SO_4)_2^- = Am^{3+} + 2SO_4^{2-}$

(IV-12) $AmAcetate^{2+} = Am^{3+} + Acetate^-$

(IV-13) $AmCitrate(aq) = Am^{3+} + Citrate^{3-}$

(IV-14) $AmEDTA^- = Am^{3+} + EDTA^{4-}$

(IV-15) $AmLactate^{2+} = Am^{3+} + Lactate^-$

(IV-16) $AmOxalate^+ = Am^{3+} + Oxalate^{2-}$

(IV-17) $AmOHCO_3(s) + 2H^+ = Am^{3+} + H_2O + HCO_3^-$

(IV-18) $Am(OH)_3(s) + 3H^+ = Am^{3+} + 3H_2O$

(IV-19) $NaAm(CO_3)_2 \cdot 6H_2O(s) + 2H^+ = Na^+ + Am^{3+} + 2HCO_3^- + 6H_2O$

(IV-20) $AmPO_4(cr) + H^+ = Am^{3+} + HPO_4^{2-}$

Source:
Am(III) Model: Literature, PNNL, SNL (Craig Novak)
Organics from FSU

# WIPP Thermodynamic Database: Am(III) Model

(IV-1) $AmCO_3^+ + H^+ = Am^{3+} + HCO_3^-$

(IV-2) $Am(CO_3)_2^- + 2H^+ = Am^{3+} + 2HCO_3^-$

(IV-3) $Am(CO_3)_3^{3-} + 3H^+ = Am^{3+} + 3HCO_3^-$

(IV-4) $Am(CO_3)_4^{5-} + 4H^+ = Am^{3+} + 4HCO_3^-$

(IV-5) $Am(OH)^{2+} + H^+ = Am^{3+} + H_2O$

(IV-6) $Am(OH)_2^+ + 2H^+ = Am^{3+} + 2H_2O$

(IV-7) $Am(OH)_3(aq) + 3H^+ = Am^{3+} + 3H_2O$

(IV-8) $AmCl^{2+} = Am^{3+} + Cl^-$

(IV-9) $AmCl_2^+ = Am^{3+} + 2Cl^-$

(IV-10) $AmSO_4^+ = Am^{3+} + SO_4^{2-}$

(IV-11) $Am(SO_4)_2^- = Am^{3+} + 2SO_4^{2-}$

(IV-12) $AmAcetate^{2+} = Am^{3+} + Acetate^-$

(IV-13) $AmCitrate(aq) = Am^{3+} + Citrate^{3-}$

(IV-14) $AmEDTA^- = Am^{3+} + EDTA^{4-}$

(IV-15) $AmLactate^{2+} = Am^{3+} + Lactate$

(IV-16) $AmOxalate^+ = Am^{3+} + Oxalate^{2-}$

(IV-17) $AmOHCO_3(s) + 2H^+ = Am^{3+} + H_2O + HCO_3^-$

(IV-18) $Am(OH)_3(s) + 3H^+ = Am^{3+} + 3H_2O$

(IV-19) $NaAm(CO_3)_2 \bullet 6H_2O(s) + 2H^+ = Na^+ + Am^{3+} + 2HCO_3^- + 6H_2O$

(IV-20) $AmPO_4(cr) + H^+ = Am^{3+} + HPO_4^{2-}$

(IV-21) $AmHB_4O_7^{2+} + 9H_2O = Am^{3+} + 4B(OH)_4^- + H^+$

Changes:
Aqueous species Am-Tetraborate Added
Revised $AmEDTA^-$

# WIPP Thermodynamic Database: Am(III) Model

(IV-1) $AmCO_3^+ + H^+ = Am^{3+} + HCO_3^-$

(IV-2) $Am(CO_3)_2^- + 2H^+ = Am^{3+} + 2HCO_3^-$

(IV-3) $Am(CO_3)_3^{3-} + 3H^+ = Am^{3+} + 3HCO_3^-$

(IV-4) $Am(CO_3)_4^{5-} + 4H^+ = Am^{3+} + 4HCO_3^-$

(IV-5) $Am(OH)^{2+} + H^+ = Am^{3+} + H_2O$

(IV-6) $Am(OH)_2^+ + 2H^+ = Am^{3+} + 2H_2O$

(IV-7) $Am(OH)_3(aq) + 3H^+ = Am^{3+} + 3H_2O$

(IV-8) $AmCl^{2+} = Am^{3+} + Cl^-$

(IV-9) $AmCl_2^+ = Am^{3+} + 2Cl^-$

(IV-10) $AmSO_4^+ = Am^{3+} + SO_4^{2-}$

(IV-11) $Am(SO_4)_2^- = Am^{3+} + 2SO_4^{2-}$

(IV-12) $AmAcetate^{2+} = Am^{3+} + Acetate^-$

(IV-13) $AmCitrate(aq) = Am^{3+} + Citrate^{3-}$

(IV-14) $AmEDTA^- = Am^{3+} + EDTA^{4-}$

(IV-15) $AmLactate^{2+} = Am^{3+} + Lactate^-$

(IV-16) $AmOxalate^+ = Am^{3+} + Oxalate^{2-}$

(IV-17) $AmOHCO_3(s) + 2H^+ = Am^{3+} + H_2O + HCO_3^-$

(IV-18) $Am(OH)_3(s) + 3H^+ = Am^{3+} + 3H_2O$

(IV-19) $NaAm(CO_3)_2 \bullet 6H_2O(s) + 2H^+ = Na^+ + Am^{3+} + 2HCO_3^- + 6H_2O$

(IV-20) $AmPO_4(cr) + H^+ = Am^{3+} + HPO_4^{2-}$

(IV-21) $Am(OH)_3(am) + 3H^+ = Am^{3+} + 3H_2O$

Source:
Am(III) Model: Literature, PNNL, SNL (Craig Novak)
Organics from FSU

*Issue 23*

# WIPP Thermodynamic Database: Th(IV) Model

(VI-1) $Th(CO_3)_5^{6-} + 5H^+ = Th^{4+} + 5HCO_3^-$

(VI-2) $Th(OH)_3(CO_3)^- + 4H^+ = Th^{4+} + 3H_2O + HCO_3^-$

(VI-3) $Th(OH)_4(aq) + 4H^+ = Th^{4+} + 4H_2O$

(VI-4) $Th(SO_4)_2(aq) = Th^{4+} + 2SO_4^{2-}$

(VI-5) $Th(SO_4)_3^{2-} = Th^{4+} + 3SO_4^{2-}$

Sources for Th(IV) Model:
Literature, PNNL, SNL (Craig Novak)

(VI-13) $ThO_2(am) + 4H^+ = Th^{4+} + 2H_2O$

(VI-14) $Th(SO_4)_2 \bullet 9H_2O(s) = Th^{4+} + 2SO_4^{2-} + 9H_2O$

(VI-15) $Th(SO_4)_2 \bullet 8H_2O(s) = Th^{4+} + 2SO_4^{2-} + 8H_2O$

(VI-16) $Th(SO_4)_2 \bullet Na_2SO_4 \bullet 6H_2O(s) = Th^{4+} + 3SO_4^{2-} + 2Na^+ + 6H_2O$

(VI-17) $Th(SO_4)_2 \bullet K_2SO_4 \bullet 4H_2O(s) = Th^{4+} + 3SO_4^{2-} + 2K^+ + 4H_2O$

(VI-18) $Th(SO_4)_2 \bullet 2K_2SO_4 \bullet 2H_2O(s) = Th^{4+} + 4SO_4^{2-} + 4K^+ + 2H_2O$

(VI-19) $2[Th(SO_4)_2 \bullet 7/2K_2SO_4(s)] = 2Th^{4+} + 11SO_4^{2-} + 14K^+$

# WIPP Thermodynamic Database: Th(IV) Model

(VI-1) $Th(CO_3)_5^{6-} + 5H^+ = Th^{4+} + 5HCO_3^-$

(VI-2) $Th(OH)_3(CO_3)^- + 4H^+ = Th^{4+} + 3H_2O + HCO_3^-$

(VI-3) $Th(OH)_4(aq) + 4H^+ = Th^{4+} + 4H_2O$

(VI-4) $Th(SO_4)_2(aq) = Th^{4+} + 2SO_4^{2-}$

(VI-5) $Th(SO_4)_3^{2-} = Th^{4+} + 3SO_4^{2-}$

(VI-13) $ThO_2(am) + 4H^+ = Th^{4+} + 2H_2O$

(VI-14) $Th(SO_4)_2 \bullet 9H_2O(s) = Th^{4+} + 2SO_4^{2-} + 9H_2O$

(VI-15) $Th(SO_4)_2 \bullet 8H_2O(s) = Th^{4+} + 2SO_4^{2-} + 8H_2O$

(VI-16) $Th(SO_4)_2 \bullet Na_2SO_4 \bullet 6H_2O(s) = Th^{4+} + 3SO_4^{2-} + 2Na^+ + 6H_2O$

(VI-17) $Th(SO_4)_2 \bullet K_2SO_4 \bullet 4H_2O(s) = Th^{4+} + 3SO_4^{2-} + 2K^+ + 4H_2O$

(VI-18) $Th(SO_4)_2 \bullet 2K_2SO_4 \bullet 2H_2O(s) = Th^{4+} + 4SO_4^{2-} + 4K^+ + 2H_2O$

(VI-19) $2[Th(SO_4)_2 \bullet 7/2K_2SO_4(s)] = 2Th^{4+} + 11SO_4^{2-} + 14K^+$

Sources for Th(IV) Model: Literature, PNNL, SNL (Craig Novak)

*Issue 18: We already used Felmy (1991) to parameterize $\mu^0/RT$ for $Th(OH)_4(aq)$ – Giambalvo did it for CRA 2004*

*Issue 19: Rai et al. (1997) was used for Pitzer parameters for Reaction 13 – therefore the data cannot be used for uncertainty quantification.*

*Issue 20: Altmaier (2005 & 2006) cannot be used for current model because solutions were submitted to ultracentrifugation. May be valuable for re-parameterization for +IV for 2024.*

# WIPP Thermodynamic Database: Th(IV) Model

(VI-1) $Th(CO_3)_5^{6-} + 5H^+ = Th^{4+} + 5HCO_3^-$

(VI-2) $Th(OH)_3(CO_3)^- + 4H^+ = Th^{4+} + 3H_2O + HCO_3^-$

(VI-3) $Th(OH)_4(aq) + 4H^+ = Th^{4+} + 4H_2O$

(VI-4) $Th(SO_4)_2(aq) = Th^{4+} + 2SO_4^{2-}$

(VI-5) $Th(SO_4)_3^{2-} = Th^{4+} + 3SO_4^{2-}$

(VI-6) $ThAcetate^{3+} = Th^{4+} + Acetate^-$

(VI-7) $Th(Acetate)_2^{2+} = Th^{4+} + 2Acetate^-$

(VI-8) $ThCitrate^+ = Th^{4+} + Citrate^{3-}$

(VI-9) $ThEDTA(aq) = Th^{4+} + EDTA^{4-}$

(VI-10) $ThLactate^{3+} = Th^{4+} + Lactate^-$

(VI-11) $Th(Lactate)_2^{2+} = Th^{4+} + 2Lactate^-$

(VI-12) $ThOxalate^{2+} = Th^{4+} + Oxalate^{2-}$

(VI-13) $ThO_2(am) + 4H^+ = Th^{4+} + 2H_2O$

(VI-14) $Th(SO_4)_2 \bullet 9H_2O(s) = Th^{4+} + 2SO_4^{2-} + 9H_2O$

(VI-15) $Th(SO_4)_2 \bullet 8H_2O(s) = Th^{4+} + 2SO_4^{2-} + 8H_2O$

(VI-16) $Th(SO_4)_2 \bullet Na_2SO_4 \bullet 6H_2O(s) = Th^{4+} + 3SO_4^{2-} + 2Na^+ + 6H_2O$

(VI-17) $Th(SO_4)_2 \bullet K_2SO_4 \bullet 4H_2O(s) = Th^{4+} + 3SO_4^{2-} + 2K^+ + 4H_2O$

(VI-18) $Th(SO_4)_2 \bullet 2K_2SO_4 \bullet 2H_2O(s) = Th^{4+} + 4SO_4^{2-} + 4K^+ + 2H_2O$

(VI-19) $2[Th(SO_4)_2 \bullet 7/2K_2SO_4(s)] = 2Th^{4+} + 11SO_4^{2-} + 14K^+$

Sources for Th(IV) Model:
Literature, PNNL, SNL (Craig Novak)
Organics from FSU

# WIPP Thermodynamic Database: Th(IV) Model

(VI-1) $Th(CO_3)_5^{6-} + 5H^+ = Th^{4+} + 5HCO_3^-$

(VI-2) $Th(OH)_3(CO_3)^- + 4H^+ = Th^{4+} + 3H_2O + HCO_3^-$

(VI-3) $Th(OH)_4(aq) + 4H^+ = Th^{4+} + 4H_2O$

(VI-4) $Th(SO_4)_2(aq) = Th^{4+} + 2SO_4^{2-}$

(VI-5) $Th(SO_4)_3^{2-} = Th^{4+} + 3SO_4^{2-}$

(VI-6) $ThAcetate^{3+} = Th^{4+} + Acetate^-$

(VI-7) $Th(Acetate)_2^{2+} = Th^{4+} + 2Acetate^-$

(VI-8) $ThCitrate^+ = Th^{4+} + Citrate^{3-}$

(VI-9) $ThEDTA(aq) = Th^{4+} + EDTA^{4-}$

(VI-10) $ThLactate^{3+} = Th^{4+} + Lactate^-$

(VI-11) $Th(Lactate)_2^{2+} = Th^{4+} + 2Lactate^-$

(VI-12) $ThOxalate^{2+} = Th^{4+} + Oxalate^{2-}$

(VI-13) $ThO_2(am) + 4H^+ = Th^{4+} + 2H_2O$

(VI-14) $Th(SO_4)_2 \bullet 9H_2O(s) = Th^{4+} + 2SO_4^{2-} + 9H_2O$

(VI-15) $Th(SO_4)_2 \bullet 8H_2O(s) = Th^{4+} + 2SO_4^{2-} + 8H_2O$

(VI-16) $Th(SO_4)_2 \bullet Na_2SO_4 \bullet 6H_2O(s) = Th^{4+} + 3SO_4^{2-} + 2Na^+ + 6H_2O$

(VI-17) $Th(SO_4)_2 \bullet K_2SO_4 \bullet 4H_2O(s) = Th^{4+} + 3SO_4^{2-} + 2K^+ + 4H_2O$

(VI-18) $Th(SO_4)_2 \bullet 2K_2SO_4 \bullet 2H_2O(s) = Th^{4+} + 4SO_4^{2-} + 4K^+ + 2H_2O$

(VI-19) $2[Th(SO_4)_2 \bullet 7/2K_2SO_4(s)] = 2Th^{4+} + 11SO_4^{2-} + 14K^+$

Changes: $\mu^0/RT$ = -622.4700 for $Th(OH)_4(aq)$ (Giambalvo 2002). Novak (2005) revised it as -626.5853 *cf.* -626.921 ± 2.678 (NEA, 2008)

*Issue 17: Justification Needed*
*Appendix GEOCHEM*

# WIPP Thermodynamic Database: Np(V) Model

(VII-1) $NpO_2CO_3^- + H^+ = NpO_2^+ + HCO_3^-$

(VII-2) $NpO_2(CO_3)_2^{3-} + 2H^+ = NpO_2^+ + 2HCO_3^-$

(VII-3) $NpO_2(CO_3)_3^{5-} + 3H^+ = NpO_2^+ + 3HCO_3^-$

(VII-4) $NpO_2(OH)(aq) + H^+ = NpO_2^+ + H_2O$

(VII-5) $NpO_2(OH)_2^- + 2H^+ = NpO_2^+ + 2H_2O$

Sources for Np(V) Model: Literature, LBNL, SNL (Craig Novak)

(VII-13) $NpO_2OH(aged) + H^+ = NpO_2^+ + H_2O$

(VII-14) $NpO_2OH(am) + H^+ = NpO_2^+ + H_2O$

(VII-15) $2[NaNpO_2CO_3 \bullet 7/2H_2O](s) + 2H^+ = 2NpO_2^+ + 2HCO_3^- + 2Na^+ + 7H_2O$

(VII-16) $Na_3NpO_2(CO_3)_2(s) + 2H^+ = NpO_2^+ + 2HCO_3^- + 3Na^+$

(VII-17) $KNpO_2CO_3(s) + H^+ = NpO_2^+ + HCO_3^- + K^+$

(VII-18) $K_3NpO_2(CO_3)_2(s) + 2H^+ = NpO_2^+ + 2HCO_3^- + 3K^+$

# WIPP Thermodynamic Database: Np(V) Model

(VII-1) $NpO_2CO_3^- + H^+ = NpO_2^+ + HCO_3^-$

(VII-2) $NpO_2(CO_3)_2^{3-} + 2H^+ = NpO_2^+ + 2HCO_3^-$

(VII-3) $NpO_2(CO_3)_3^{5-} + 3H^+ = NpO_2^+ + 3HCO_3^-$

(VII-4) $NpO_2(OH)(aq) + H^+ = NpO_2^+ + H_2O$

(VII-5) $NpO_2(OH)_2^- + 2H^+ = NpO_2^+ + 2H_2O$

(VII-6) $NpO_2Acetate(aq) = NpO_2^+ + Acetate^-$

(VII-7) $NpO_2Citrate^{2-} = NpO_2^+ + Citrate^{3-}$

(VII-8) $NpO_2H_2EDTA^- = NpO_2^+ + EDTA^{4-} + 2H^+$

(VII-9) $NpO_2HEDTA^{2-} = NpO_2^+ + EDTA^{4-} + H^+$

(VII-10) $NpO_2EDTA^{3-} = NpO_2^+ + EDTA^{4-}$

(VII-11) $NpO_2Lactate(aq) = NpO_2^+ + Lactate^-$

(VII-12) $NpO_2Oxalate^- = NpO_2^+ + Oxalate^{2-}$

(VII-13) $NpO_2OH(aged) + H^+ = NpO_2^+ + H_2O$

(VII-14) $NpO_2OH(am) + H^+ = NpO_2^+ + H_2O$

(VII-15) $2[NaNpO_2CO_3 \bullet 7/2H_2O](s) + 2H^+ = 2NpO_2^+ + 2HCO_3^- + 2Na^+ + 7H_2O$

(VII-16) $Na_3NpO_2(CO_3)_2(s) + 2H^+ = NpO_2^+ + 2HCO_3^- + 3Na^+$

(VII-17) $KNpO_2CO_3(s) + H^+ = NpO_2^+ + HCO_3^- + K^+$

(VII-18) $K_3NpO_2(CO_3)_2(s) + 2H^+ = NpO_2^+ + 2HCO_3^- + 3K^+$

Sources for Np(V) Model: Literature, LBNL, SNL (Craig Novak)
Organics: FSU

# WIPP Thermodynamic Database: U(VI) Model

## U(VI) Value: Set to ~$10^{-5}$ M

Source: Hobart and Moore (1996)

# WIPP Thermodynamic Database: U(VI) Model

## U(VI) Value: Set to ~$10^{-5}$ M

Source: Hobart and Moore (1996)

Changes:
EPA mandated the value of $10^{-3}$ M after CRA-2004

# WIPP Thermodynamic Database: Lead Chemistry

Appendix A, Table 8. Reactions Included in DATA0.FM2 for Pb Species

| | |
|---|---|
| (VIII-1) | $Pb^{2+} + Cl^- = PbCl^+$ |
| (VIII-2) | $Pb^{2+} + 2Cl^- = PbCl_2(aq)$ |
| (VIII-3) | $Pb^{2+} + 3Cl^- = PbCl_3^-$ |
| (VIII-4) | $Pb^{2+} + Oxalate^{2-} = PbOxalate(aq)$ |
| (VIII-5) | $Pb^{2+} + 2Oxalate^{2-} = Pb(Oxalate)_2^{2-}$ |
| (VIII-6) | $Pb^{2+} + CO_3^{2-} = PbCO_3(aq)$ |
| (VIII-7) | $Pb^{2+} + 2CO_3^{2-} = Pb(CO_3)_2^{2-}$ |
| (VIII-8) | $Pb^{2+} + CO_3^{2-} + Cl^- = Pb(CO_3)Cl^-$ |
| (VIII-9) | $Pb^{2+} + H_2O(l) \rightleftarrows PbOH^+ + H^+$ |
| (VIII-10) | $Pb^{2+} + 2H_2O(l) \rightleftarrows Pb(OH)_2(aq) + 2H^+$ |
| (VIII-11) | $Pb^{2+} + 3H_2O(l) \rightleftarrows Pb(OH)_3^- + 3H^+$ |
| (VIII-12) | $PbB_4O_7(aq) + 9H_2O(l) \rightleftarrows Pb^{2+} + 4B(OH)_4^- + 2H^+$ |
| (VIII-13) | $PbB(OH)_4^+ \rightleftarrows Pb^{2+} + B(OH)_4^-$ |
| (VIII-14) | $Pb[B(OH)_4]_2(aq) \rightleftarrows Pb^{2+} + 2B(OH)_4^-$ |
| (VIII-15) | $Pb^{2+} + EDTA^{4-} = PbEDTA^{2-}$ |
| (VIII-16) | $Pb^{2+} + Citrate^{3-} = PbCitrate^-$ |
| (VIII-17) | $PbOxalate(cr) = Pb^{2+} + Oxalate^{2-}$ |
| (VIII-18) | $PbCO_3(cerussite) = Pb^{2+} + CO_3^{2-}$ |
| (VIII-19) | $PbO(litharge) + 2H^+ = Pb^{2+} + H_2O$ |
| (VIII-20) | $Pb(BO_2)_2 \cdot H_2O + 3H_2O(l) \rightleftarrows Pb^{2+} + 2B(OH)_4^-$ |

Sources:

Lead chloride species:

Millero and Byrne (1984), Felmy et al. (2000)

Pb Oxalate species:

Xiong et al. (2013)

Lead carbonate species:

Easley and Byrne (2011), Woosley and Millero (2013) Xiong (2015)

Pb Borate species: Xiong (2015)

Pb EDTA: Xiong et al. (2017)

Pb Citrate: Xiong et al. (2017)

Back:

# WIPP Thermodynamic Database: Lead Chemistry

Appendix A, Table 8. Reactions Included in DATA0.FM2 for Pb Species

| | |
|---|---|
| (VIII-1) | $Pb^{2+} + Cl^- \rightleftarrows PbCl^+$ |
| (VIII-2) | $Pb^{2+} + 2Cl^- \rightleftarrows PbCl_2(aq)$ |
| (VIII-3) | $Pb^{2+} + 3Cl^- \rightleftarrows PbCl_3^-$ |
| (VIII-4) | $Pb^{2+} + Oxalate^{2-} \rightleftarrows PbOxalate(aq)$ |
| (VIII-5) | $Pb^{2+} + 2Oxalate^{2-} \rightleftarrows Pb(Oxalate)_2^{2-}$ |
| (VIII-6) | $Pb^{2+} + CO_3^{2-} \rightleftarrows PbCO_3(aq)$ |
| (VIII-7) | $Pb^{2+} + 2CO_3^{2-} \rightleftarrows Pb(CO_3)_2^{2-}$ |
| (VIII-8) | $Pb^{2+} + CO_3^{2-} + Cl^- \rightleftarrows Pb(CO_3)Cl^-$ |
| (VIII-9) | $Pb^{2+} + H_2O(l) \rightleftarrows PbOH^+ + H^+$ |
| (VIII-10) | $Pb^{2+} + 2H_2O(l) \rightleftarrows Pb(OH)_2(aq) + 2H^+$ |
| (VIII-11) | $Pb^{2+} + 3H_2O(l) \rightleftarrows Pb(OH)_3^- + 3H^+$ |
| (VIII-12) | $PbB_4O_7(aq) + 9H_2O(l) \rightleftarrows Pb^{2+} + 4B(OH)_4^- + 2H^+$ |
| (VIII-13) | $PbB(OH)_4^+ \rightleftarrows Pb^{2+} + B(OH)_4^-$ |
| (VIII-14) | $Pb[B(OH)_4]_2(aq) \rightleftarrows Pb^{2+} + 2B(OH)_4^-$ |
| (VIII-15) | $Pb^{2+} + EDTA^{4-} \rightleftarrows PbEDTA^{2-}$ |
| (VIII-16) | $Pb^{2+} + Citrate^{3-} \rightleftarrows PbCitrate^-$ |
| (VIII-17) | $PbOxalate(cr) \rightleftarrows Pb^{2+} + Oxalate^{2-}$ |
| (VIII-18) | $PbCO_3(cerussite) \rightleftarrows Pb^{2+} + CO_3^{2-}$ |
| (VIII-19) | $PbO(litharge) + 2H^+ \rightleftarrows Pb^{2+} + H_2O$ |
| (VIII-20) | $Pb(BO_2)_2 \cdot H_2O + 3H_2O(l) \rightleftarrows Pb^{2+} + 2B(OH)_4^-$ |
| (VIII-21) | $PbS(galena) + H^+ \rightleftarrows Pb^{2+} + HS^-$ |

Sources:

Lead chloride species:

Millero and Byrne (1984), Felmy et al. (2000)

Pb Oxalate species:

Xiong et al. (2013)

Lead carbonate species:

Easley and Byrne (2011), Woosley and Millero (2013) Xiong (2015)

Pb Borate species: Xiong (2015)

Pb EDTA: Xiong et al. (2017)

Pb Citrate: Xiong et al. (2017)

Changes: DATA0.FM3

Added Galena

# WIPP Thermodynamic Database: Iron Chemistry

(IX-1) $FeOH^{+} + H^{+} = Fe^{2+} + H_2O$

(IX-2) $Fe(OH)_2(aq) + 2H^{+} = Fe^{2+} + 2H_2O$

(IX-3) $Fe(OH)_3^{-} + 3H^{+} = Fe^{2+} + 3H_2O$

(IX-4) $Fe(OH)_4^{2-} + 4H^{+} = Fe^{2+} + 4H_2O$

(IX-5) $FeCO_3(aq) + H^{+} = Fe^{2+} + HCO_3^{-}$

(IX-6) $Fe(CO_3)_2^{-2} + 2H^{+} = Fe^{2+} + 2HCO_3^{-}$

(IX-7) $Fe(OH)_2(s) + 2H^{+} = Fe^{2+} + 2H_2O$

(IX-8) $Fe_2Cl(OH)_3(hibbingite) + 3H^{+} = 2Fe^{2+} + Cl^{-} + 3H_2O$

(IX-9) $FeCO_3(siderite) + H^{+} = Fe^{2+} + HCO_3^{-}$

(IX-11) $Fe_2CO_3(OH)_2(siderite) + 3H^{+} = 2Fe^{2+} + HCO_3^{-} + 2H_2O$

(IX-12) $FeOxalate(aq) = Fe^{2+} + Oxalate^{2-}$

(IX-13) $Fe(Oxalate)_2^{-2} = Fe^{+2} + 2Oxalate^{-2}$

(IX-14) $FeHEDTA^{-} = Fe^{+2} + H^{+} + EDTA^{-4}$

(IX-15) $FeEDTA^{2-} = Fe^{2+} + EDTA^{4-}$

(IX-16) $FeOHEDTA^{-3} + H^{+} = Fe^{+2} + EDTA^{-4} + H_2O$

(IX-17) $Fe(OH)_2EDTA^{-4} + 2H^{+} = Fe^{+2} + EDTA^{-4} + 2H_2O$

(IX-19) $FeOHCitrate^{-2} + H^{+} = Fe^{2+} + Citrate^{3-} + H_2O$

(IX-20) $FeCitrate^{-} = Fe^{2+} + Citrate^{3-}$

(IX-21) $FeHCitrate(aq) = Fe^{2+} + H^{+} + Citrate^{3-}$

(IX-22) $FeOxalate.2H_2O(s) = Fe^{2+} + Oxalate^{2-} + 2H_2O$

(IX-23) $FeSO_4(s) = Fe^{2+} + SO_4^{2-}$

Back:

Sandia National Laboratories

# Issue 21: Hydromagnesite

Selection of the value for hydromagnesite:

- The value from Xiong (2011), which is similar to that of Konigsberger et al. (1992), ***versus*** the values from Robie and Hemingway (1973), Berninger et al. (2014), Gautier et al. (2014). [Notice that Berninger et al. (2014), Gautier et al. (2014) were from the same research group.]
- DOE's evaluation: The values from Xiong (2011) and Konigsberger et al. (1992) are consistent with geological field observations, whereas those from Robie and Hemingway contradict with geological field observations.
- DOE's position: Selection of the value from Xiong (2011).

---


Berninger, U.N., Jordan, G., Schott, J. and Oelkers, E.H., 2014. The experimental determination of hydromagnesite precipitation rates at 22.5–75° C. *Mineralogical Magazine*, *78*(6), pp.1405-1416.

Gautier, Q., Bénézeth, P., Mavromatis, V. and Schott, J., 2014. Hydromagnesite solubility product and growth kinetics in aqueous solution from 25 to 75 C. *Geochimica et Cosmochimica Acta*, *138*, pp.1-20.

Königsberger, E., Schmidt, P., and Gamsjäger, H., 1992. Solid-solute phase equilibria in aqueous solution. VI. Solubilities, complex formation, and ion-interaction parameters for the system $Na^{+}$–$Mg^{2+}$–$ClO_4$–$CO_2$–$H_2O$ at 25°C. Journal of Solution Chemistry, 21: 1195–1216.

Robie, R.A. and Hemingway, B.S., 1973. The enthalpies of formation of nesquehonite, MgCO3· 3H2O, and hydromagnesite, 5MgO· 4CO2· 5H2O. *Journal of Research of the US Geological Survey*, *1*, pp.543-547.

Xiong, Y. 2011. Experimental determination of solubility constant of hydromagnesite (5424) in NaCl solutions up to 4.4 m at room temperature. Chemical Geology 284:262-269.

# Issue 21: Hydromagnesite

DOE selects the solubility constant from Xiong (2011) for DATA0.FM2, because that value:

- ✓ Correctly predicts the saturation states for natural lakes in which hydromagnesite forms, and therefore is consistent with geological field observations
- ✓ Consequently, reliably predicts the correct near-field geochemical conditions for the WIPP, a geological repository
- ✓ The selection of recent data is aligned with FR Notice
  - ✓ "The DOE's updates of the chemical database for future performance assessments should more comprehensively incorporate recent data."

# Issue 21: Hydromagnesite

DOE selects the solubility constant from Xiong (2011) for DATA0.FM2, because that value:

- ✓ Has been widely used in various research investigations outside the WIPP project subsequently after its publication (e.g, Hollingbery 2011; Hollingbery and Hull 2012; Wang and Li 2012; Chaka and Felmy 2014; Chen et al. 2014; Shalabi-Navid et al. 2014; Shalabi-Navid 2015; Harriharan and Mazzotti 2016; Harriharan and Mazzotti 2017).

---


Chaka, A.M. and Felmy, A.R., 2014. Ab initio thermodynamic model for magnesium carbonates and hydrates. *The Journal of Physical Chemistry A*, *118*(35), pp.7469-7488.

Chen, M., Felmy, A.R. and Dixon, D.A., 2014. Structures and Stabilities of $(MgO)_n$ Nanoclusters. *The Journal of Physical Chemistry A*, *118*(17), pp.3136-3146.

Hariharan, S. and Mazzotti, M., 2016. Growth Kinetics of Synthetic Hydromagnesite at 90°C. *Crystal Growth & Design*, *17*(1), pp.317-327.

Hariharan, S. and Mazzotti, M., 2017. Kinetics of flue gas $CO_2$ mineralization processes using partially dehydroxylated lizardite. *Chemical Engineering Journal*, *324*, pp.397-413.

Hollingbery, L.A., 2011. *Decomposition and Fire Retardancy of Naturally Occurring Mixtures of Huntite and Hydromagnesite* (Doctoral dissertation, University of Central Lancashire).

Hollingbery, L.A. and Hull, T.R., 2012. The thermal decomposition of natural mixtures of huntite and hydromagnesite. *Thermochimica acta*, *528*, pp.45-52.

Shahabi-Navid, M., 2015. *Atmospheric Corrosion of Mg and MgAl Alloys: Characterization and Mechanisms*. Chalmers University of Technology.

Shahabi-Navid, M., Esmaily, M., Svensson, J.E., Halvarsson, M., Nyborg, L., Cao, Y. and Johansson, L.G., 2014. NaCl-induced atmospheric corrosion of the MgAl alloy AM50-the influence of $CO_2$. *Journal of The Electrochemical Society*, *161*(6), pp.C277-C287.

Wang, J. and Li, Z., 2012. Crystallization and Agglomeration Kinetics of Hydromagnesite in the Reactive System $MgCl_2$–$Na_2CO_3$–NaOH–$H_2O$. *Industrial & Engineering Chemistry Research*, *51*(23), pp.7874-7883.

Sandia National Laboratories

# Issue 21: Hydromagnesite

The values from Robie and Hemingway (1973), Gautier et al. (2014) and Berninger et al. (2014) are similar, and may suffer various shortcomings. [Notice that Gautier et al. (2014) and Berninger et al. (2014) were from the same research group.] Using the value from Berninger et al. (2014) as an example, they

- Incorrectly predict that natural lakes in which hydromagnesite forms are strongly undersaturated with respect to hydromagnesite, and therefore directly contradict with geological field observations.
- These values are inconsistent with independent experimental solubility data for hydromagnensite.

Consequently, using any of these values will lead to the incorrect representations of near-field geochemical conditions for the WIPP.

# Issue 21: Hydromagnesite

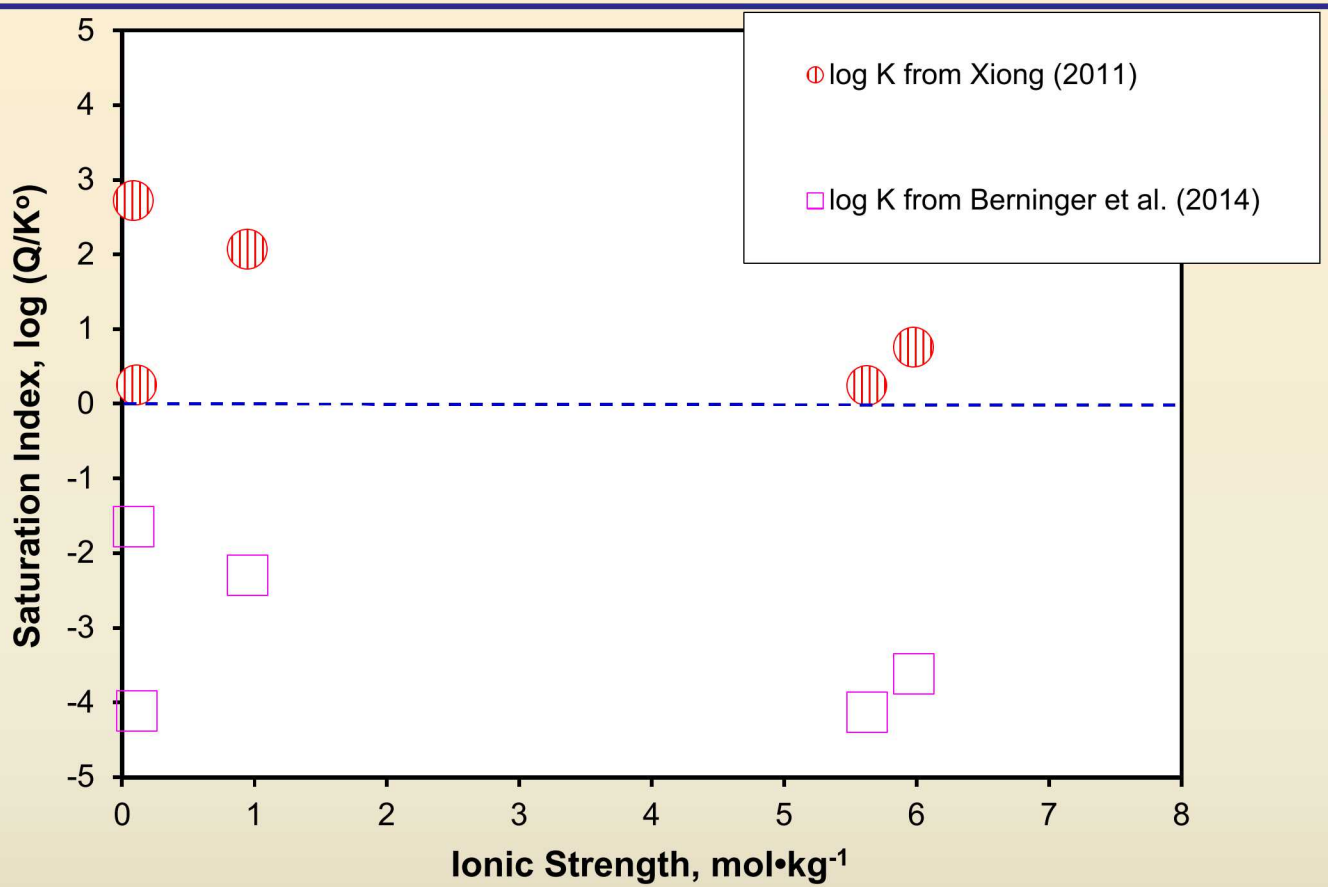


Figure 1. A plot showing saturation indices of hydromagnesite for the carbonate lakes in Qinghai-Xizang Plateau, China, based on the solubility constants of hydromagnesite, from Xiong (2011) on synthetic hydromagnesite, and from Berninger et al. (2014). The hydrochemical data are from Zheng and Liu (2009) (reproduced from Xiong and Cetiner 2017). Hydromagnesite forms in these lakes.

Log (Q/K) = 0 , saturation equilibrium. log(Q/K) > 0, precipitation; log(Q/K) < 0, unstable, completely dissolved

# Issue 21: Hydromagnesite

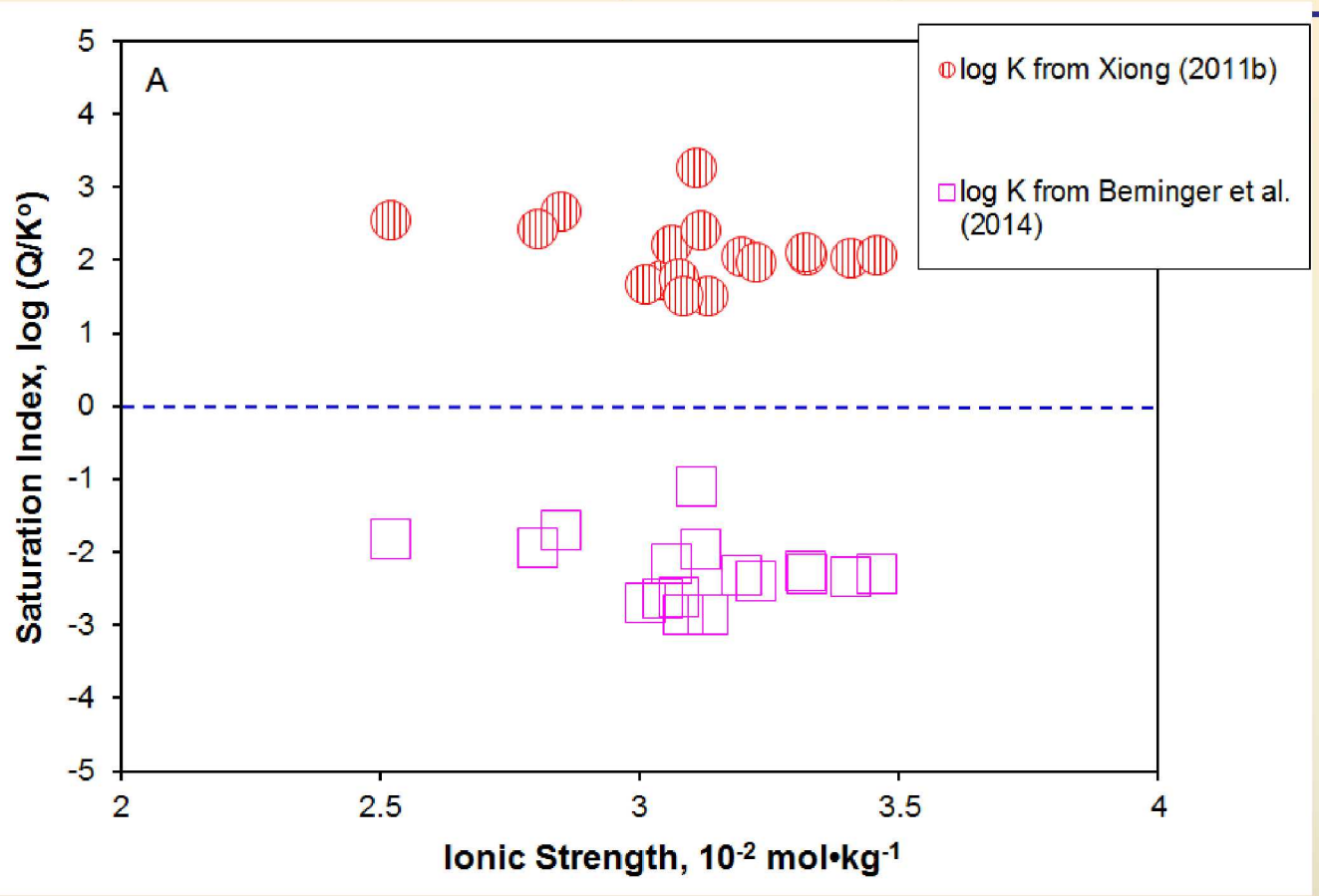


Figure 2. A plot showing saturation indices of hydromagnesite for the Salda Lake in Turkey, based on the solubility constants of hydromagnesite, from Xiong (2011) on synthetic hydromagnesite, and from Berninger et al. (2014). The hydrochemical data are from Sezer (2004) (reproduced from Xiong and Cetiner 2017). Hydromagnesite forms in this lake. Surface water.

Log (Q/K) = 0 , saturation equilibrium. log(Q/K) > 0, precipitation; log(Q/K) < 0, unstable, completely dissolved

# Issue 21: Hydromagnesite

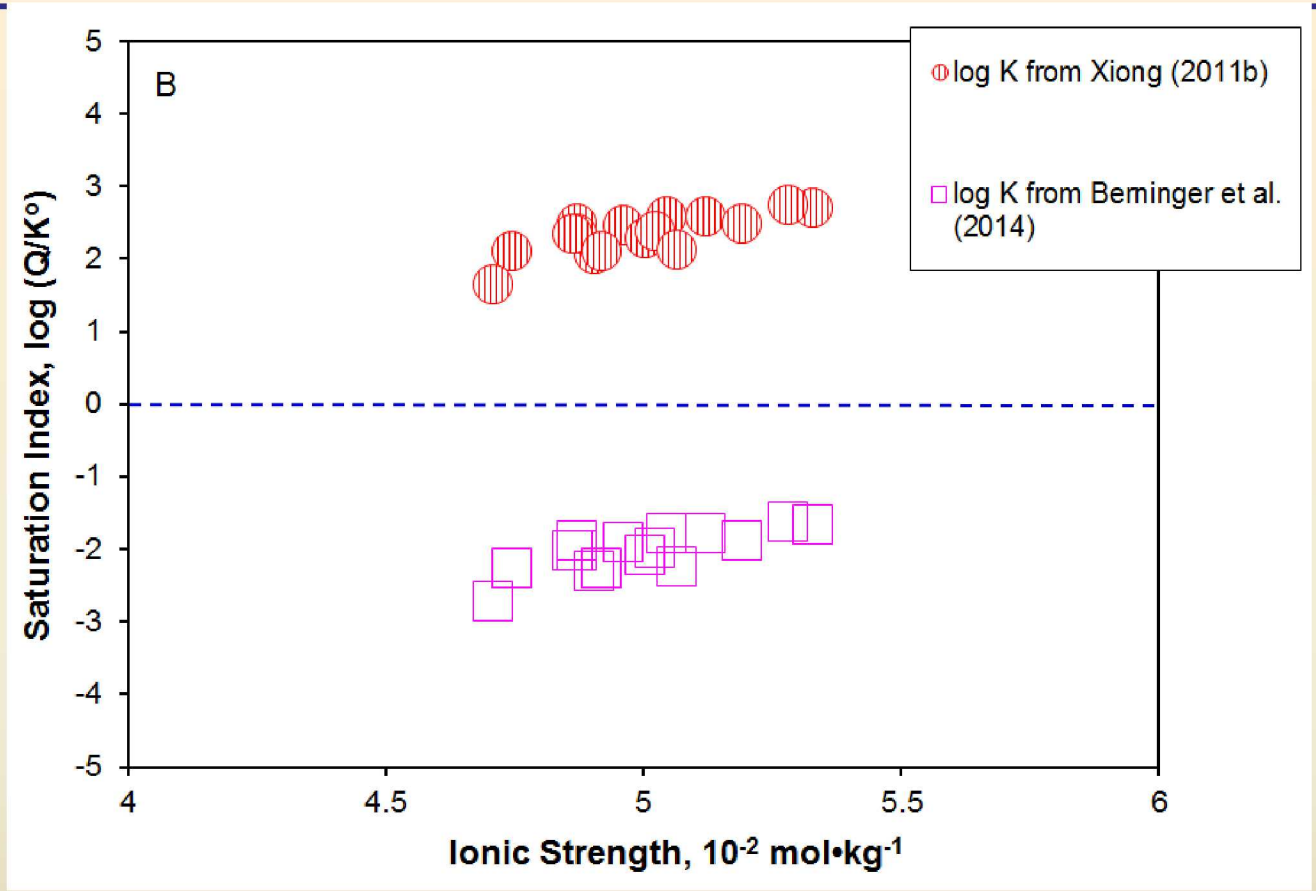


Figure 3. A plot showing saturation indices of hydromagnesite for the Salda Lake in Turkey, based on the solubility constants of hydromagnesite, from Xiong (2011) on synthetic hydromagnesite, and from Berninger et al. (2014). The hydrochemical data are from Sezer (2004) (reproduced from Xiong and Cetiner 2017). Hydromagnesite forms in this lake. Water at 20 m below the surface.

Log (Q/K) = 0 , saturation equilibrium. log(Q/K) > 0, precipitation; log(Q/K) < 0, unstable, completely dissolved

# Issue 21: Hydromagnesite

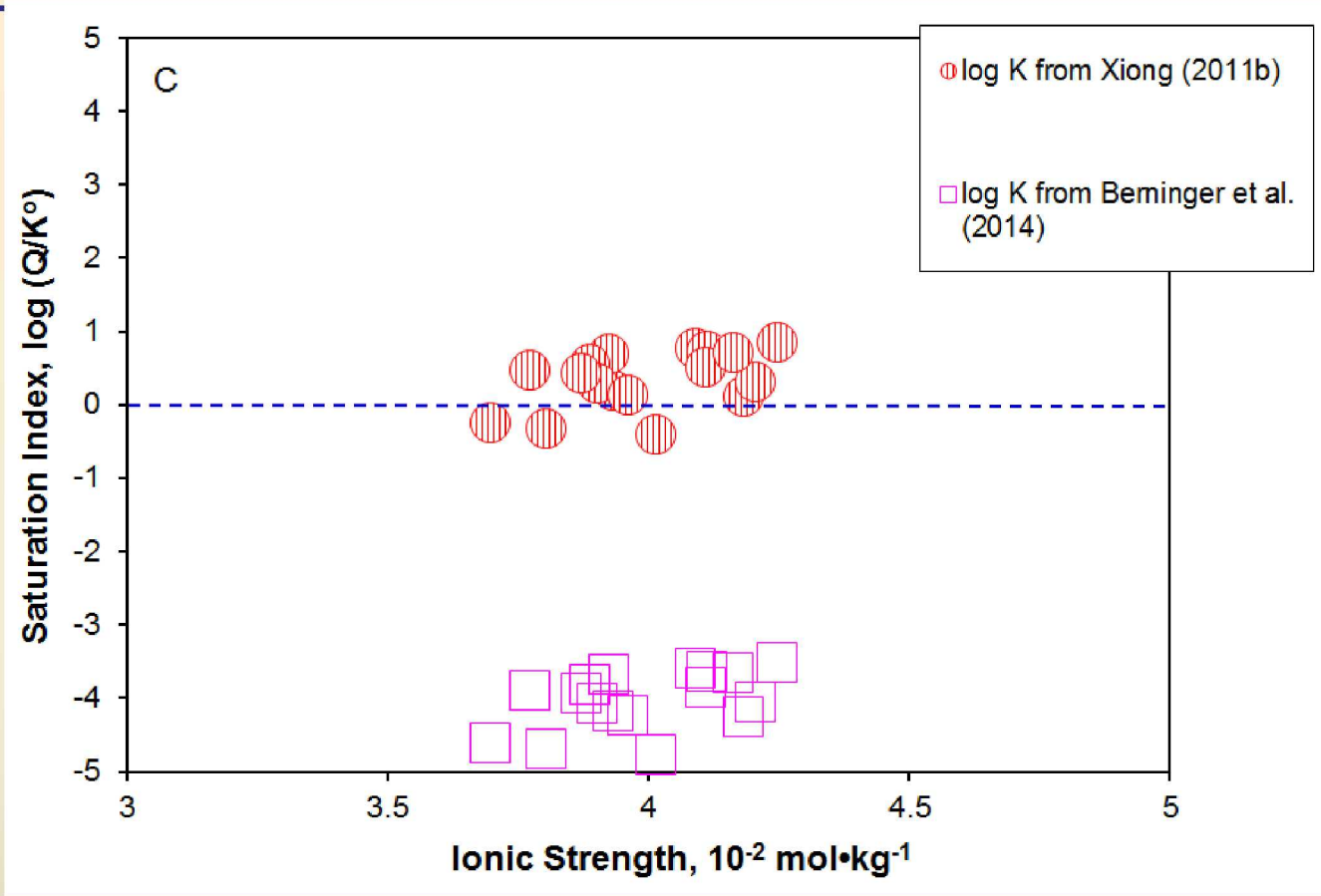


Figure 4. A plot showing saturation indices of hydromagnesite for the Salda Lake in Turkey, based on the solubility constants of hydromagnesite, from Xiong (2011) on synthetic hydromagnesite, and from Berninger et al. (2014). The hydrochemical data are from Sezer (2004) (reproduced from Xiong and Cetiner 2017). Hydromagnesite forms in this lake. Water at 40 m below surface.

Log (Q/K) = 0 , saturation equilibrium. log(Q/K) > 0, precipitation; log(Q/K) < 0, unstable, completely dissolved

# Issue 21: Hydromagnesite

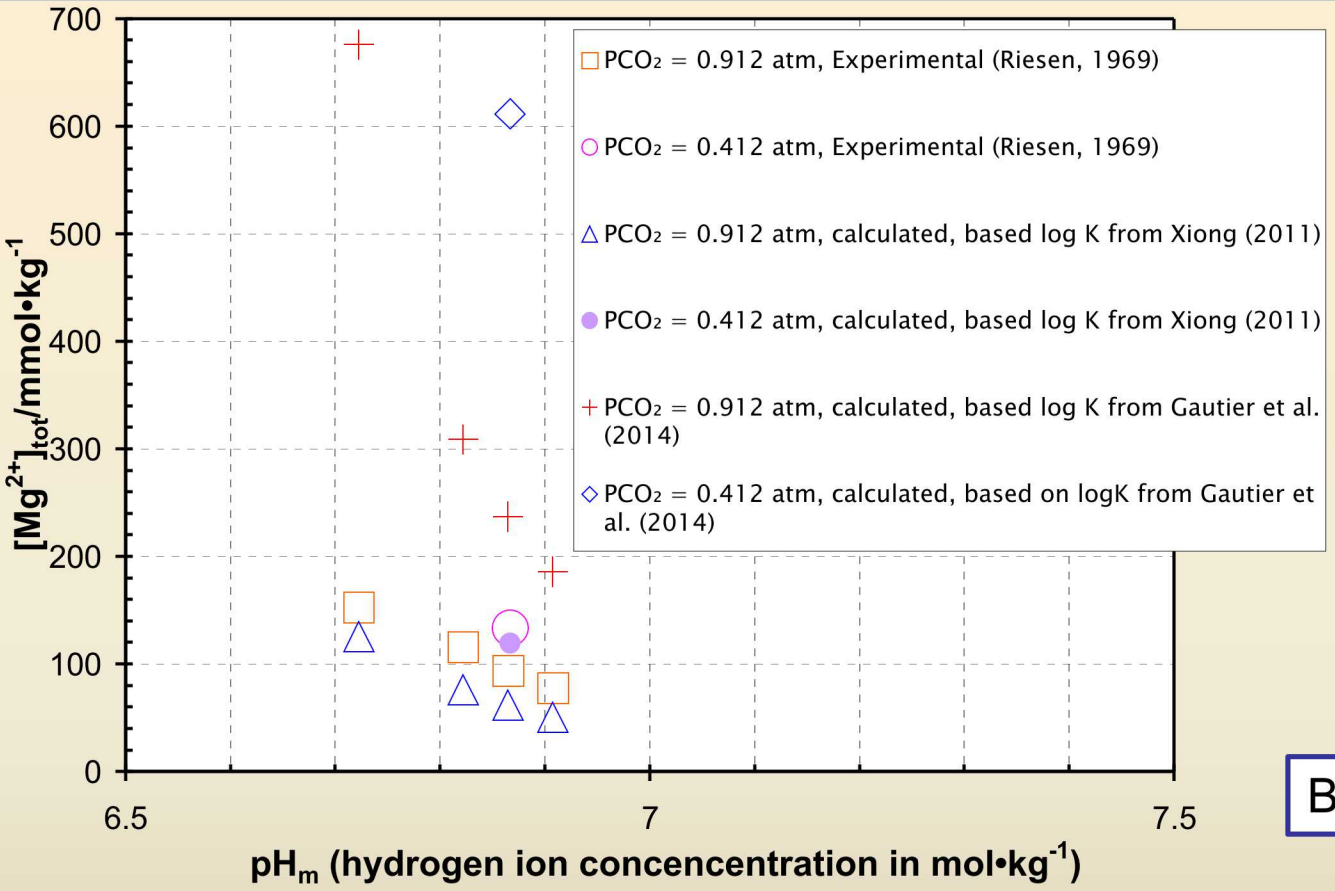


Back:

Figure 5. A plot showing the comparison of magnesium concentrations in equilibrium with hydromagnesite predicted by using the solubility product constants from Gautier et al. (2014) and from Xiong (2011) with the independent experimental values in 3.0 mol•kg$^{-1}$ $NaClO_4$ from Riesen (1969) (*reproduced from Xiong 2017).*

# Issue 22: $AmHB_4O_7^{2+}$

## New Stability Constant for $AmHB_4O_7^{2+}$ and Its associated Pitzer Parameters

$$Am^{3+} + 4B(OH)_4^- + H^+ \rightleftharpoons AmHB_4O_7^{2+} + 9H_2O$$

The equilibrium constant for above reaction and the Pitzer parameters associated with $AmHB_4O_7^{2+}$ , consistent with the speciation scheme of the WIPP thermodynamic database (Xiong, 2017), are incorporated into the DATA0.FM2, based on the raw solubility data on Nd(III) from Borkowski et al. (2010).

- ✓ Incorporation of Am will account for the contributions from $AmHB_4O_7^{2+}$ to ΣAm(III).

---

Borkowski, M., M. Richmann, D.T. Reed and Y. Xiong. 2010. Complexation of Nd(III) with tetraborate ion and its effect on actinide(III) solubility in WIPP brine. Radiochimica Acta 98:577-582.

Xiong, Y., 2017. Solution Chemistry for Actinide Borate Species to High Ionic Strengths: Equilibrium Constants for $AmHB_4O_7^{2+}$ and $AmB_9O_{13}(OH)_4$ (cr) and Their Importance to Nuclear Waste Management. *MRS Advances*, *2*(13), pp.741-746.

# Issue 22: $AmHB_4O_7^{2+}$

Table 2. Equilibrium constant for $AmHB_4O_7^{2+}$ at infinite dilution at 25 °C (298.15 K), and its associated Pitzer interaction parameters

| Reaction | | | log K at 25 °C | |
|---|---|---|---|---|
| $4B(OH)_4^- + 3H^+ + Am^{3+} \rightleftharpoons AmHB_4O_7^{2+} + 9H_2O(l)$ | | | 37.3416 | |
| Pitzer Binary Interaction Cofficients | | | | |
| Species *i* | Species *j* | $\beta^{(0)}$ | $\beta^{(1)}$ | $C^{\phi}$ |
| $AmHB_4O_7^{2+}$ | $Cl^-$ | 0.9163 | 1.74 | 0 |

# Issue 22: $AmHB_4O_7^{2+}$

## Speciation of Am(III) in NaCl in the Presence of Borate

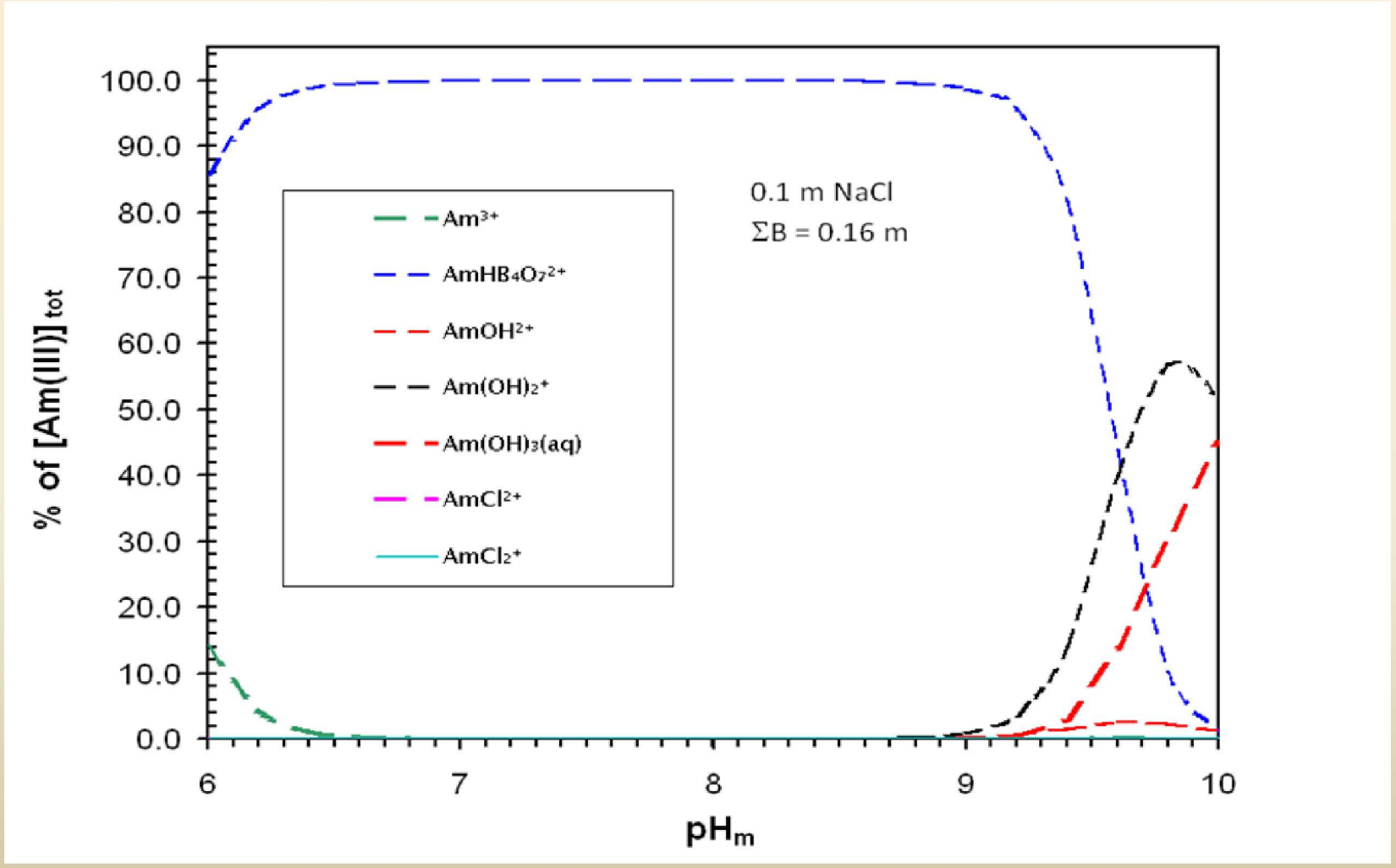

# Issue 22: $AmHB_4O_7^{2+}$

## Speciation of Am(III) in NaCl in the Presence of Borate

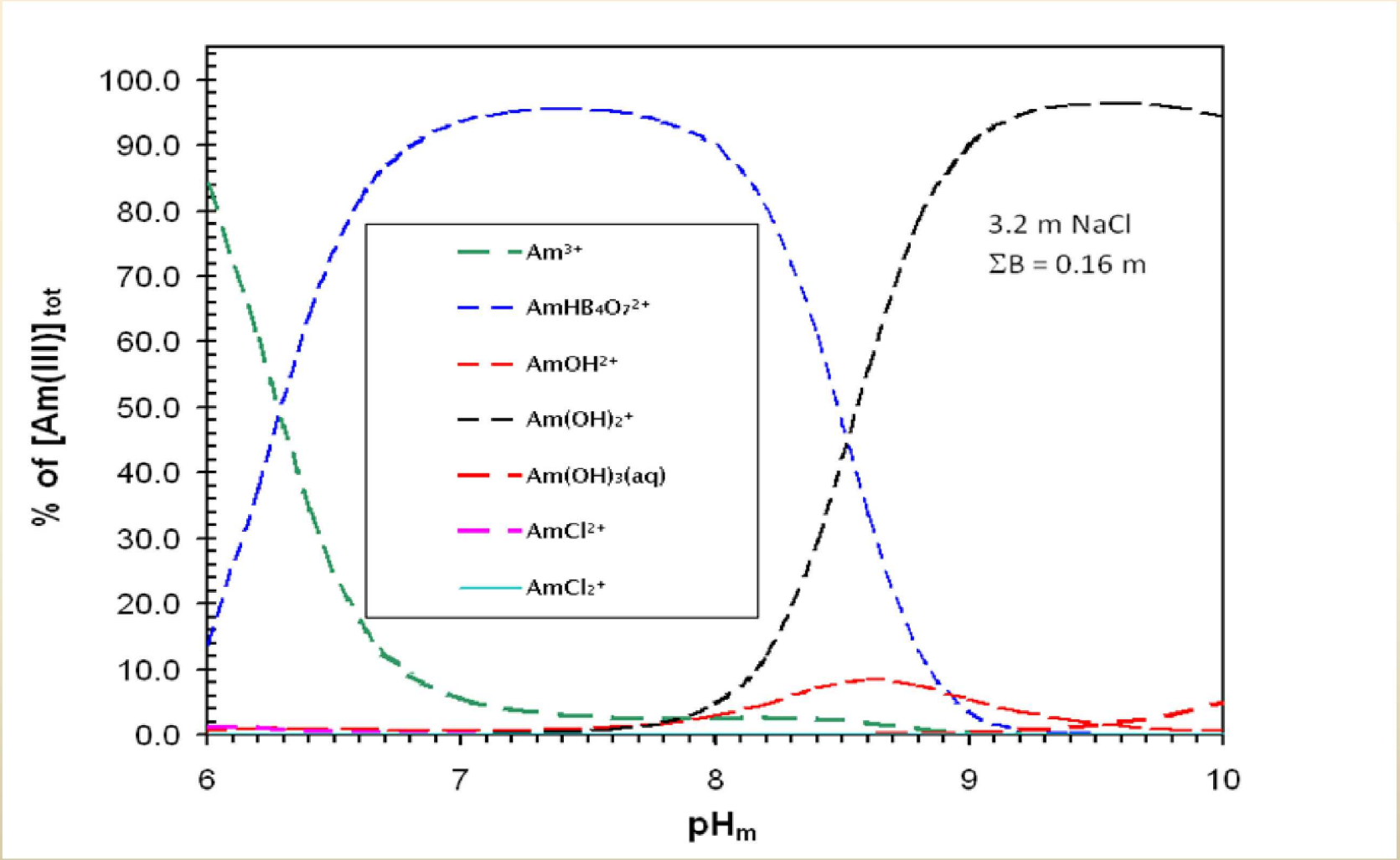

# Issue 22: $AmHB_4O_7^{2+}$

## Speciation of Am(III) in NaCl in the Presence of Borate

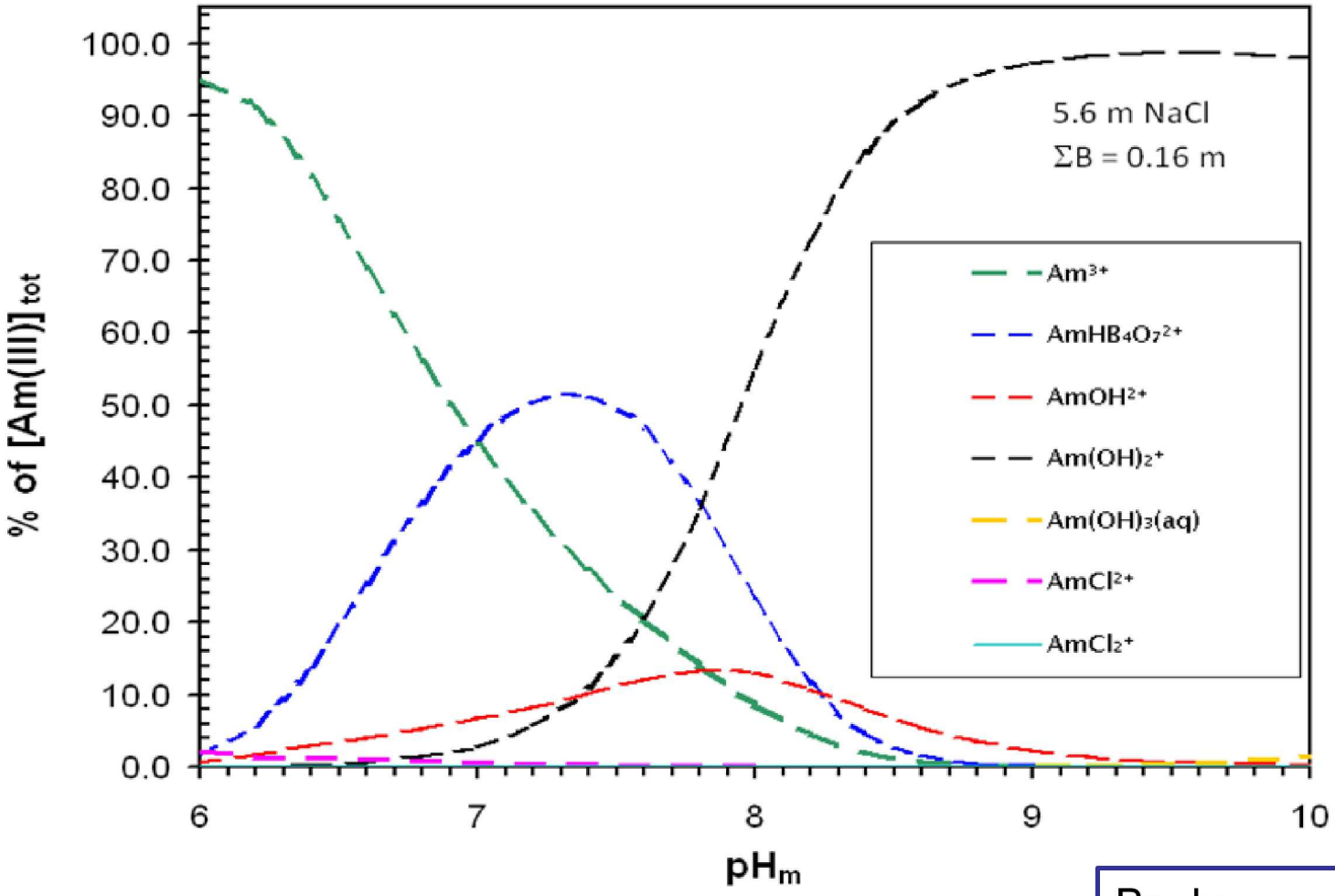


Back:

# Issue 22: Am(III)-borate Solid

## New Stability Constant for $AmB_9O_{13}(OH)_4(cr)$

$$AmB_9O_{13}(OH)_4(cr) + 19H_2O = Am^{3+} + 9B(OH)_4^- + 6H^+$$

The equilibrium constant for above reaction, consistent with the speciation scheme including $AmHB_4O_7^{2+}$, of the WIPP thermodynamic database (DATA0.FM2) (Xiong and Domski, 2016), has been evaluated (Xiong, 2017) from the literature raw solubility.

- ✓ The value has not been entered in DATA0.FM2 yet.
- ✓ We plan to add it to DATA0.FM2 to increase the capability of the database.

Xiong, Y., 2017. Solution Chemistry for Actinide Borate Species to High Ionic Strengths: Equilibrium Constants for $AmHB_4O_7^{2+}$ and $AmB_9O_{13}(OH)_4$ (cr) and Their Importance to Nuclear Waste Management. *MRS Advances*, *2*(13), pp.741-746.

Xiong, Y.-L., Domski, P.S., 2016. "Updating the WIPP Thermodynamic Database, Revision 1, Supersedes ERMS 565730." Carlsbad, NM: Sandia National Laboratories. ERMS 566047.

Back:

# Revised Stability Constant for $CaEDTA^{2-}$

## Revised Stability Constant for $CaEDTA^{2-}$

$$Ca^{2+} + EDTA^{4-} = CaEDTA^{2-}$$

The Am(III) solubilities predicted by Domski and Xiong (2015) using DATA0.FM2 are indeed lower than those predicted by Brush and Domski (2014) using DATA0.FM1. The decrease in Am(III) solubilities is actually attributed to

- ✓ The improvement and refinement for the stability constant of $CaEDTA^{2-}$ and,
- ✓ Its associated Pitzer interaction parameters.

# Revised Stability Constant for $CaEDTA^{2-}$

## Revised Stability Constant for $CaEDTA^{2-}$

$$Ca^{2+} + EDTA^{4-} \rightleftharpoons CaEDTA^{2-}$$

In the DATA0.FM1, the log $\beta^{o}_{1}$ with a value of 10.1260 for the above was based on the value for $MgEDTA^{2-}$ , using $MgEDTA^{2-}$ as an analog to $CaEDTA^{2-}$

$$Mg^{2+} + EDTA^{4-} \rightleftharpoons MgEDTA^{2-}$$

# Revised Stability Constant for $CaEDTA^{2-}$

## Revised Stability Constant for $CaEDTA^{2-}$

$$Ca^{2+} + EDTA^{4-} \rightleftharpoons CaEDTA^{2-}$$

In the DATA0.FM2, we determined the log $\beta^o_1$ with a value of 11.50 at 25°C for the above reaction (Xiong et al., 2017), based on the solubility data of $Ca_2EDTA \bullet 7H_2O(s)$ in NaCl and $MgCl_2$ solutions produced at Sandia National Laboratories.

- ✓ The log $\beta^o_1$ with a value of 11.50 for the above reaction recently determined by us is in excellent agreement with the literature value.
- ✓ The log $\beta^o_1$ experimentally determined by Carini and Martell (1954) at 25°C is 10.98.

---

Xiong, Y., Kirkes, L. and Westfall, T., 2017. Experimental determination of solubilities of di-calcium ethylenediaminetetraacetic acid hydrate [Ca 2 C 10 H 12 N 2 O 8· 7H 2 O (s)] in NaCl and MgCl 2 solutions to high ionic strengths and its Pitzer model: Applications to geological disposal of nuclear waste and other low temperature environments. *Chemical Geology*, *454*, pp.15-24.

# Revised Stability Constant for $CaEDTA^{2-}$

## Revised Stability Constant for $CaEDTA^{2-}$

$$Ca^{2+} + EDTA^{4-} \rightleftharpoons CaEDTA^{2-}$$

In the NEA review, they got a value of 12.69 for the above reaction (Hummel et al., 2005), evaluated with the SIT model. It is worth noting:

- ✓ the NEA review is based on experimental data in low ionic strength range, i.e., the majority of them is at 0.1 $mol \bullet dm^{-3}$.
- ✓ Our data cover a wide range of ionic strengths from 0.01 to 7.5 $mol \bullet kg^{-1}$.
- ✓ The NEA review series mention that when the Pitzer and SIT models apply to the same data set for a reaction involving highly charged species, logK will be different.
- ✓ As we use the Pitzer model for the data sets with a wide range of ionic strengths, whereas the NEA uses the SIT for the data set at low ionic strength, the difference is expected.

---

Hummel, W., Anderegg, G., Puigdomenech, I., Rao, L., Tochiyama, O., 2005. Chemical Thermodynamics of Compounds and Complexes of U, Np, Pu, Am, Tc, Zr, Ni and Se with Selected Organic Ligands. Chemical Thermodynamics, Volume 9, OECD Nuclear Energy Agency, Data Bank, Issy-les-Moulineaux, France, Elsevier B.V. Amsterdam, The Netherlands, p. 1088.

# Revised Stability Constant for $CaEDTA^{2-}$

## Revised Stability Constant for $CaEDTA^{2-}$

$$Ca^{2+} + EDTA^{4-} \rightleftharpoons CaEDTA^{2-}$$

In the DATA0.FM1, the Pitzer interaction parameters for $Na^+$–$CaEDTA^{2-}$ were assumed to be the same as those for $Na^+$–$MgEDTA^{2-}$, again using the interactions of $Na^+$–$MgEDTA^{2-}$ as analogs for $Na^+$–$CaEDTA^{2-}$.

- ✓ In the DATA0.FM2, we evaluated the Pitzer parameters for $Na^+$–$CaEDTA^{2-}$ (Xiong et al., 2017), based on the solubility data of $Ca_2EDTA \bullet 7H_2O(s)$ in NaCl and $MgCl_2$ solutions produced at Sandia National Laboratories.

---

Xiong, Y., Kirkes, L. and Westfall, T., 2017. Experimental determination of solubilities of di-calcium ethylenediaminetetraacetic acid hydrate [Ca 2 C 10 H 12 N 2 O 8· 7H 2 O (s)] in NaCl and MgCl 2 solutions to high ionic strengths and its Pitzer model: Applications to geological disposal of nuclear waste and other low temperature environments. *Chemical Geology*, *454*, pp.15-24.

# Revised Stability Constant for $CaEDTA^{2-}$

## Revised Stability Constant for $CaEDTA^{2-}$

$$Ca^{2+} + EDTA^{4-} \rightleftharpoons CaEDTA^{2-}$$

In the DATA0.FM1, there were no Pitzer interaction parameters for $Mg^{2+}$–$CaEDTA^{2-}$.

- ✓ In the DATA0.FM2, we evaluated the Pitzer parameters for $Mg^{2+}$–$CaEDTA^{2-}$ (Xiong et al., 2017), based on the solubility data of $Ca_2EDTA \bullet 7H_2O(s)$ in NaCl and $MgCl_2$ solutions produced at Sandia National Laboratories.

---

Xiong, Y., Kirkes, L. and Westfall, T., 2017. Experimental determination of solubilities of di-calcium ethylenediaminetetraacetic acid hydrate [Ca 2 C 10 H 12 N 2 O 8· 7H 2 O (s)] in NaCl and MgCl 2 solutions to high ionic strengths and its Pitzer model: Applications to geological disposal of nuclear waste and other low temperature environments. *Chemical Geology*, *454*, pp.15-24.

# Revised Stability Constant for $CaEDTA^{2-}$

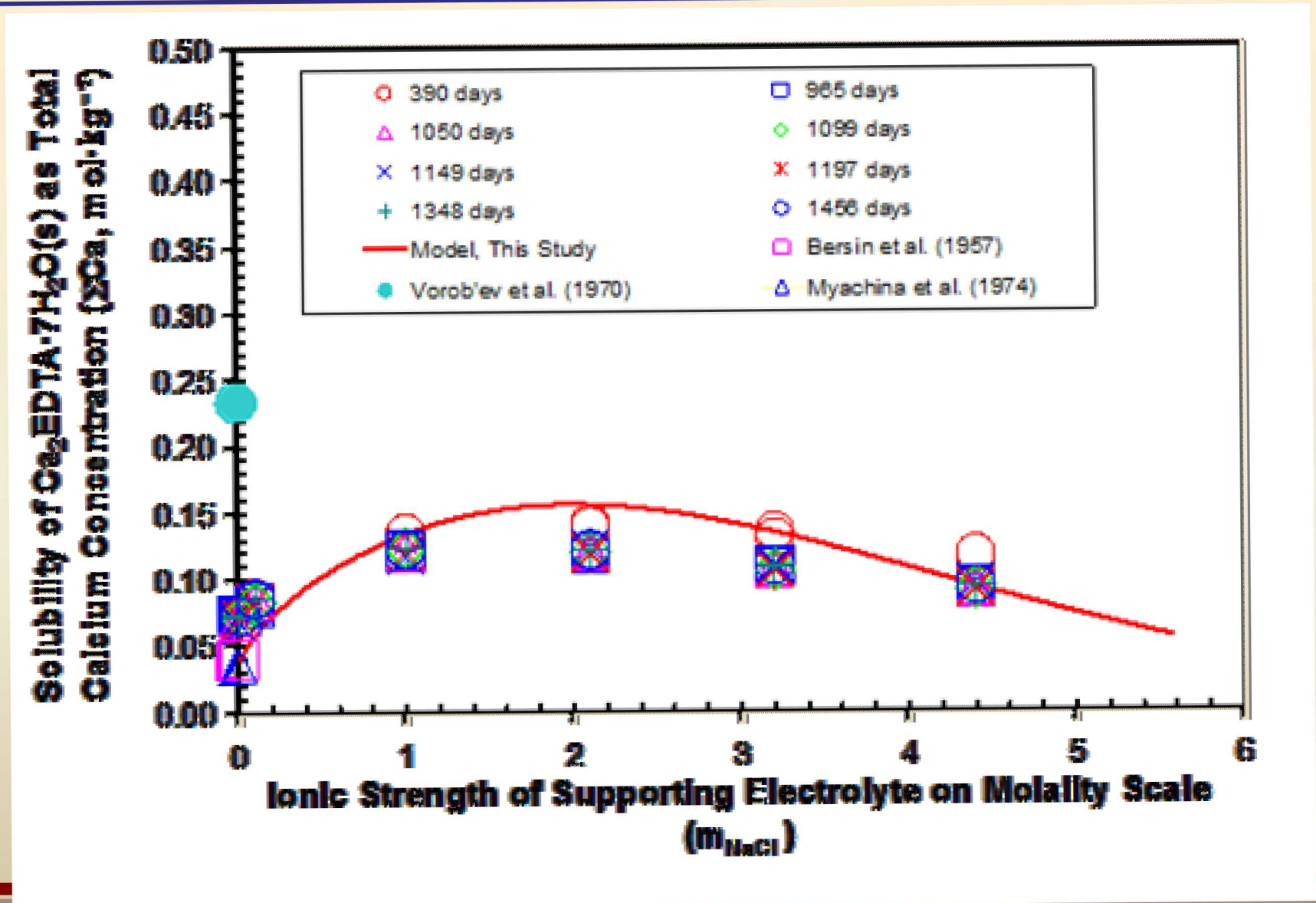

# Revised Stability Constant for $CaEDTA^{2-}$

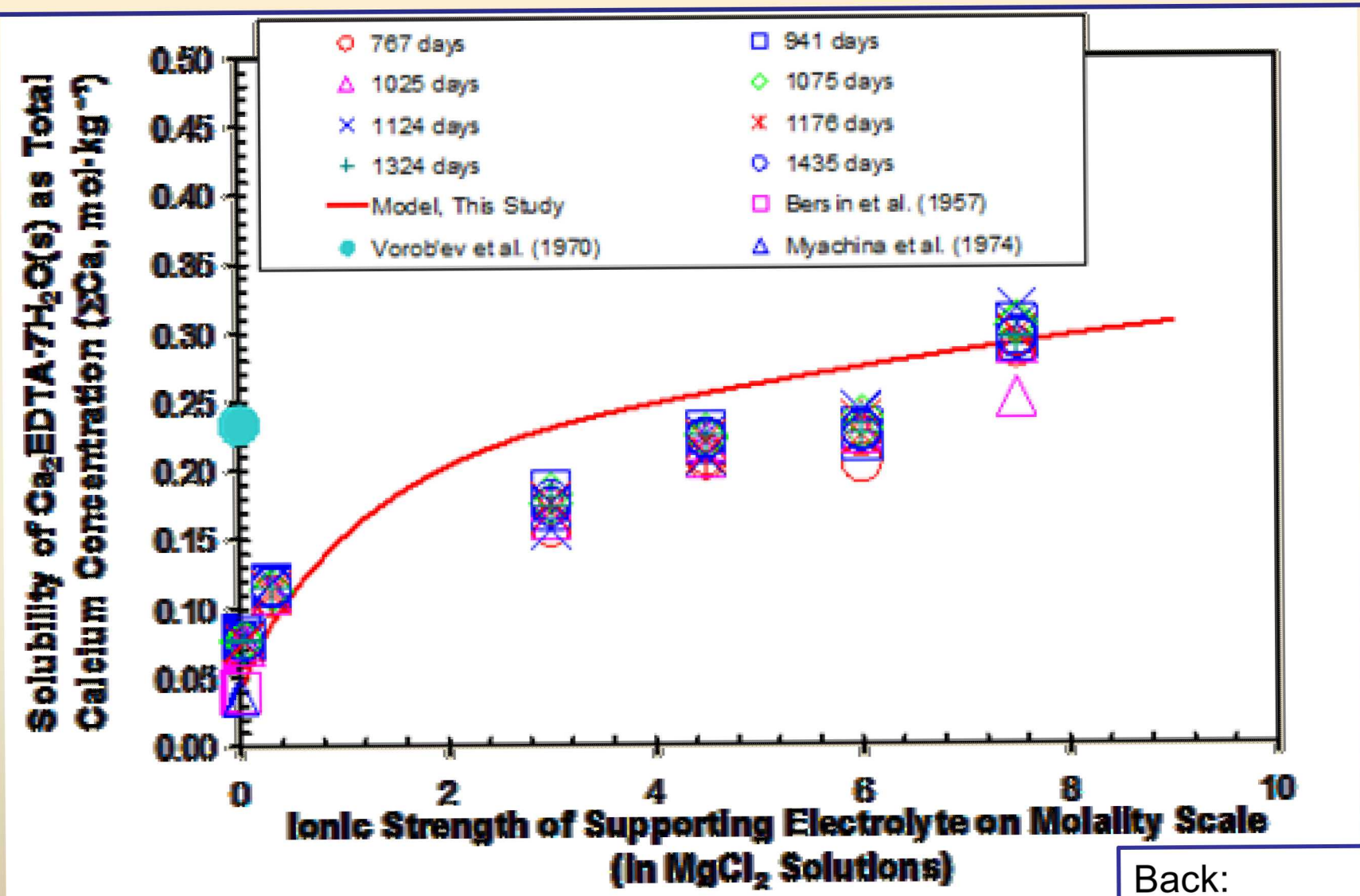


Back:

# Issue 23: Data for $Nd(OH)_3$ from Neck et al.

The experimental data from Neck et al. (2009) were for an amorphous phase, $Nd(OH)_3(am)$.

- ✓ We have evaluated the equilibrium constant for $Nd(OH)_3(am)$ from the experimental data of Neck et al. (2009).
- ✓ We plan to add the equilibrium constant for $Am(OH)_3(am)$ in the DATA0.FM2 for the upcoming updated actinide uncertainty distribution analysis.
- ✓ Specifically, we will use it to simulate experiments in which the solubility-controlling phase was $Nd(OH)_3(am)$ or $An(OH)_3(am)$, per selection criteria G7, to compare with the selected experimental data.

---

Neck, V., Altmaier, M., Rabung, T., Lützenkirchen, J., and Fanghänel, T. (2009) Thermodynamics of trivalent actinides and neodymium in NaCl, $MgCl_2$, and $CaCl_2$ solutions: Solubility, hydrolysis, and ternary Ca-M (III)-OH complexes. Pure and Applied Chemistry, 81, 1555–1568.

# Issue 23: Data for $Nd(OH)_3$ from Neck et al.

| Thermodynamic properties in form of Gibbs free energy of formation | |
|---|---|
| Species | $\Delta_f G$, kJ $mol^{-1}$ |
| $Am^{3+}$ | -599.116 |
| $AmOH^{2+}$ | -793.123 |
| $Am(OH)_2^{+}$ | -983.819 |
| $Am(OH)_3^{o}$ | -1,163.880 |
| $AmCl^{2+}$ | -731.747 |
| $AmCl_2^{+}$ | -857.424 |
| $Am(OH)_3(s)$ | -1227.809 |
| $Am(OH)_3(am)$ | -1214.322** |
| Thermodynamic properties in form of equilibrium constants | |
| Reactions | log $K^0$ |
| $AmOH^{2+} + H^{+} = Am^{3+} + H_2O(l)$ | 7.5556 |
| $Am(OH)_2^{+} + 2H^{+} = Am^{3+} + 2H_2O(l)$ | 15.6915 |
| $Am(OH)_3^{0} + 3H^{+} = Am^{3+} + 3H_2O(l)$ | 25.6905 |
| $AmCl^{2+} = Am^{3+} + Cl^{-}$ | -0.2393 |
| $AmCl_2^{+} = Am^{3+} + 2Cl^{-}$ | 0.7400 |
| $Am(OH)_3(s) + 3H^{+} = Am^{3+} + 3H_2O(l)$ | 14.4900 |
| $Am(OH)_3(am) + 3H^{+} = Am^{3+} + 3H_2O(l)$ | 16.85±0.20** |
| $Nd(OH)_3(am) + 3H^{+} = Nd^{3+} + 3H_2O(l)$ | 16.85±0.20** |

# Issue 23: Data for $Nd(OH)_3$ from Neck et al.

* The computer code employed for the WIPP CCA-1996, CRA-2004, and CRA-2009 was the Fracture Matrix Transport (FMT) code. That code used dimensionless standard chemical potentials ($\mu^o/RT$ ) for the WIPP thermodynamic model. On September 17, 2011, U.S. U.S. Environment Protection Agency approved the migration from the FMT code to EQ3/6 Version 8.0a. EQ3/6 Version 8.0a uses equilibrium constants. In this table, Gibbs free energies of formation are from Xiong et al. (2010), which were converted from dimensionless standard chemical potentials by using the equation, $\Delta_f G^0 = ( \mu^o/RT) \times 298.15 \times 8.314$. Equilibrium constants are from the EQ3/6 Version 8.0a database, DATA0.FMT (Wolery et al., 2010; Xiong, 2011).

** Evaluated by this study with the WIPP thermodynamic model, using the data for $Nd(OH)_3$(am) from literature, and the same value for the equilibrium constant is applied to $Am(OH)_3$(am). Notice that the equilibrium constant was first evaluated. Then, the $\Delta_f G^0$ for $Am(OH)_3$(am) was derived in consistency with the FMT database (Xiong et al., 2010, and references therein).

# Issue 23: Data for $Nd(OH)_3$ from Neck et al.

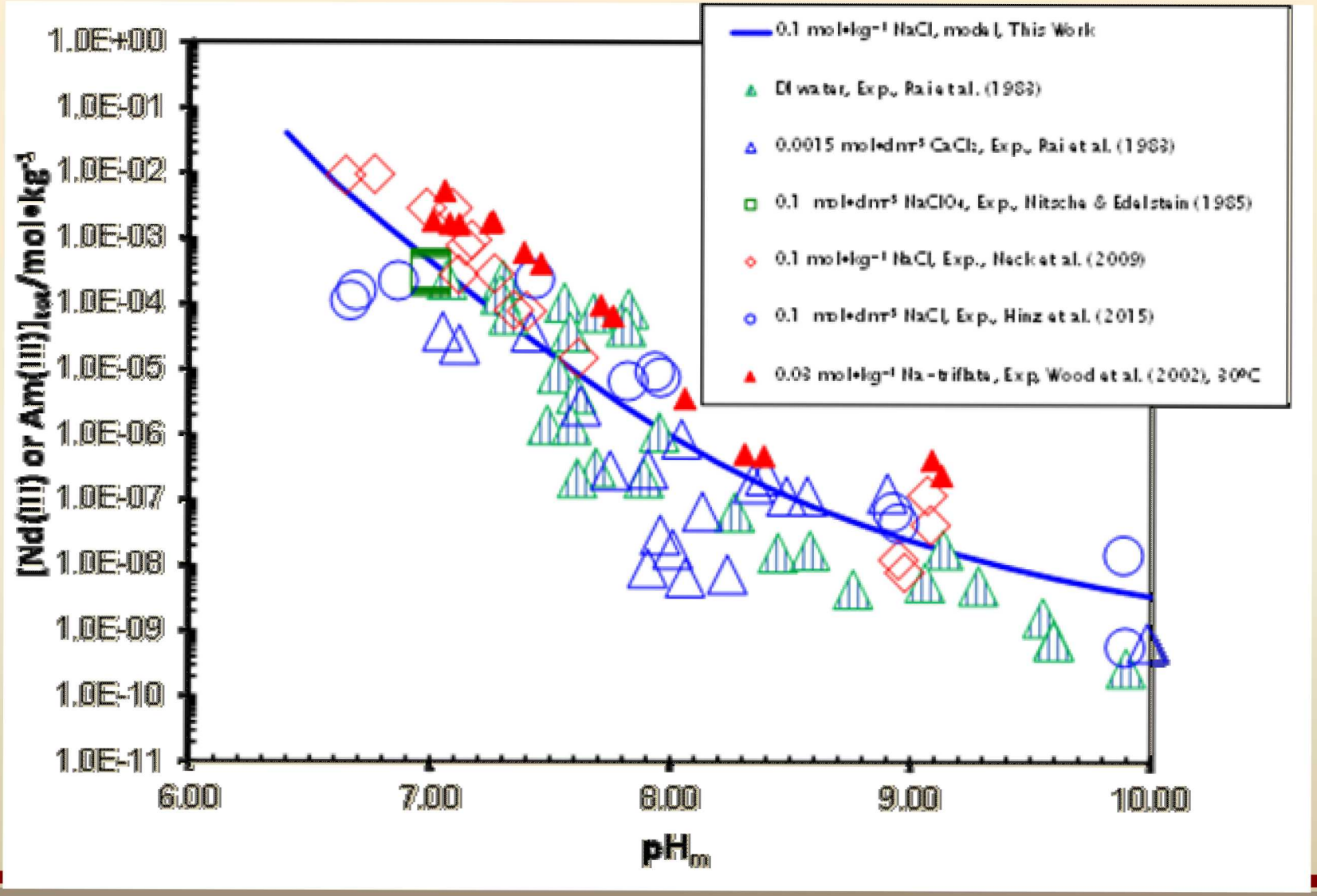

# Issue 23: Data for $Nd(OH)_3$ from Neck et al.

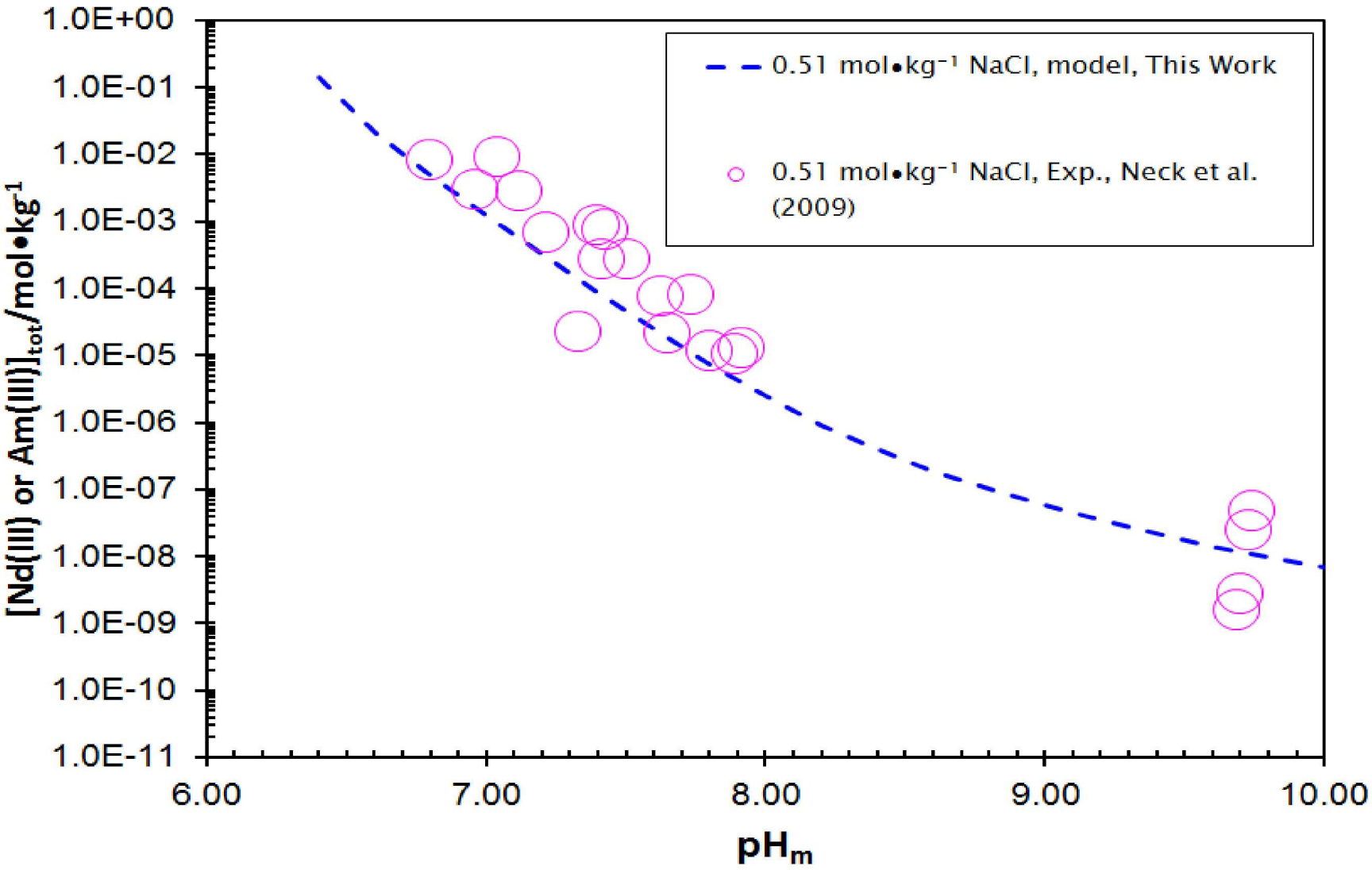

# Issue 23: Data for $Nd(OH)_3$ from Neck et al.

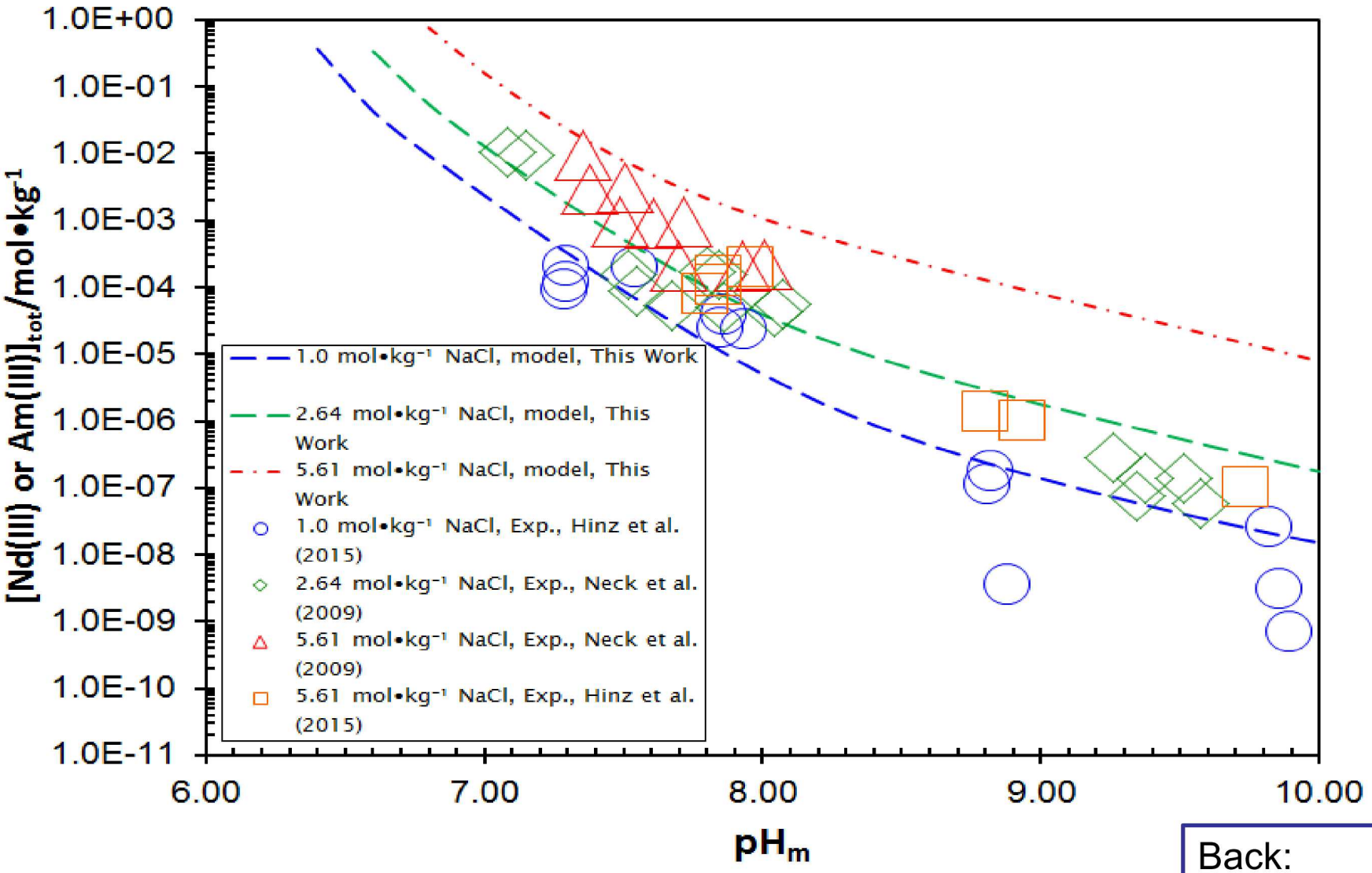


Back:

# Stability Constant for $MgSO_4(aq)$

## Stability Constant for $MgSO_4(aq)$

$$Mg^{2+} + SO_4^{2-} \rightleftharpoons \mathbf{MgSO_4(aq)}$$

The addition of $MgSO_4(aq)$ into the database provides more accurate descriptions about the performance of the WIPP engineered barrier, MgO, because sulfate is a major species in the WIPP brines,

- ✓ Generic Weep Brine (GWB): 0.203 $mol \bullet kg^{-1}$ and,
- ✓ U.S. Energy Research and Development Administration Well 6 (ERDA-6): 0.187 $mol \bullet kg^{-1}$.

# Stability Constant for $MgSO_4(aq)$

## Stability Constant for $MgSO_4(aq)$

$$Mg^{2+} + SO_4^{2-} \rightleftharpoons MgSO_4(aq)$$

Xiong et al. (2018, in press) experimentally determined the stability constant for the above reaction as 2.38 ± 0.08, based on brucite solubility data in $Na_2SO_4$ solutions

- ✓ Brucite has higher solubilities in $Na_2SO_4$ solutions.
- ✓ The higher solubilities are due to formation of $MgSO_4(aq)$.

---

Xiong, Y.-L., Leslie Kirkes, Terry Westfall, 2018. Experimental Determination Of Solubilities of Brucite [$Mg(OH)_2(cr)$] In $Na_2SO_4$ Solutions With Borate To High Ionic Strengths. In press, Journal of Solution Chemistry

# Stability Constant for $MgSO_4(aq)$

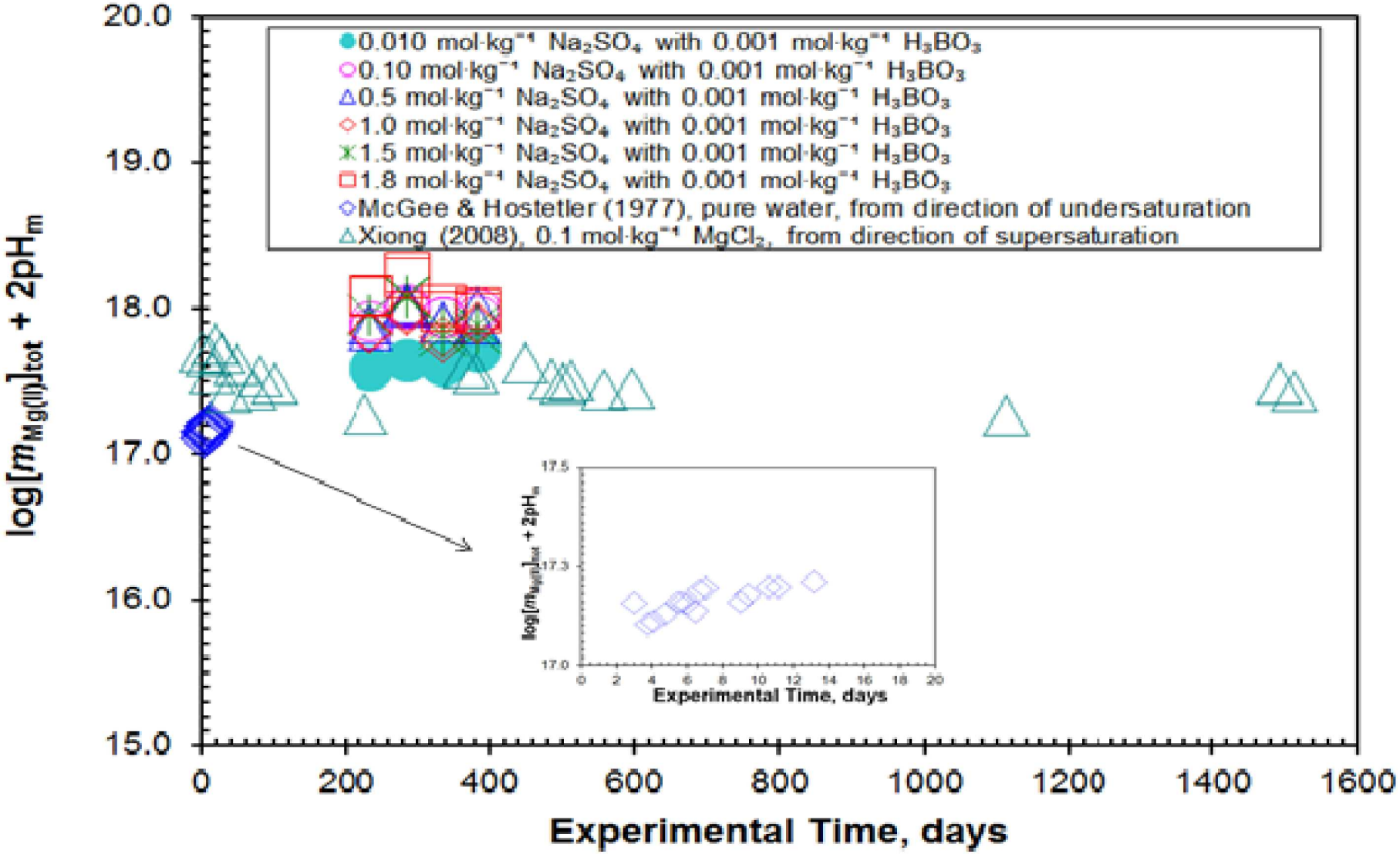

# Stability Constant for $MgSO_4(aq)$

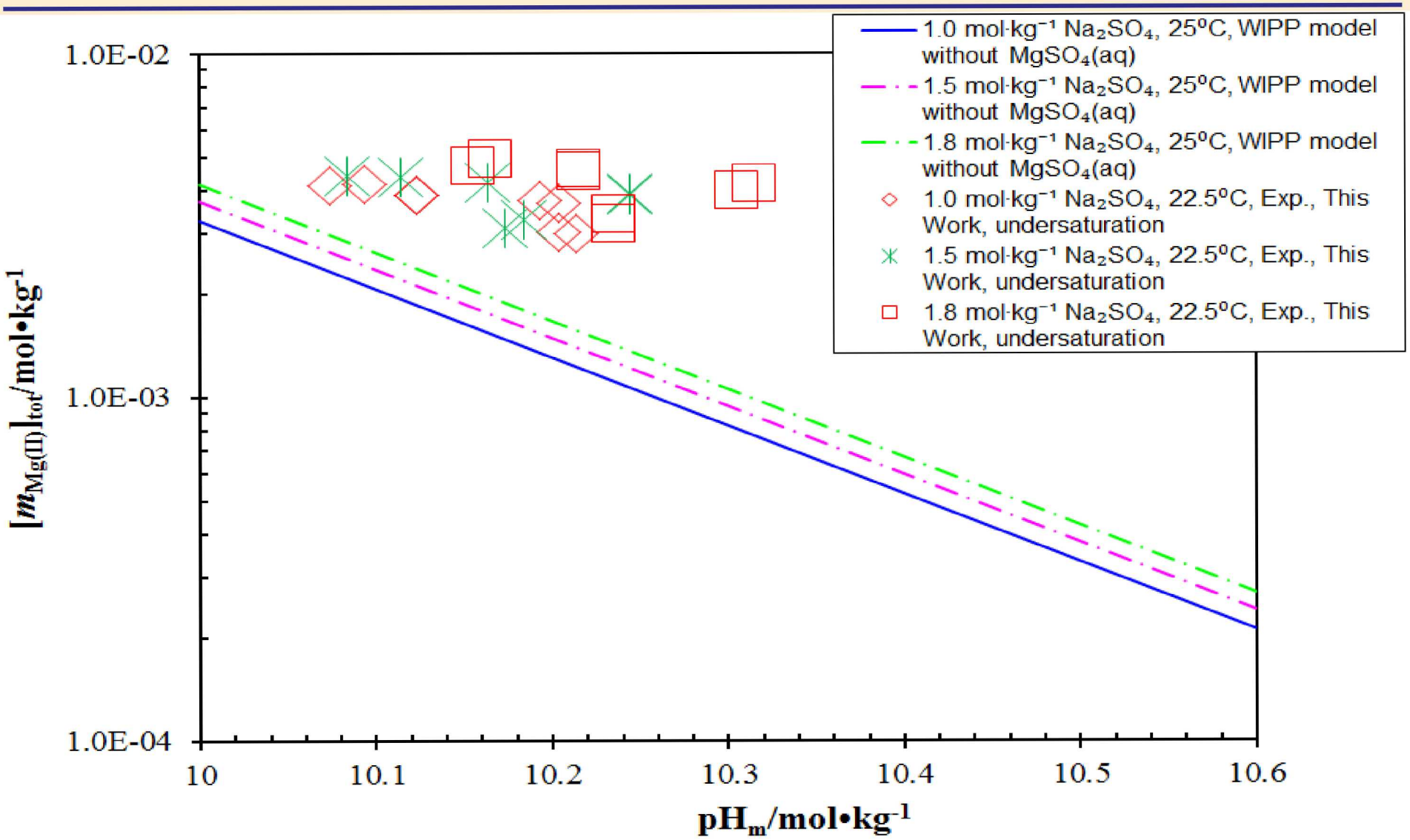

# Stability Constant for $MgSO_4(aq)$

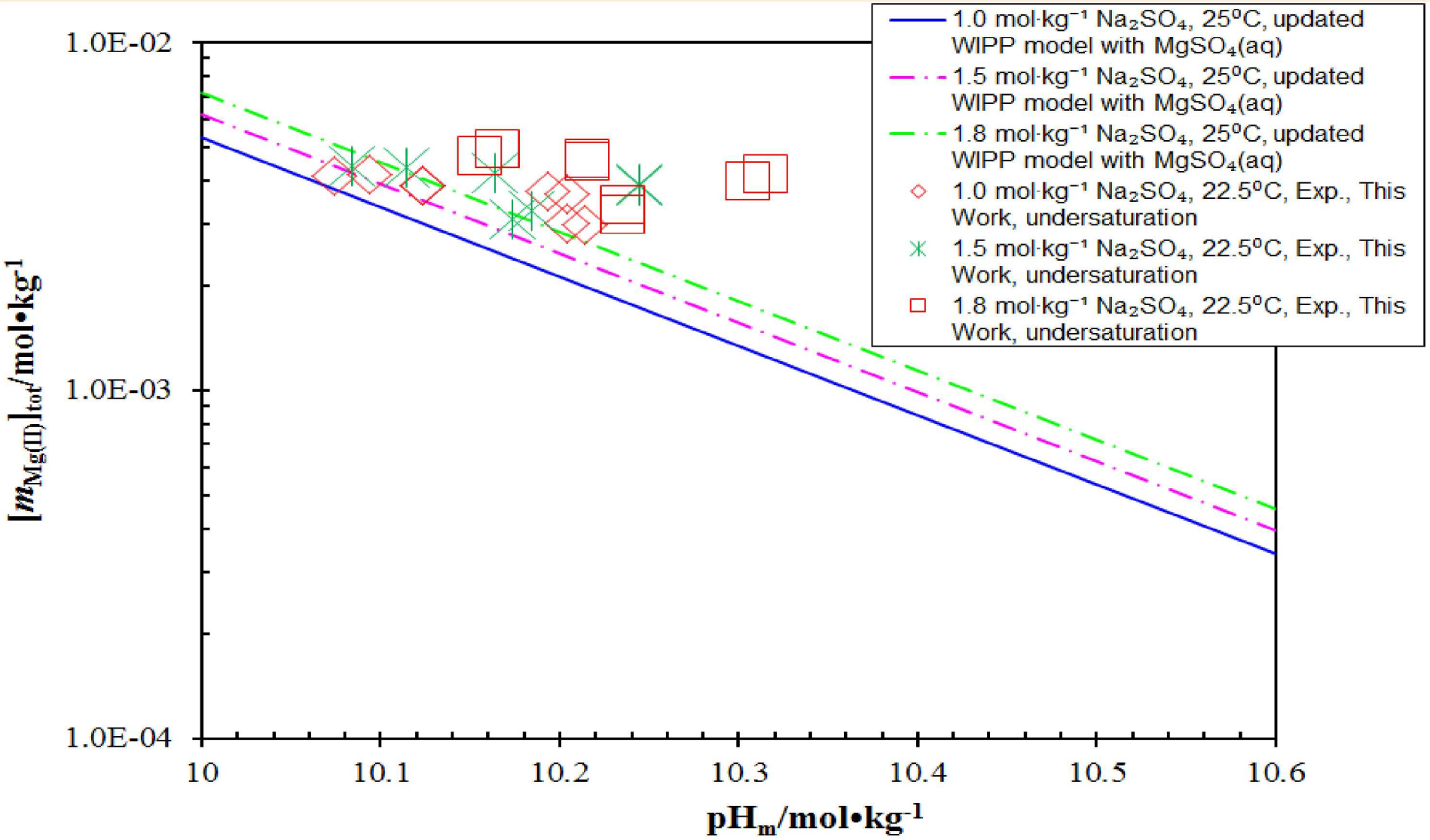

# Stability Constant for $MgSO_4(aq)$

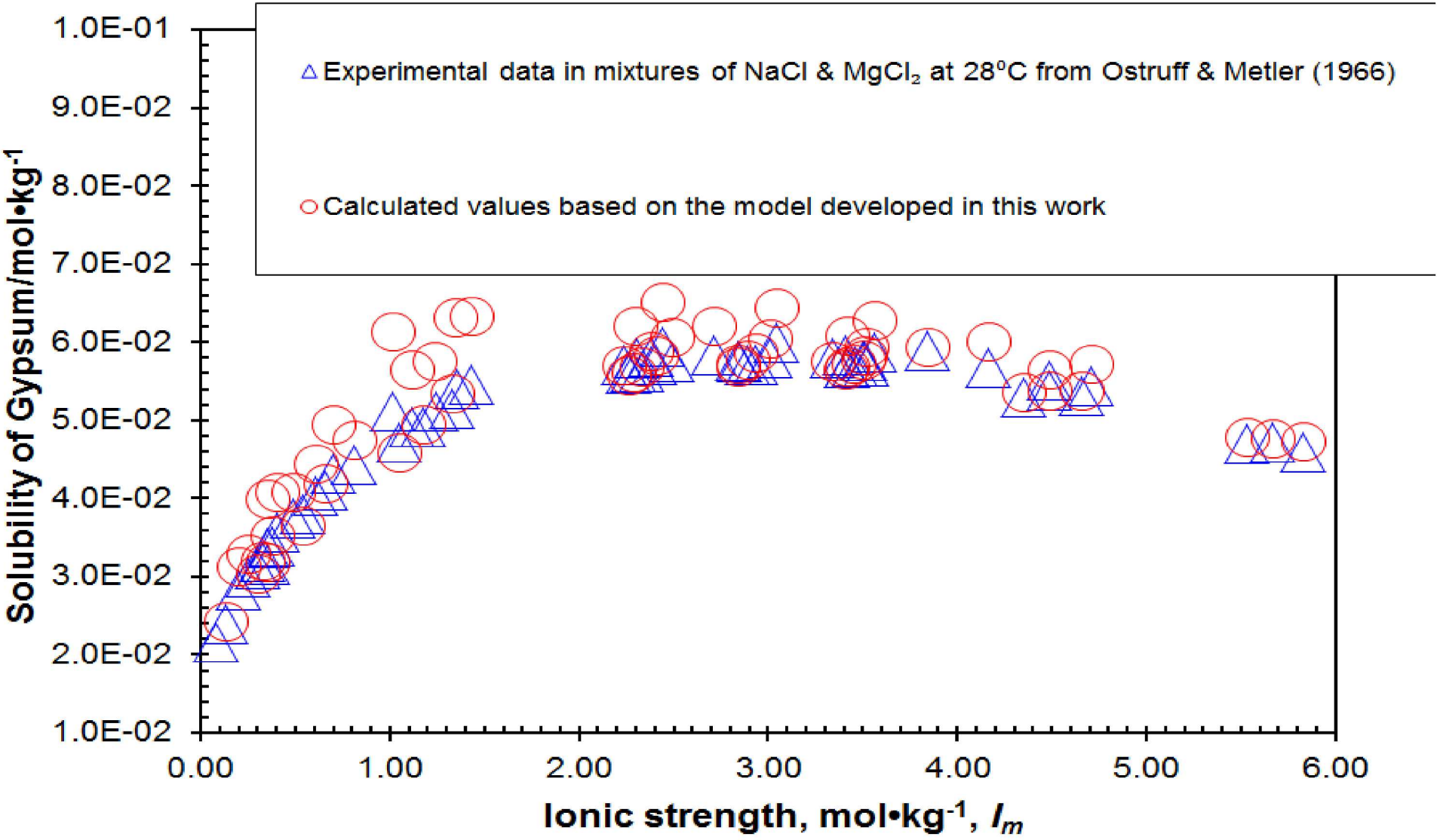

# Stability Constant for $MgSO_4(aq)$

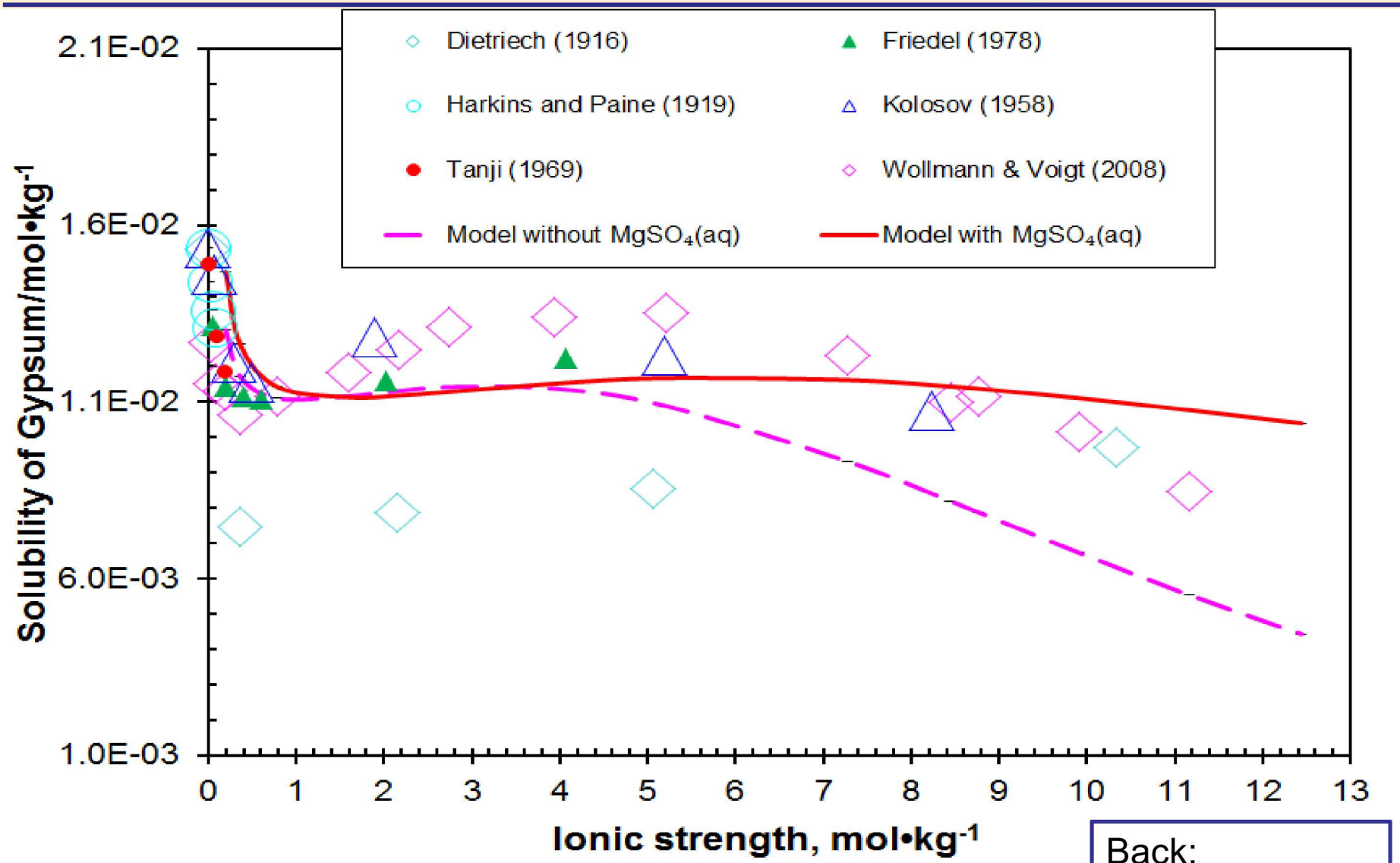


Back:

# Stability Constant for $AmEDTA^-$

## Stability Constant for $AmEDTA^-$

$$Am^{3+} + EDTA^{4-} \rightleftharpoons AmEDTA^-$$

- ✓ The value in DATA0.FM1 ($\log \beta^0_1 = 18.97$) was derived from data in the ionic strength range from 0.3 m to 5.0 m in NaCl solutions.
- ✓ Since the 2009 Recertification of WIPP, new experimental data in the ionic strength range from 0.10 m to 6.60 m in $NaClO_4$ solutions have been produced at the Choppin Group at Florida State University.
- ✓ A revised value ($\log \beta^0_1 = 20.55$) derived using the new data is valid to higher ionic strengths (e.g., Thakur, Xiong, Borkowski, and Choppin, 2014).
- ✓ $\log \beta^0_1 = 20.55$ was incorporated in DATA0.FM2

# Stability Constant for $AmEDTA^-$

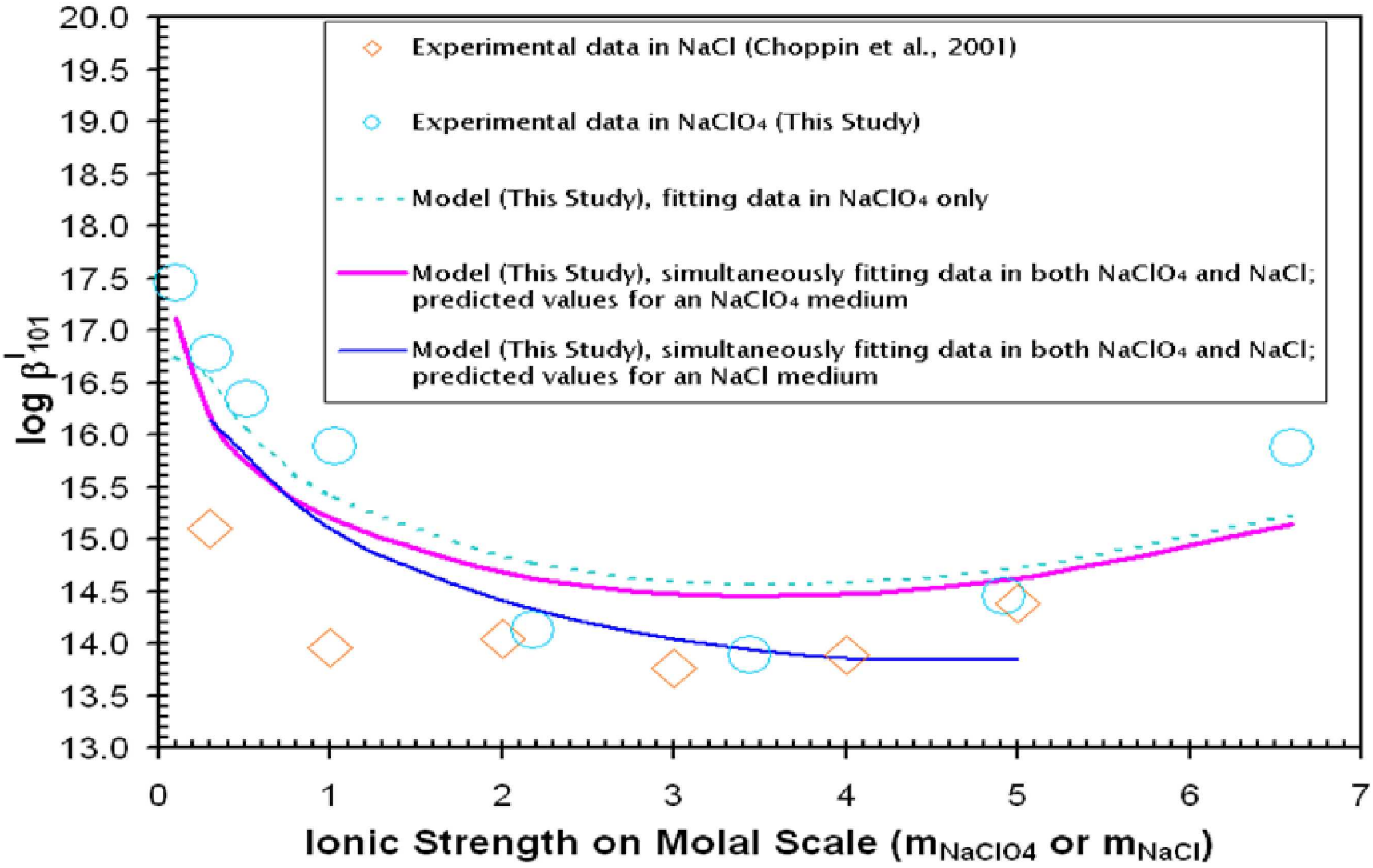

# Stability Constant for $NaB(OH)_4(aq)$

## Stability Constant for $NaB(OH)_4(aq)$

$$Na^+ + B(OH)_4^- \rightleftharpoons NaB(OH)_4(aq)$$

- This is a new reaction that has no parameters in DATA0.FM1
- Numerous researchers have suggested the existence of this complex in solutions containing sodium (e.g., Reardon, 1976; Corti et al., 1980; Rowe et al., 1989; Pokrovski et al., 1995; Akinfiev et al., 2006).
- Experimental solubility data for sodium tetraborate in NaCl solutions was produced by Xiong et al. (2013).
- The log $\beta_1 = 0.25 \pm 0.01$ for the above reaction evaluated by Xiong et al. (2013) is in excellent agreement with the most recent conductivity measurements (Arcis et al., 2016).

---

Arcis, H., Ferguson, J.P., Zimmerman, G.H. and Tremaine, P.R., 2016. The limiting conductivity of the borate ion and its ion-pair formation constants with sodium and potassium under hydrothermal conditions. *Physical Chemistry Chemical Physics*, *18*(34), pp.24081-24094

Xiong, Y., Kirkes, L. and Westfall, T., 2013. Experimental determination of solubilities of sodium tetraborate (borax) in NaCl solutions, and a thermodynamic model for the Na-B (OH) 3-Cl-SO4 system to high-ionic strengths at 25 C. *American Mineralogist*, *98*(11-12), pp.2030-2036.

# Stability Constant for $NaB(OH)_4(aq)$

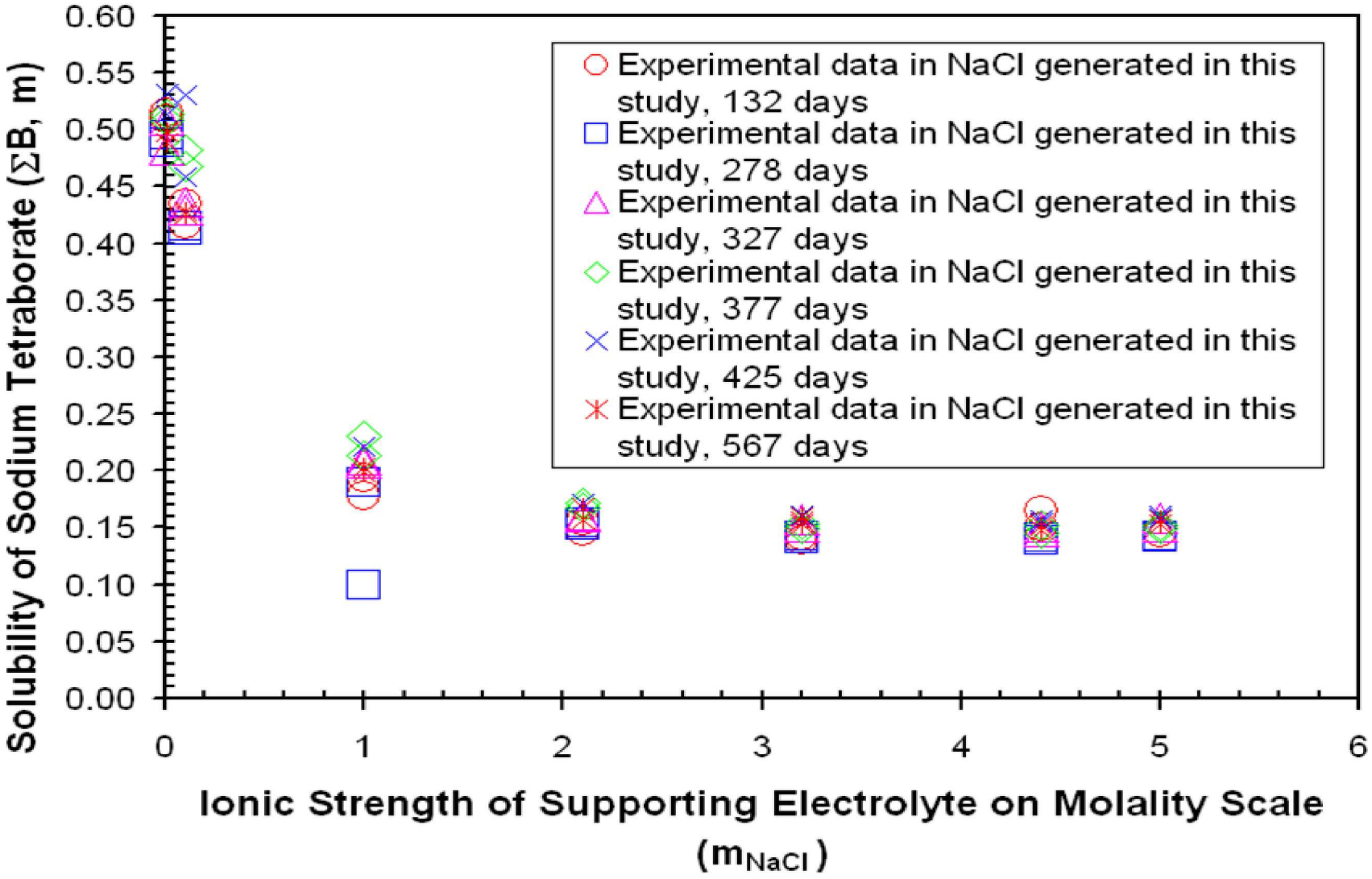

# Stability Constant for $NaB(OH)_4(aq)$

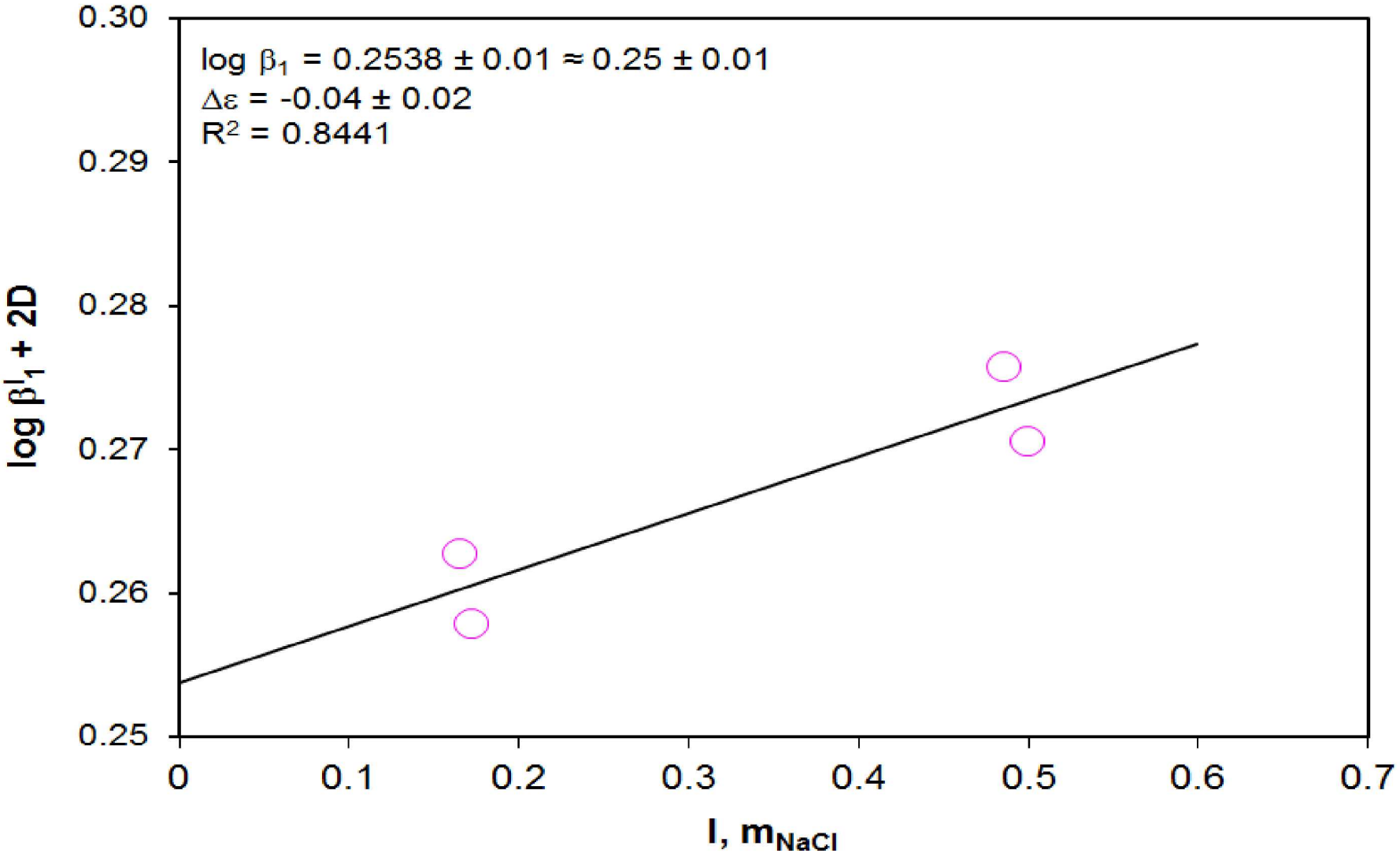

# Stability Constant for $NaB(OH)_4(aq)$

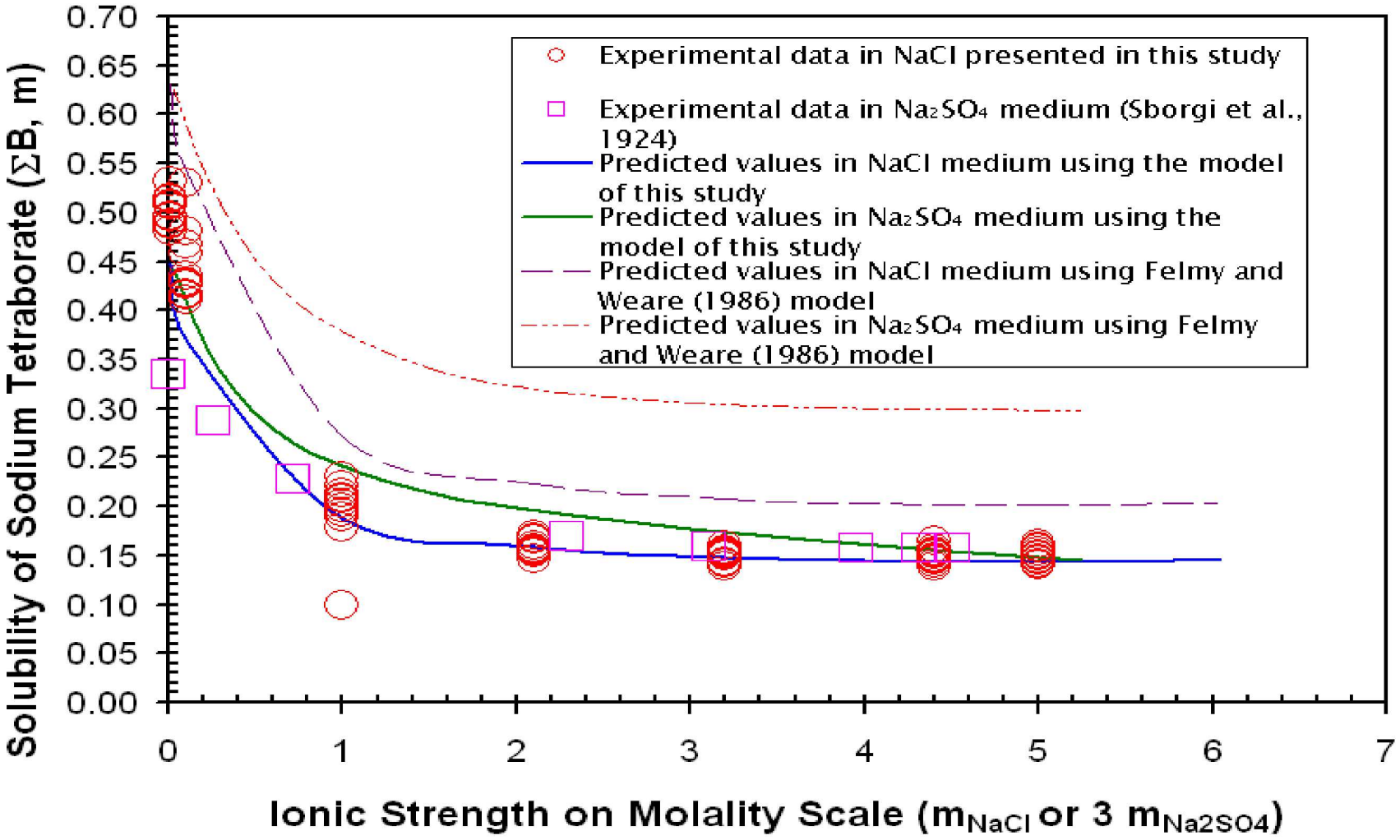

# Stability Constant for $NaB(OH)_4(aq)$

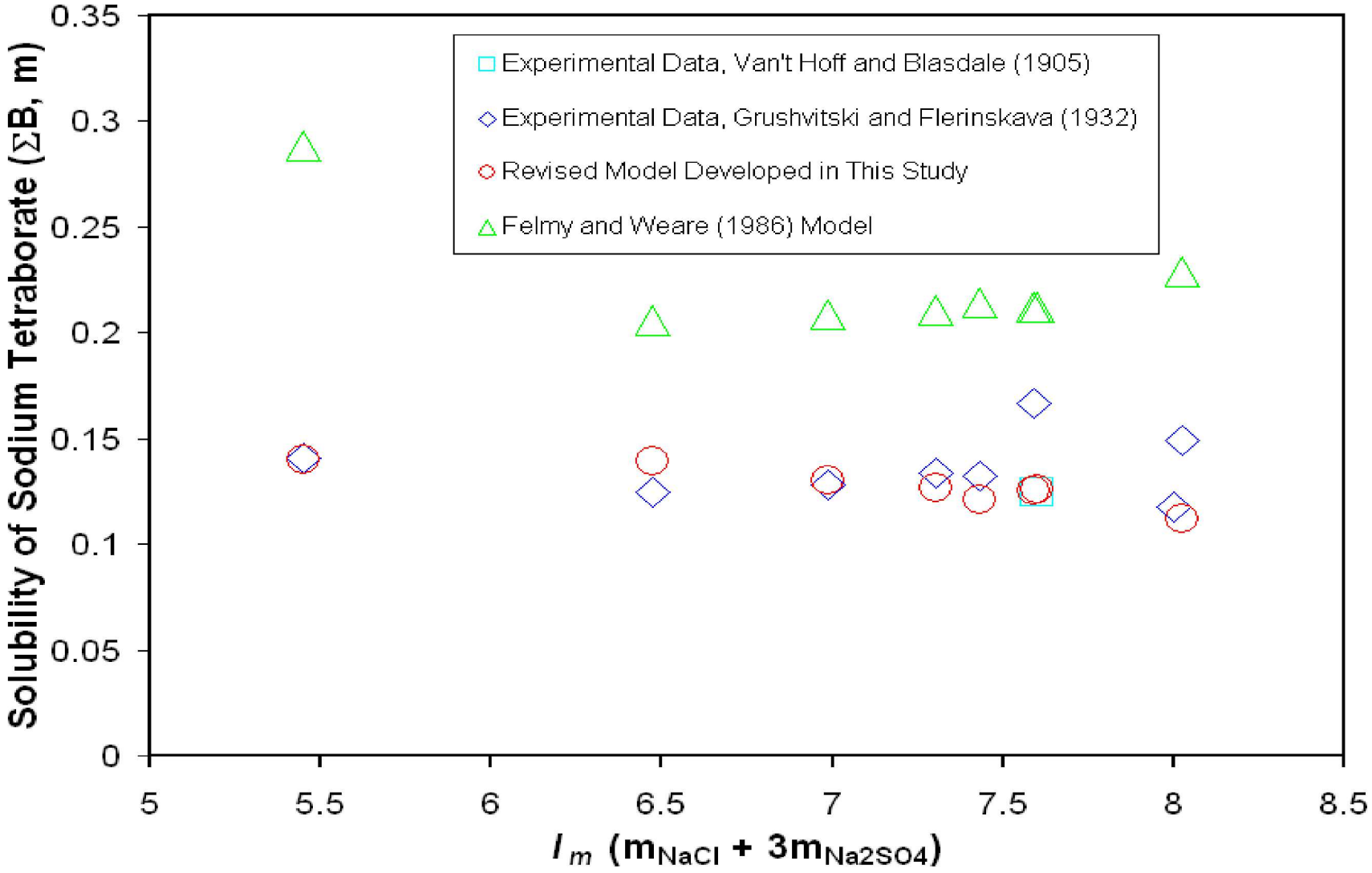

# Lead Chemistry

- We added the lead parameters into the DATA0.FM2 for near-field geochemistry predictions.
- This comprehensive lead model significantly improves our understanding of the near-field geochemistry because
  - There are sizable inventories of lead in both the waste and shielding .
- These reactions were parameterized with data gathered at Sandia National Laboratories (e.g., Xiong 2013, 2014a, 2014b, 2014c, 2015a) and from literature.
- The reactions involving lead chloride complexes, lead oxalate complexes, and lead carbonate complexes have already been published as peer-reviewed journal publications (Xiong et al., 2013; Xiong, 2015b).

---

Xiong, Y., Kirkes, L., Westfall, T. and Roselle, R., 2013. Experimental determination of solubilities of lead oxalate (PbC2O4 (cr)) in a NaCl medium to high ionic strengths, and the importance of lead oxalate in low temperature environments. *Chemical Geology*, *342*, pp.128-137.

Xiong, Y., 2015b. Experimental determination of lead carbonate solubility at high ionic strengths: a Pitzer model description. *Monatshefte für Chemie-Chemical Monthly*, *146*(9), pp.1433-1443..

# Lead Chemistry

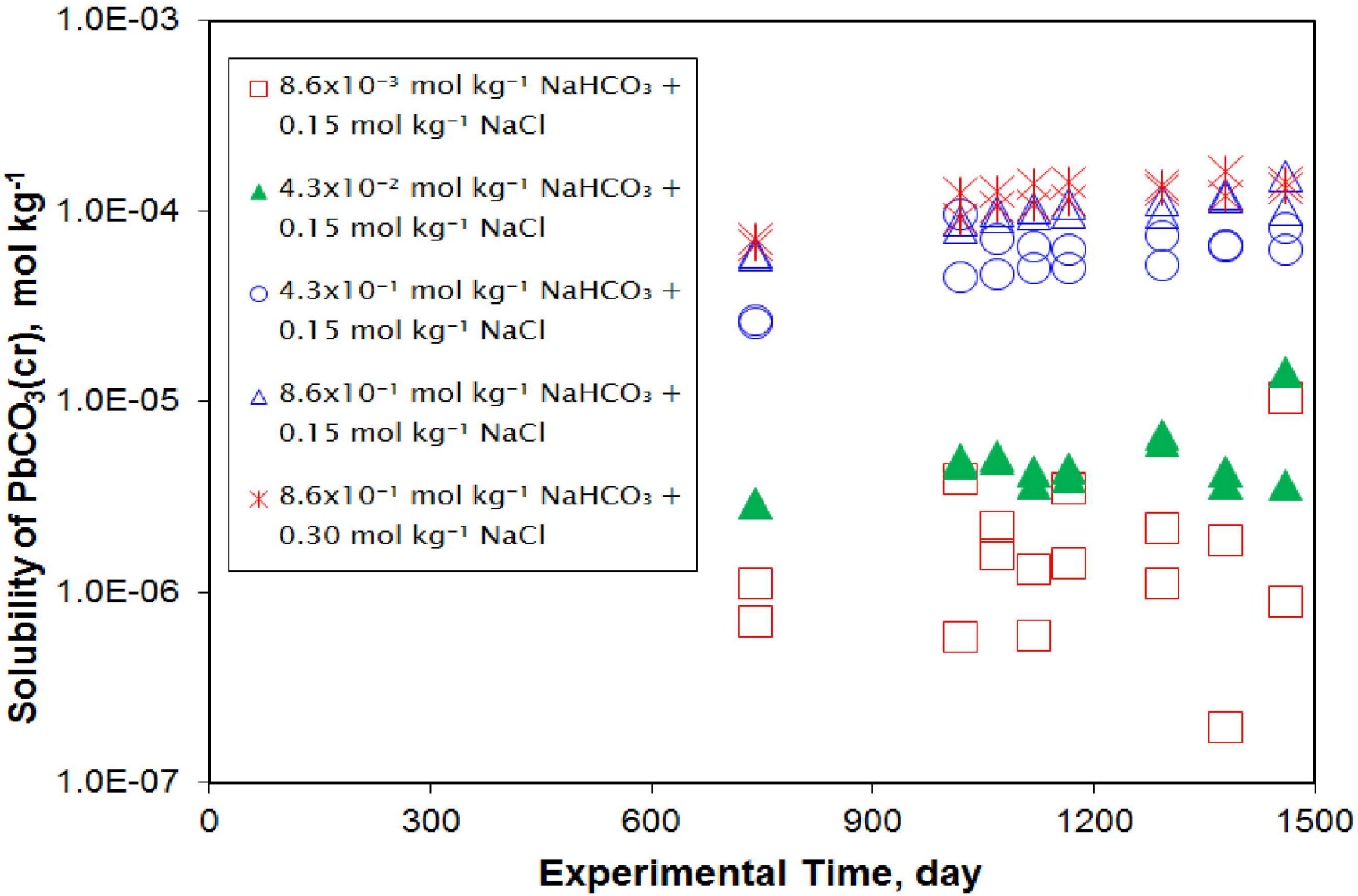

# Lead Chemistry

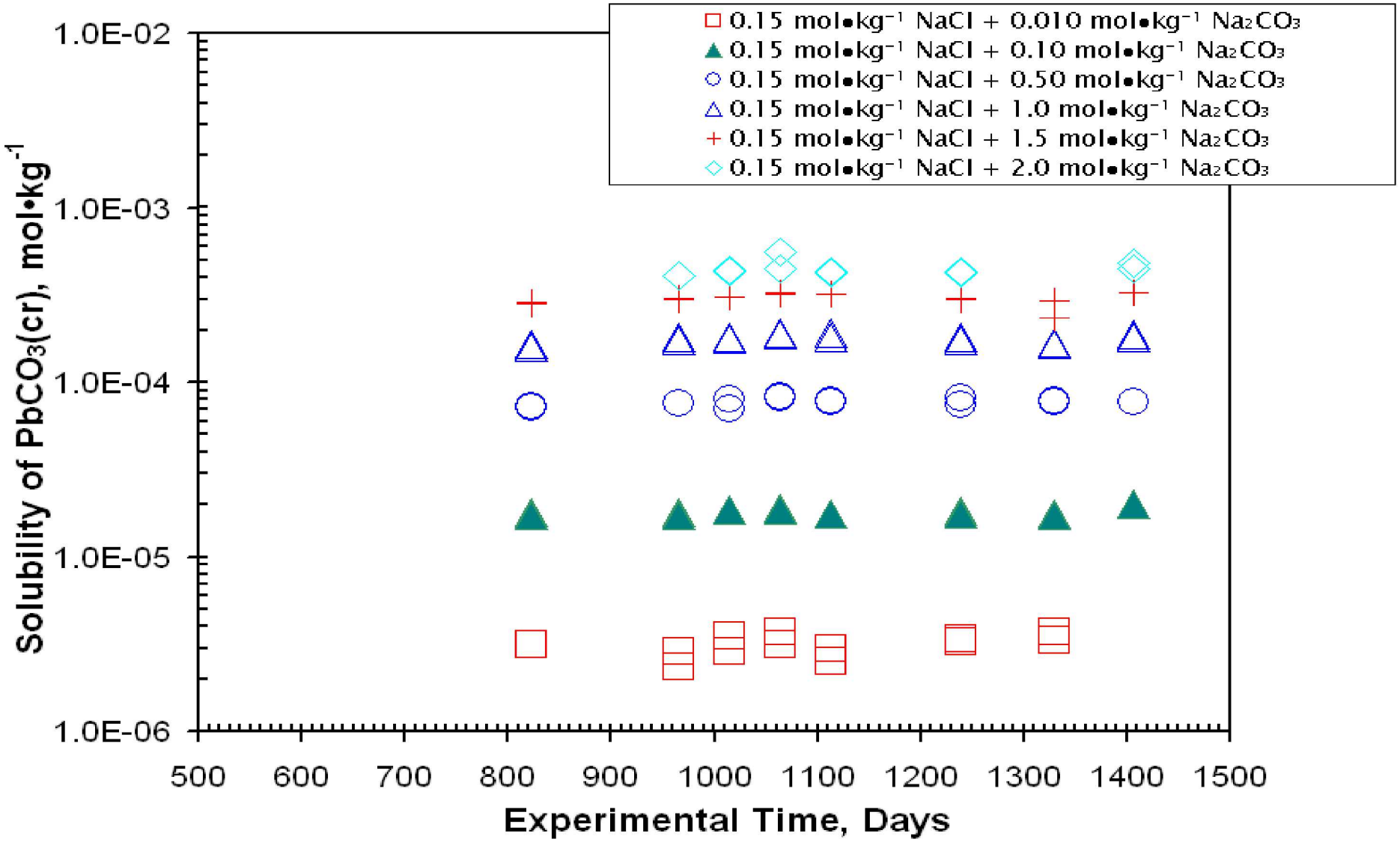

# Lead Chemistry

Table 1. Equilibrium constants at infinite dilution at 25°C and 1 bar for the $Na^+$—$Pb^{2+}$—$Cl^-$—$HCO_3^-$—$CO_3^{2-}$ system

| Reactions | $\log K_s^o$, $\log \beta_1^o$, $\log \beta_2^o$ or $\log \beta_{11}^o$ | Reference and Remarks |
|---|---|---|
| $PbCO_3(cr) = Pb^{2+} + CO_3^{2-}$ | $-13.76 \pm 0.15$ (2σ) | This study, based on solubility of $PbCO_3$(cr) in the mixtures of $NaHCO_3$ and NaCl and in the mixture of $NaHCO_3$ and $Na_2CO_3$ |
| $Pb^{2+} + CO_3^{2-} = PbCO_3(aq)$ | $6.87 \pm 0.09$ (2σ) | Woosley and Millero (2013) |
| $Pb^{2+} + 2CO_3^{2-} = Pb(CO_3)_2^{2-}$ | $10.41 \pm 0.18$ (2σ) | Easley and Byrne (2011) |
| $Pb^{2+} + CO_3^{2-} + Cl^- = Pb(CO_3)Cl^-$ | $7.23 \pm 0.74$ (2σ) | Woosley and Millero (2013) |

# Lead Chemistry

Table 2. Pitzer interaction parameters at 25°C and 1 bar for the $Na^+$—$Pb^{2+}$—$Cl^-$—$HCO_3^-$—$CO_3^{2-}$ system

| Pitzer Binary Interaction Parameters | | | | | |
|---|---|---|---|---|---|
| Species *i* | Species *j* | $\beta^{(0)}$ | $\beta^{(1)}$ | $C^{\phi}$ | Reference |
| $Na^+$ | $Pb(CO_3)_2^{2-}$ | 0.1975 | 1.74 | –0.2105 | This study |
| $Na^+$ | $Pb(CO_3)Cl^-$ | 0.3799 | 0.29 | 0.1921 | This study |
| Pitzer Mixing Interaction Parameters (theta parameter) and Interaction Parameters Involving Neutral Species (lambda and zeta parameters) | | | | | |
| Species *i* | Species *j* | Species *k* | $\lambda_{ij}$ or $\theta_{ij}$ | $\zeta_{ijk}$ | Reference |
| $HCO_3^-$ | $Pb(CO_3)_2^{2-}$ | | 0.1476 | | This study |
| $CO_3^{2-}$ | $Pb(CO_3)_2^{2-}$ | | 0.2223 | | This study |
| $Cl^-$ | $PbCO_3(aq)$ | | –0.02 | | Woosley and Millero (2013) |
| $Na^+$ | $PbCO_3(aq)$ | $Cl^-$ | 0 | –0.145 | Woosley and Millero (2013) |

# Lead Chemistry

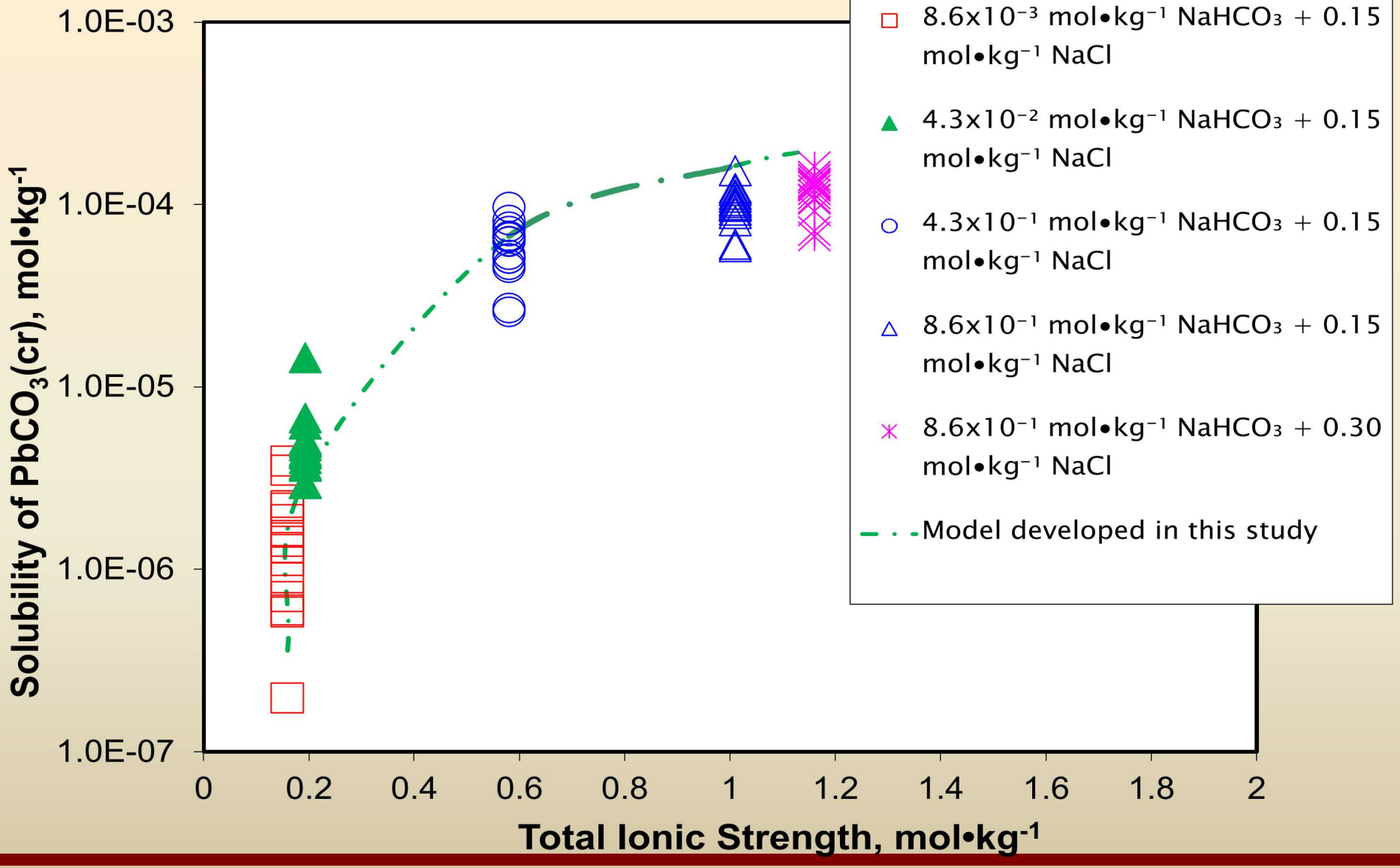

# Lead Chemistry

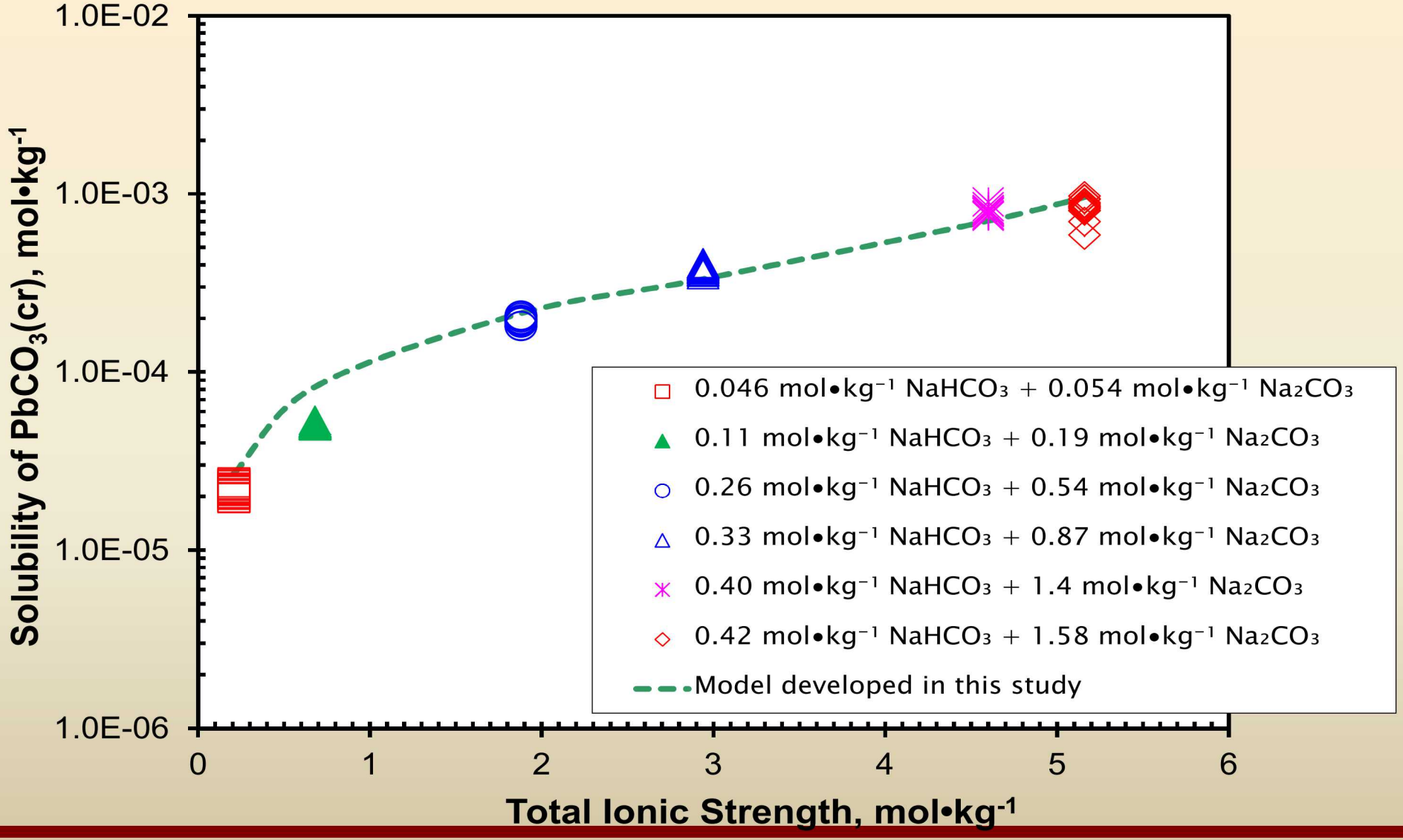

# Lead Chemistry

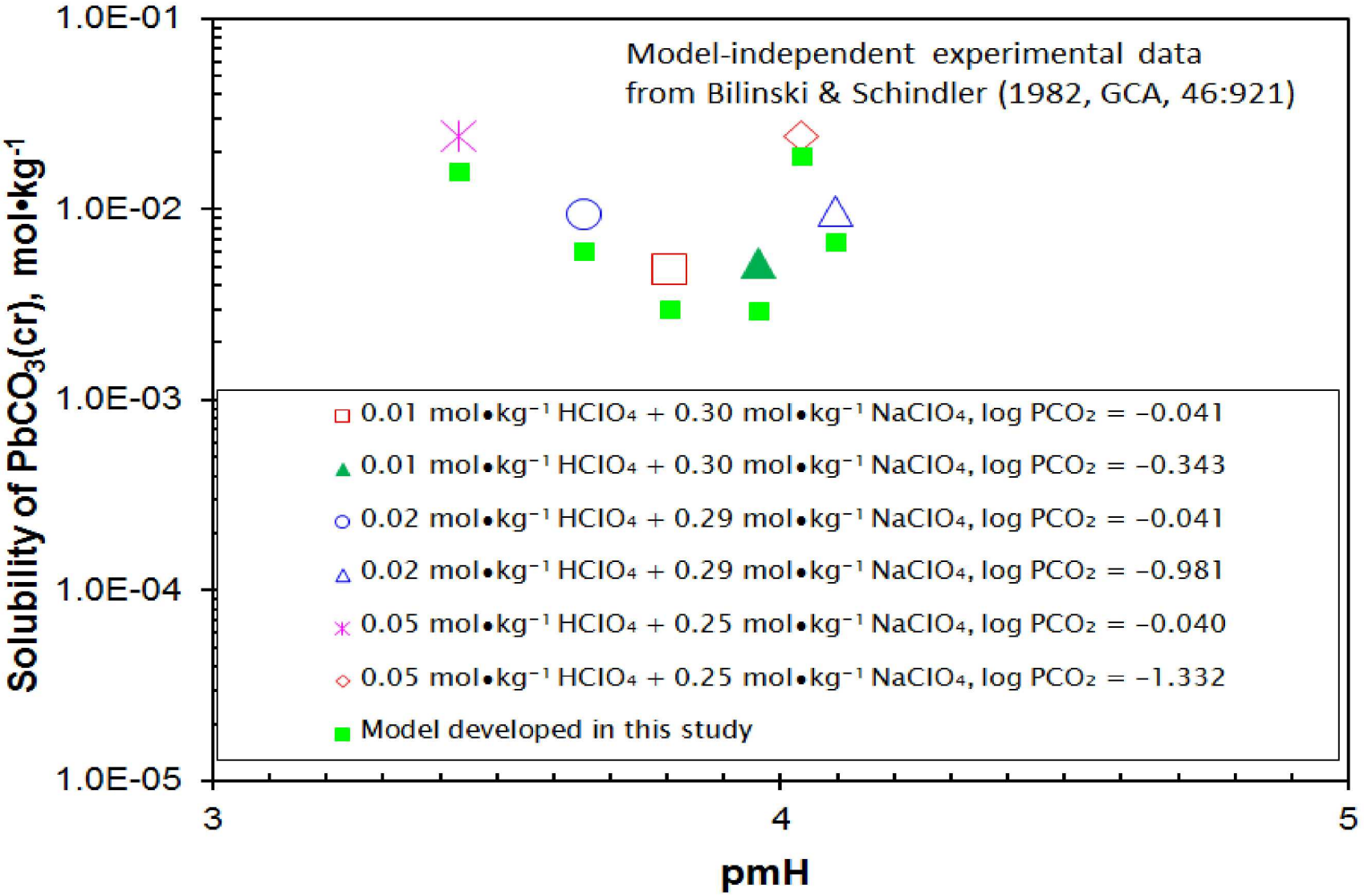

# Lead Chemistry

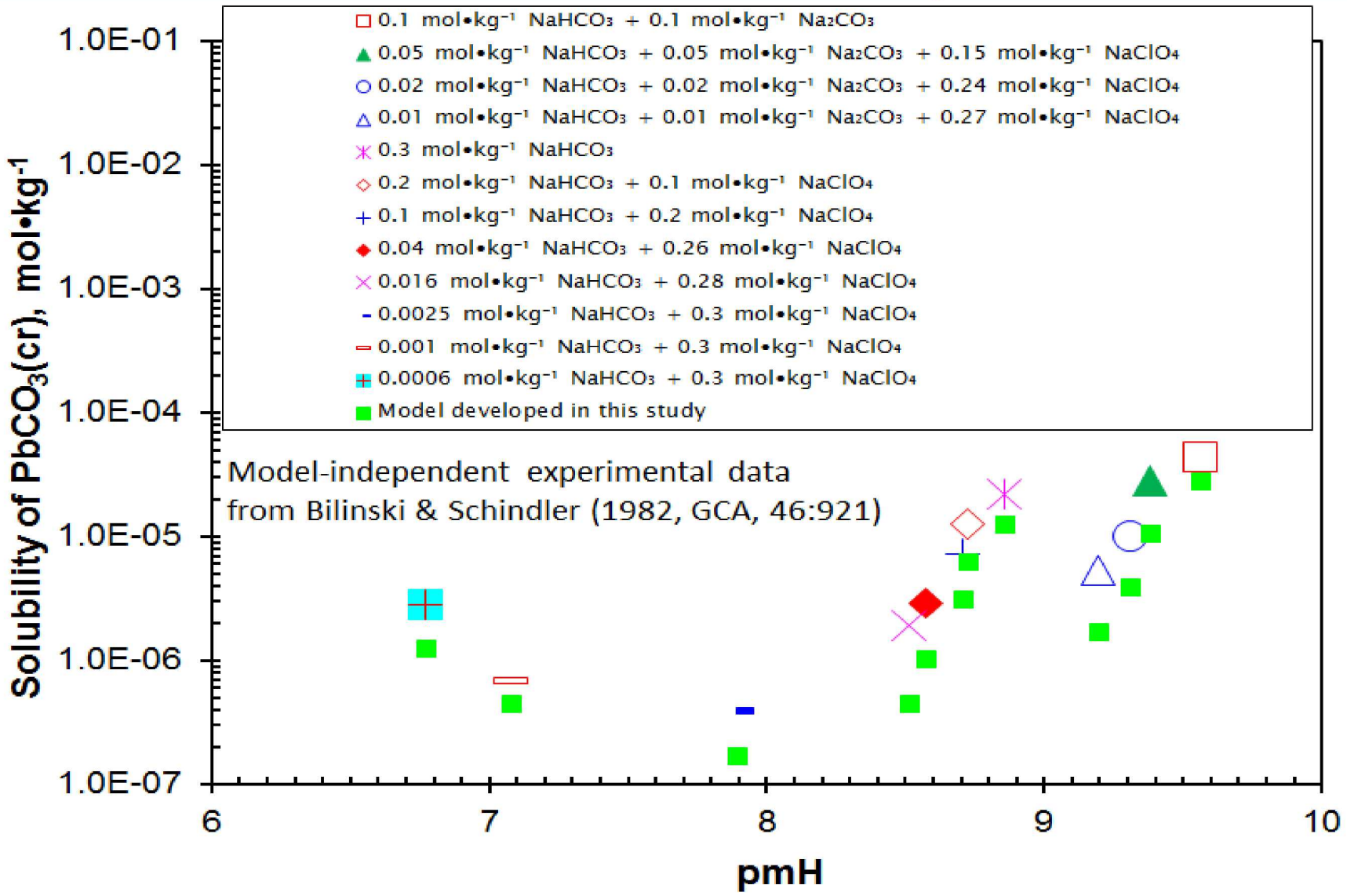

# Lead Chemistry

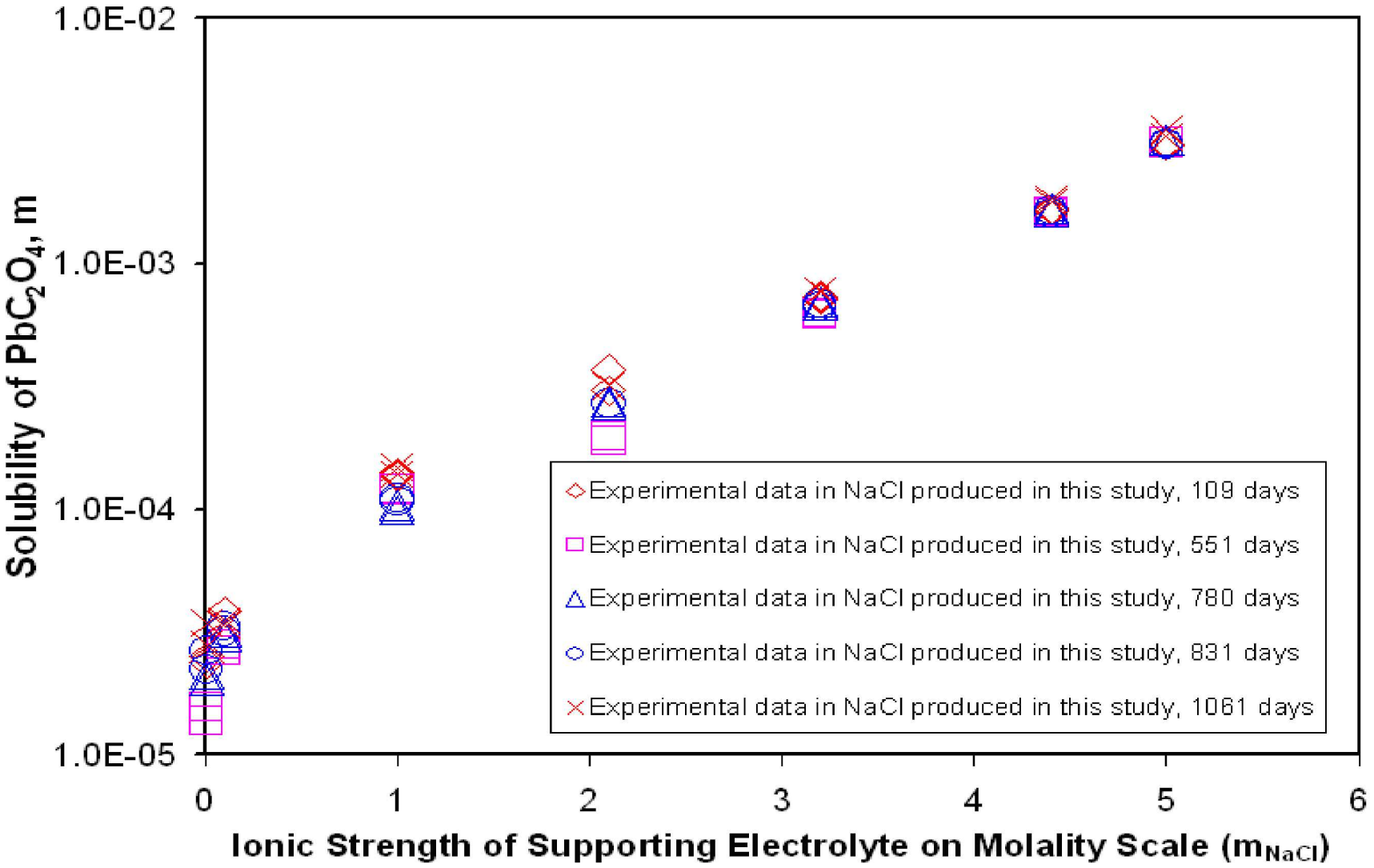

# Lead Chemistry

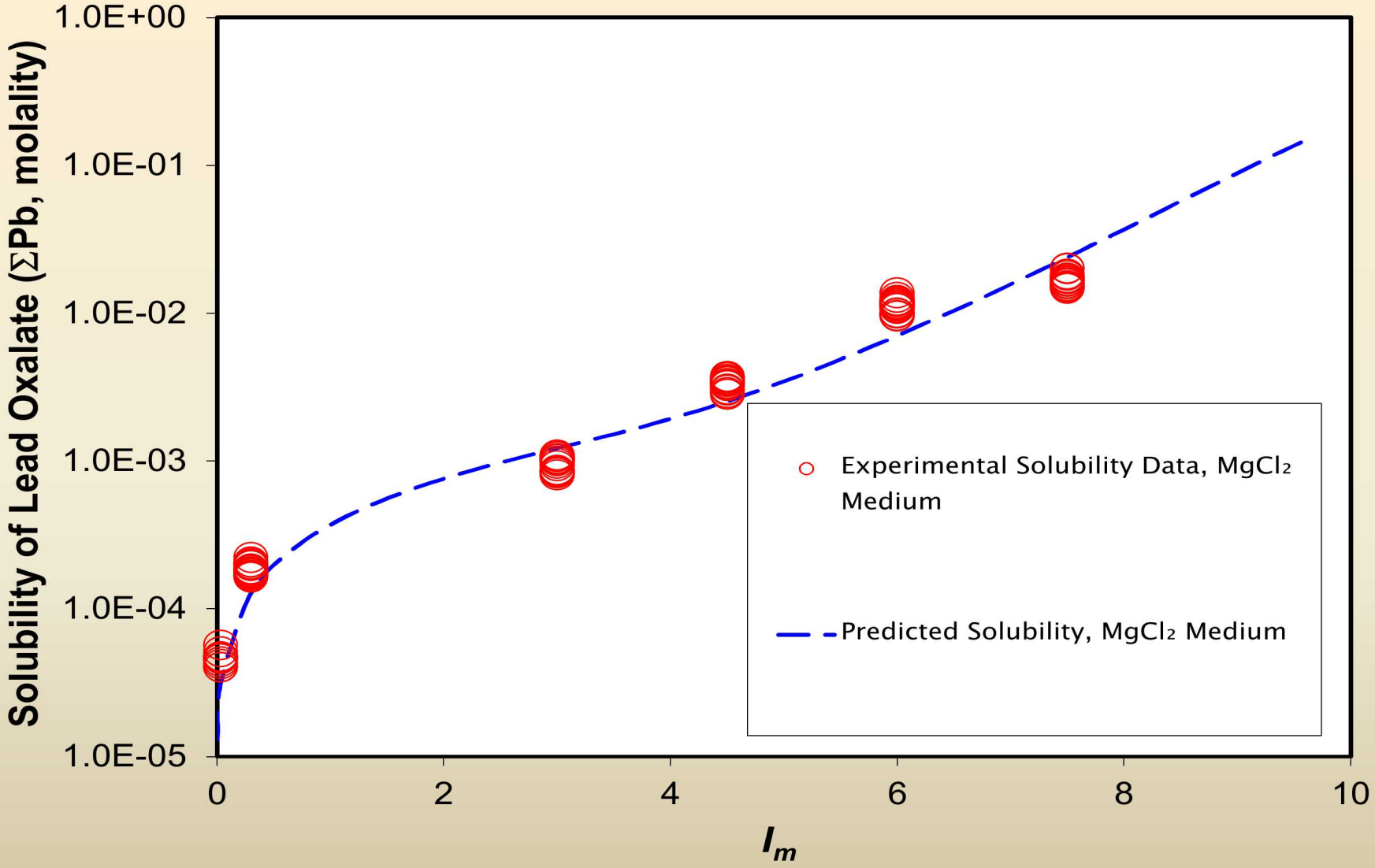

# Lead Chemistry

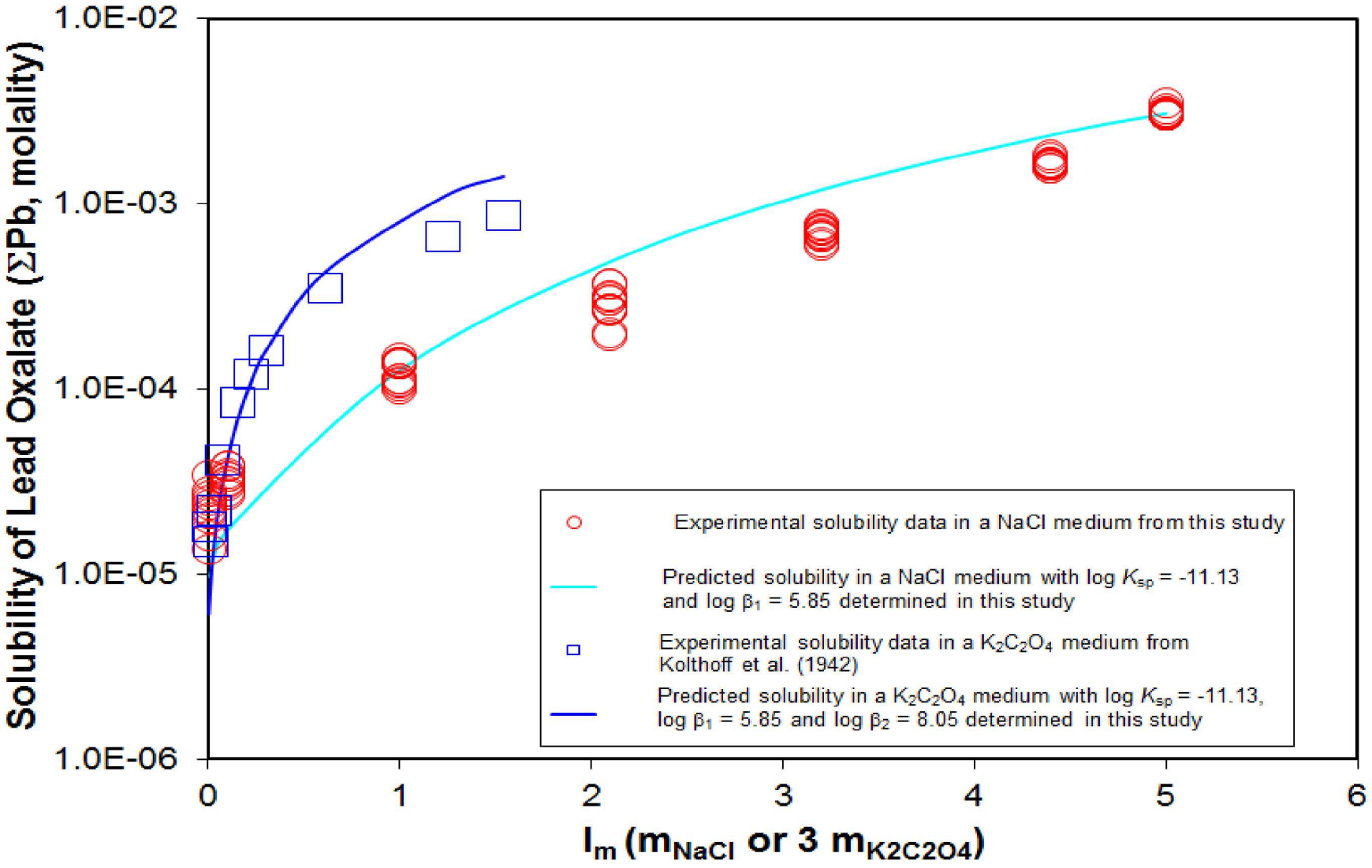

# Lead Chemistry

Table 4. Equilibrium constants at infinite dilution, 25°C and 1 bar, Pitzer interaction parameters, in $Na^+$—$K^+$—$Pb^{2+}$—$Cl^-$—$C_2O_4^{2-}$ system

| Reactions | log $K_{sp}$ or log $\beta_n$ | Reference and Remarks |
|---|---|---|
| $PbC_2O_4(cr) = Pb^{2+} + C_2O_4^{2-}$ | $-11.13 \pm 0.15$ ($2\sigma$) | This study, based on solubility of $PbC_2O_4(cr)$ in NaCl medium presented in the present work, Pitzer model |
| $Pb^{2+} + C_2O_4^{2-} = PbC_2O_4(aq)$ | $5.85 \pm 0.10$ ($2\sigma$) | This study, based on solubility of $PbC_2O_4(cr)$ in NaCl medium presented in the present work, Pitzer model |
| $Pb^{2+} + 2C_2O_4^{2-} = Pb(C_2O_4)_2^{2-}$ | $8.05 \pm 0.15$ ($2\sigma$) | This study, evaluated from solubilities of $PbC_2O_4(cr)$ in $K_2C_2O_4$ medium from Kolthoff et al. (1942), Pitzer model |

# Lead Chemistry

Table 4. Equilibrium constants at infinite dilution, 25°C and 1 bar, Pitzer interaction parameters, in $Na^+$—$K^+$—$Pb^{2+}$—$Cl^-$—$C_2O_4^{2-}$ system (cont.)

| | | |
|---|---|---|
| $Pb^{2+} + Cl^- = PbCl^+$ | 1.48 | Millero and Byrne (1984), evaluated by using Pitzer model; uncertainty not given |
| $Pb^{2+} + 2Cl^- = PbCl_2(aq)$ | 2.03 | Millero and Byrne (1984), evaluated by using Pitzer model; uncertainty not given |
| $Pb^{2+} + 3Cl^- = PbCl_3^-$ | 1.86 | Millero and Byrne (1984), evaluated by using Pitzer model; uncertainty not given |

# Lead Chemistry

| Pitzer Binary Interaction Parameters | | | | | |
|---|---|---|---|---|---|
| Species *i* | Species *j* | $\beta^{(0)}$ | $\beta^{(1)}$ | $C^{\phi}$ | |
| $Pb^{2+}$ | $Cl^-$ | 0.26 | 1.64 | 0.088 | Millero and Byrne (1984) |
| $PbCl^+$ | $Cl^-$ | 0.15 | 0 | 0 | Millero and Byrne (1984) |
| $Na^+$ | $PbCl_3^-$ | –0.0605 | 0 | 0.091 | This study |
| $K^+$ | $Pb(C_2O_4)_2^{2-}$ | 0 | –1.86 | 0.198 | This study |
| $Na^+$ | $Pb(C_2O_4)_2^{2-}$ | 0 | –1.86 | 0.198 | This study, in analog to $K^+$—$Pb(C_2O_4)_2^{2-}$ |
| Pitzer Mixing Interaction Parameters and Interaction Parameters Involving Neutral Species | | | | | |
| Species *i* | Species *j* | Species *k* | $\lambda_{ij}$ or $\theta_{ij}$ | $\zeta_{ijk}$ | |
| $Cl^-$ | $PbCl_2(aq)$ | | –0.14 | | This study |
| $Na^+$ | $PbCl_2(aq)$ | | –0.11 | | Felmy et al. (2000) |
| $Na^+$ | $Pb^{2+}$ | | 0.10 | | Felmy et al. (2000) |
| $Na^+$ | $PbCl_2(aq)$ | $Cl^-$ | | 0 | This study |
| $Na^+$ | $PbC_2O_4(aq)$ | $Cl^-$ | 0 | 0 | This study |

# Summary

- We have summarized the changes that have been made in the database since CRA-2004.
- The updated database, DATA0.FM2, provides more accurate representations of the near-field geochemistry of the WIPP, owing to
  - Revised solubility constant of hydromagnesite that is consistent with geological field observations and independent experimental data.
  - Updated Am(III) model with addition of $AmHB_4O_7^{2+}$ and revised constant for $AmEDTA^-$
  - Revised parameters for $CaEDTA^{2-}$
  - Updated MgO model with addition of $MgSO_4(aq)$
  - Updated borate model with addition of $NaB(OH)_4(aq)$ and revised constant for borax
  - Lead chemistry model

# Backup slides

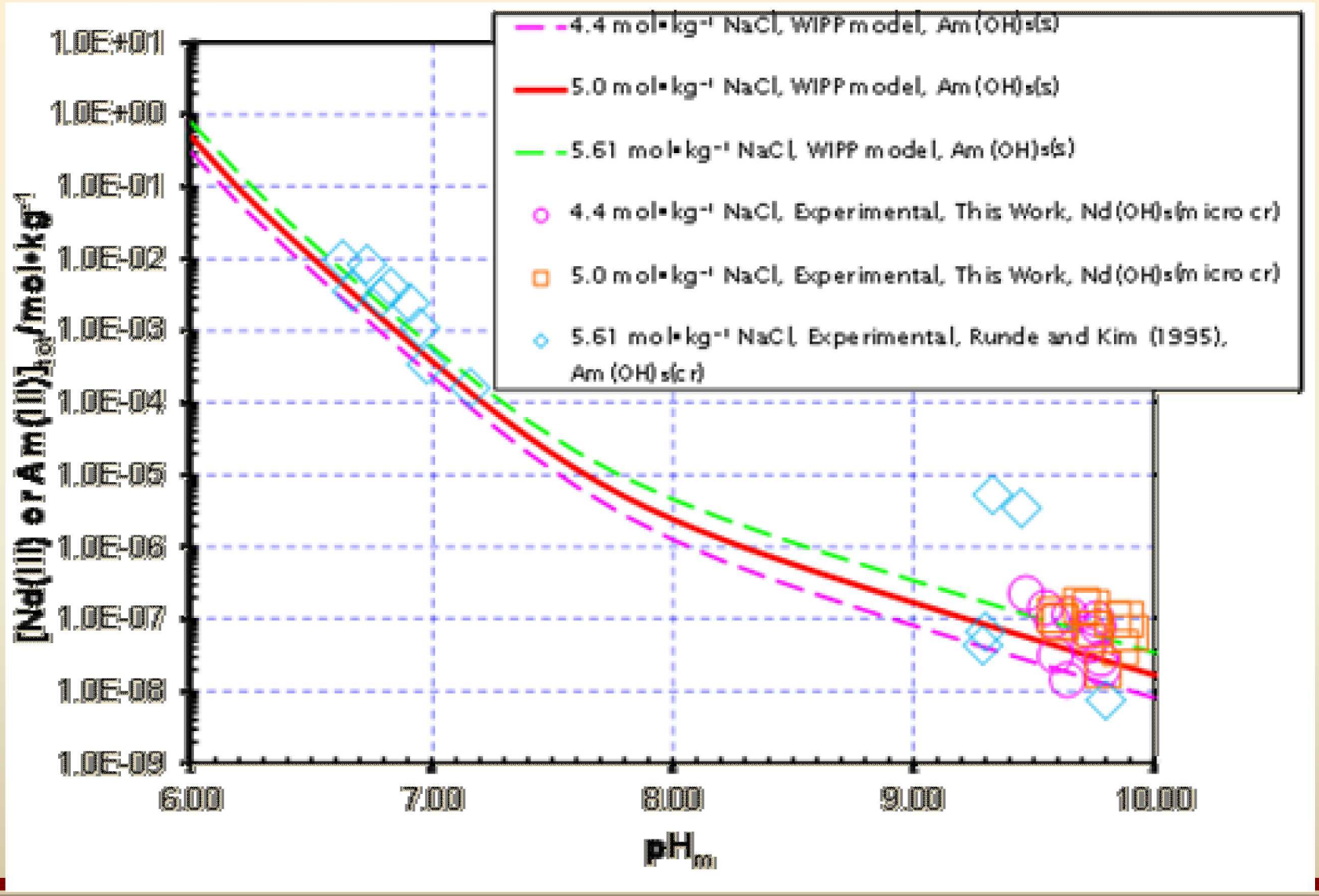

# Backup slides